DESIGN OF AN ADVENTITIAL TYPE REINFORCEMENT OF PROSTHETIC VASCULAR GRAFTS THROUGH MECHANICALLY AFFIRMED MATERIAL AND STRUCTURE MODULATION

by

Ross David Alexander Millam

A thesis submitted to the Faculty of Health Sciences, University of Cape Town on the completion of the degree of Master of Science (Medicine)

Department of Cardiovascular Research
University of Cape Town
August 2001

Declaration

I, Ross Millam, hereby declare that the following work is my own work and no part of it has been submitted for a degree at any academic institution.

Signed by candidate

Ross Millam

August 2001

Abstract

The high occurrence of vascular disease in the 20th century has been the driving force for researchers to produce a successful small diameter synthetic graft. Large diameter synthetic grafts remain patent for extended periods due to a higher flow rate, while smaller diameter grafts occlude more readily. Mechanical property mismatch between graft and host artery has been cited as one of the major factors that contribute to graft occlusion. It has thus been important to develop a readily available graft that is accepted by the body and does not cause flow abnormalities and stress-concentrations at graft-artery junctions. The object of this project was to ascertain the effect of an adventitial reinforcement on elastic compliance of synthetic porous polyurethane grafts. Non-reinforced grafts were over-compliant and continued to distend over an extended time period when subjected to cyclic stress. An automated winding apparatus was employed to wind different reinforcing fibres at various configurations. A fine elastane fibre was used to imitate elastin, the elastic component of a natural adventitia, a stiff nylon monofilament was used to imitate collagen which is much stiffer, and a polyurethane fibre with intermediate properties was also used. Porous polyurethane grafts manufactured by a salt-cast method and a gelatin bead-cast method were reinforced with the fibres at winding pitches of 1, 2.5 and 5mm. Two sets of grafts were reinforced with a combination of elastane and nylon reinforcement in an attempt to imitate the properties of a natural adventitia. Static and dynamic compliance tests were performed on all sets of grafts. Static compliance was measured by incrementally increasing the pressure by 20mm Hg over a range of 40-300mm Hg. The compliance was determined by measuring the corresponding diameter change over this pressure range. The non-reinforced salt-cast grafts showed the highest compliance values, having a static compliance of 9.21%/100mm Hg over the 80-120mm Hg pressure range, while the non-reinforced bead-cast grafts had a compliance of 5.21%/100mm Hg, indicating the bead-cast structure to be less compliant. The graft with the lowest static compliance was a nylon-reinforced graft, with a winding pitch of 1mm. The compliance over the 80-120mm Hg range being 1.76% per 100mm Hg. Dynamic compliance testing was also performed on all the graft types and a simulated physiological pressure pulse was applied to the grafts. Compliance was calculated over an 80-120mm Hg range as well as a 180-220mm Hg range. Dynamic compliances were generally lower than the static values for each set of graft, most likely due to the effect of testing rate. The grafts were also tested for maximum bursting pressure, the strongest graft tested being a bead graft reinforced with 290μm diameter PU monofilament at 2.5mm pitch, failing at 652mm Hg. The non-reinforced grafts were shown to gradually distend with extended

dynamic testing. By applying an external fibre-type reinforcement it was shown that the mechanical properties of an over-compliant porous polyurethane graft prosthesis could be improved. Moreover, it was shown that these properties could be manipulated by applying different reinforcing materials and by using different reinforcing configurations.

Acknowledgements

I would like to thank all the staff of the Cardiovascular research unit for their support during the writing of this thesis, in particular my supervisors Prof. Zilla and Deon Bezuidenhout for their guidance and suggestions. Special thanks also go to Mr. Bruno Orlandi who helped with the design and construction of the winding apparatus used to reinforce the grafts, as well as help with the setup of the compliance testing apparatus. I would also like to thank Mr. Eike von Guerard in this regard, who built the testing chamber for the apparatus. Also thanks to Mark Yeoman for his support and suggestions regarding the testing of the grafts, as well as Mrs. Elria Collocott and Ms. Dorothy Daws for their help in administrative matters.

Glossary of symbols

PTFE	Polytetraflouroethylene (Teflon®)	Δd	Change in diameter
ePTFE	Expanded polytetrafluoroethylene	LVDT	Linear variable displacement transducer
PET	Polyester	A/D	Analogue to digital
PU	Polyurethane	NMP	1-Methyl-2-Pyrrolidinone
bpm	beats per minute	dtex	Decitex (grams per 10000 m)
mm Hg	Millimetres mercury		
GPa	Gigapascals (10^9 pascals)		
MPa	Megapascals (10^6 pascals)		
kPa	kilopascals (10^3 pascals)		
E	Young's modulus		
E_L	Young's modulus, longitudinal direction		
E_T	Young's modulus, transverse direction		
E_g	Young's modulus, porous graft		
E_w	Young's modulus, reinforcing fibre		
σ	Stress		
σ_g	Stress in graft		
σ_w	Stress in winding		
ε	Strain		
ε_w	Strain in winding		
nm	nanometres		
μm	micrometres		
ϕ	winding angle, degrees		
ν	Poisson's ratio		
C	Compliance		
R	Radius		
d	Diameter		
d_w	Diameter of winding		
t	Wall thickness		
p	Internal pressure		
l	Length		
γ	Winding pitch, mm		

List of definitions

Adventitia	The membranous outer covering of an organ or a blood vessel.
Anastomosis	The surgical connection of separate or severed tubular hollow organs to form a continuous channel.
Autologous	Derived or transferred from the same individual's body.
Compliance	Extension or displacement of a loaded structure per unit load (in the case of blood vessels, the percentage diameter or volume change per unit increase in internal pressure.
Creep	The change in dimension of a specimen when subjected to a constant stress, the change being in the direction of the applied stress.
Distal	Anatomically located far from a point of reference, such as an origin or a point of attachment.
Elastane	Generic name for elastic polymer materials, usually comprising polyurethane-urea.
Heterogeneous	Consisting of dissimilar elements or parts, not homogeneous.
Heterograft (xenograft)	A living tissue graft that is made from one animal species to another.
Homogenous	Uniform in structure or composition throughout.
Hysteresis	The amount of energy absorbed by a material when it is stressed and the stress then removed.
Intima	The innermost membrane of an organ or a part, especially the inner lining of a lymphatic vessel, an artery, or a vein.
Intimal hyperplasia	The proliferation of smooth muscle and endothelial cells on the inside of a blood vessel.
Media	The middle, muscular layer of the wall of a blood vessel.
Occlusion	The closing or obstruction of a hollow organ or part.
Patency	The state or quality of being open, expanded, or unblocked.
Poisson's ratio	The ratio of lateral to transverse strain under an applied stress.
Proximal	Nearer to a point of reference such as an origin, a point of attachment, or the midline of the body.
Stress relaxation	The reduction in stress in a specimen after applying a force to the specimen and holding at a specific dimension.

Thrombogenic	Causing thrombosis or clotting of the blood.
Thromboresistant	The ability to resist thrombosis or blood clotting.
Thrombosis	A condition in which the blood changes from a liquid to a solid and produces a blood clot.
Xenograft	A living tissue graft that is made from one animal species and implanted in another.
Young's modulus	The ratio of stress to strain in a linear elastic material

Table of contents

Index of figures

Index of tables

Introduction

The development of a compliant small diameter vascular graft has been the topic of cardiovascular research for a number of years. This is due to its importance in the treatment of cardiovascular disease, which remains a major cause of mortality world-wide.

Synthetic grafts of polymeric materials have already been used with success in the replacement of large vessels with diameters of up to 3 centimetres, where differences in properties between graft and vessel are of less consequence. Grafts of smaller diameters (generally 6mm and less), made of the same synthetic materials, have had considerably less success. This has generally been attributed to surface thrombogenicity and intimal hyperplasia. While surface thrombogenicity is due to a lack of living endothelial cells, intimal hyperplasia is due to the proliferation of ingrowing host tissue on the blood surface of the graft. The cause of intimal hyperplasia is multifactorial, and one of the causes seems to be the difference in mechanical properties and compliance between graft and host artery. Compliance is a term used to describe the change in diameter of a vessel under a given change in internal pressure. Compliance mismatch between graft and vessel can lead to considerable problems, which eventually result in failure of the graft. Difference in stresses at the anastomotic junction can result in a proliferation of smooth muscle cells, due to an increased release of growth enzymes. This leads to a thickening of the vessel wall and eventual occlusion. The objective therefore has been to create a graft with the same or similar mechanical properties to that of a natural vessel and overcome these effects. In this respect, various approaches have been researched to solve this problem. Some have decided to take the 'natural' route while others have preferred to look for a synthetic alternative. The biological approach includes cell cultivation and in vitro 'growing' of an artery, or use of treated natural vessels transplanted to replace diseased ones. The synthetic approach details manufacturing a tube from a biocompatible material, usually polymeric in nature. In both cases it is necessary that the grafts are accepted by the body and are effectively incorporated. Some researchers have taken a compromise approach, seeking to combine synthetic and biological approaches. This entails the use of a porous structure that allows cell ingrowth and endothelialisation of the inner surface of the graft. Other researchers have sought to develop a graft made from a bioresorbable material that is resorbed by the body and eventually replaced by vascular tissue. In all of these approaches, however, it is realised that the matching of the material properties of the graft and vessel is of great importance to ensure long-life functionality.

Currently, the choice of materials suitable for implant is limited. While there has been some success with Dacron® and PTFE as materials for larger diameter implants, they still remain unsuitable for the smaller diameter implants partly due to their lack of compliance. Polyurethane has been a likely substitute and has an advantage due to its great variability of properties and good acceptance rate. However, the mechanical properties of this material are still not ideal as polyurethanes used currently for synthetic grafts are visco-elastic in nature and would have the tendency to creep or distend over a period, causing the graft to eventually fail.

In this project, the aim was to improve the mechanical properties of an existing polyurethane graft, in essence to manufacture an adventitially-reinforced graft with a compliance close to that of a human femoral artery which has a compliance of around 6%/100mm Hg. Reinforcing fibres were wound helically on the external surface of the grafts, at different winding pitches (the gap between adjacent fibres) and some grafts having more than one layer of fibre. In some cases more than one type of fibre was employed. The static and dynamic compliance of these grafts was then appraised by testing them on a custom-built apparatus, to determine the effect these reinforcements had on the mechanical properties. The effect of extended testing on the mechanical properties was also investigated. Burst testing and suture tearing strength were also performed on some of the graft types to determine their ultimate failure strength and suturability.

1. Literature Review

This chapter gives an overview of some of the history of vascular prostheses as well as the different types of grafts being used currently. Aspects of vascular grafting that determine the ultimate success of grafts are also discussed, in particular the matching of mechanical properties and compliance to that of natural vessels.

1.1 BACKGROUND OF VASCULAR PROSTHESES

1.1.1 Arterial Grafts of Natural Tissue

Autologous grafts (grafts from the same subject) remain to date the replacement vessels of choice in vascular and cardiac surgery. The problems associated with synthetic arterial grafts result in a lower patency, especially for grafts with a diameter less than 6mm. For example, the internal mammary arteries are usually the first choice of surgeons for coronary bypass operations, followed by the radial artery, the superior gastroepiploica artery and the saphenous vein. The disadvantage of this approach is that these vessels themselves are often diseased, and there is the problem of the presence of valves in veins even when placing the vein in the reverse flow direction (to prevent the valves closing). Some success has been had using other types of natural tissue grafts, for example umbilical vein reinforced with Dacron® mesh, or bovine heterografts that have undergone fixation treatment and detoxification to prevent an immune response. Hokanson and Strandness [1] showed that out of several types of arterial grafts implanted (including knitted & woven Dacron®, knitted and woven Teflon® grafts, autologous vein grafts and bovine heterografts), the bovine grafts had the best patency. The other grafts showed a decrease in patency after implantation, with exception of the vein graft. Out of vein, Dacron® and PTFE grafts, vein grafts showed the best patency in a canine bypass model after 2 weeks (83% remaining patent). Some recent research has been carried out in growing arteries in vitro, by means of cell culture techniques L'Heureux et al [2], showed that cells could be cultured in layers and wrapped around a mandrel to produce a graft. Firstly, human smooth muscle cells were cultured and then a layer of human fibroblasts added to provide an adventitia. After a maturation

time of about 7 weeks, the grafts were found to have developed a bursting strength of above 2000 mm Hg. Non-endothelialised grafts were implanted in a canine model and assessed after 7 days. Fifty percent of the grafts were found to remain patent. This low figure can be attributed to the fact that they were xenografts (ie. grafts of human tissue in a canine model). Another attempt at a cultured graft was undertaken by Ramshaw et al [3], who grew collagen-impregnated grafts by implanting silicone mandrels wrapped with Dacron® mesh in sheep. However, these grafts were not implanted into any vascular models and therefore cannot be assessed in terms of their biocompatibility or physical properties.

1.1.2 Prosthetic Vascular Grafts

To date, various materials have been used in the manufacture of synthetic artery grafts. Most of these materials have been polymeric in nature and include Teflon®, or polytetrafluoroethylene, Dacron® (PET), and polyurethane. Different manufacturing techniques have been employed to give the final desired properties (for example, Dacron® grafts are knitted with a concertina-type structure that gives them longitudinal stretch and prevents kinking). Until now, these materials have been successfully used in larger diameter vessels, and compliant behaviour has been of less importance, as the grafts have had only to withstand the maximum pressure in the vessel and not necessarily match compliance. Thus their role was merely to provide a conduit in which blood can flow. Problems arise, however as the diameter of the vessel decreases and pressure increases. Physiologically, vessels further away from the heart are smaller in diameter and have different tissue composition and hence different mechanical and elastic properties than those closer to the heart. It has generally been recognised that below a diameter of about 6mm, the patency of grafts is reduced dramatically [4,5]. More recently, graft materials have been chosen on their ability to be accepted in the body and remain inert. Also, graft microstructures have been developed that allow better incorporation into the body. Knitted or woven grafts such as Dacron®, or expanded poly(tetrafluroethylene) (PTFE) have spaces between fibres which are mostly prohibitive for tissue ingrowth. Researchers such as McGregor, Wilson [6,7] and Gershon, Cohn and Marom [8,9] have attempted to produce filament-wound grafts either with polyurethane fibres or with fibres coated with polyurethane [8]. By varying the pitch (wind angle), they could vary the amount of porosity as well as the mechanical properties of the graft. Other filament – type grafts have been made by Gupta and Kasyanov [10] who used 2 different types of fibres to imitate the properties of elastin and collagen, using a stiff Polyester fibre for the collagen and an elastic

Lycra® fibre for the elastin. These were woven together to form a composite graft which was shown to have comparable mechanical properties to a human carotid artery (upon which they modelled the graft.)

Since polyurethane has had some success as an implant material, some attempts have been made to produce a porous polyurethane graft. Some have used a phase separation technique to produce a porous structure [11,12,] or a soluble filler to create the porosity which is extracted when the graft is cured [13] or by bubbling a gas through the polymer solution before it sets [14]. With all of these methods however, there is a limit to the extent to which pore morphology can be controlled. Despite all these developments, a suitable small diameter graft that does not fail due to poor mechanical properties or poor biologic compatibility has yet to be found.

1.1.3 The Advantages and Disadvantages of Natural and Synthetic Vessels

Natural vessels, especially autologous implants (ie. from the same subject) have generally had more success as small diameter implants than synthetic grafts. In terms of mechanical properties, the natural tissue provides a fairly close match in terms of compliance or elasticity, even when using saphenous vein grafts (veins have a lower compliance than arteries). Autologous vein grafts have been widely used and are preferred over heterogeneous treated tissue or xenografts, as there is no immune response to foreign tissue. The only concern, as mentioned previously, is that autologous vessels are often in too diseased a state to be used. The beneficial quality of these grafts, however, is that they possess an endothelial lining which makes them thromboresistant (ie. they resist the onset of coagulation). The thromboresistance of a material depends primarily on its surface features and chemical make up, since this determines the types and ease with which proteins may be adsorbed. Following protein adsorption, platelet adhesion occurs and then blood cell interaction. Most synthetic materials being used currently for implants have a poor thromboresistance. Thus efforts are being made to treat the graft surfaces such that the adsorption of proteins associated with thrombus formation is limited. Heparin treatment shows some promise in preventing clot formation and also has the added benefit of inhibiting smooth muscle cell proliferation, which would naturally be beneficial in preventing intimal hyperplasia (which is the excessive growth of arterial tissue from the natural vessel into the synthetic one at the anastomosis)[4]. Another avenue being explored are synthetic grafts with an established endothelial layer, since this is the only known surface that does not cause a thrombogenic response. To do this, one would either have to implant a graft with a surface that encourages the formation of an endothelial lining, or alternatively 'seed' a graft in vitro with endothelial cells

from the patient, and implanting once a cultured endothelial layer has formed. Obviously, the time it would take to culture endothelium is a drawback.

Polyurethane has gained favour as an implant material because of its more elastic response and relative inertness when implanted. Dacron® in comparison has a high tendency for platelet adhesion and activation, which explains why it has not had much success in small diameter vessel replacement. There is still some uncertainty as to what exactly causes intimal hyperplasia but in most small diameter grafts there is always a proliferation of natural tissue at the anastomosis. This tissue is comprised mostly of smooth muscle and extracellular matrix. Loss of patency occurs when the vessel becomes stenosed. Blood flow velocity is reduced below a critical point and thrombosis (clot formation) occurs, resulting in occlusion of the vessel. Interestingly, the hyperplastic response is always found to be more pronounced at the distal (or downstream) anastomosis. It has been hypothesised that as blood platelets pass through the non-endothelialised synthetic graft, they become activated and stimulate the release of growth factors that in turn stimulate the proliferation of smooth muscle at the site of greatest stress concentration [4]. However, the true cause could be related to compliance and size mismatch, which in turn results in uneven shear stress distributions. In all cases graft failure simply occurs by blockage or occlusion after clot formation which is the result of flow abnormality (turbulence, reduced flow velocity).

1.2. THE IMPORTANCE OF COMPLIANCE MATCHING

At a junction between a natural artery and a synthetic graft (or anastomosis), there is always a degree of mismatch between natural and synthetic properties. This difference in properties invariably results in complications and has a direct effect on pressure and flow characteristics in that region. The greater the degree of mismatch, the more pronounced the problems. If the synthetic graft has a lower compliance than the artery (ie. more stiff), the dilation of the artery is restrained at the anastomosis, and at maximum distension the graft remains at a smaller diameter than the artery and the blood has to flow through a narrower path. This results in an increased blood velocity in this area. Conversely, if the graft is of higher compliance (or less stiff) than the host artery, 'ballooning' occurs after the anastomosis, as the graft distends to a higher degree than the artery. Hence pressure and flow velocity decrease due to the greater diameter. Both of these cases are detrimental to the long-life functionality of the graft, and have deleterious effects on cell growth around the anastomosis, which in turn leads to a compounding of the problem and

eventual failure. Numerous authors have cited the direct cause of intimal hyperplasia to be compliance mismatch between host and synthetic vessels. Chandran and Kim [15] have shown by numerical modelling that compliance mismatch in the case of end-to-end anastomoses is a major cause of abnormal flow conditions which ultimately results in loss of patency. In the case of end-to-side anastomoses however, they claim geometry of the junction to be the primary factor and mismatch a secondary contributor to flow abnormality. Kidson [16,17] showed a correlation between graft compliance and patency by implanting vein, Dacron® and PTFE grafts in a canine model. The stiffest, least compliant ePTFE (expanded polytetrafluoroethylene) grafts had the poorest patency (15% after 12 weeks), while Dacron® and vein grafts had a patency of 30 and 80% respectively). Walden et al [18] conducted a similar study and also confirmed that ePTFE had the lower patency when compared to autologous vein grafts. Stansby et al [19] and Giudiceandrea [20] seeded ePTFE and polyurethane grafts with endothelial cells and tested them on an artificial circulation device. They found that the more compliant polyurethane grafts had a better cell adhesion percentage than the less compliant ePTFE grafts, suggesting that more compliant materials reduce the fluid shear on endothelial cells. In the case of porous grafts there is also the added effect of tissue ingrowth after implantation. Generally, this will cause a decrease in compliance as shown by White, Klein and Shors [21] who implanted over-compliant porous silicone grafts in dogs. After 2 weeks, the compliance had decreased to a similar value to that of a natural artery. In humans, Dacron® and ePTFE grafts decrease in compliance over time due to a fibroplastic response [22] which consists of the proliferation of fibroblasts and collagen.

1.2.1. Haemodynamic Aspects of Arterial Grafting

As mentioned above, there has been defined or hypothesised a critical flow velocity below which thrombus will form. Also, at elevated flow rates, turbulence occurs which results in increased shear stress on the intimal layer, causing an erosive effect on the endothelial lining of the vessel. This obviously results in a decrease in thromboresistance and ultimately loss of patency. Burkel [4], citing work by Sauvage et al., defines a critical flow velocity below which thrombus forms. Research suggests this velocity to be 6-8ml/s. This also explains the high patency rates of large diameter grafts compared to small diameter ones. In large vessels, the flow velocity is high and a stable intimal layer of platelets and fibrin forms. In smaller vessels, the flow rate is considerably lower and the likelihood of thrombus formation is far greater. The anastomotic geometry is also an important factor to consider in arterial grafting. In an effort to reduce the occlusive effects of hyperplasia, some experiments have been done implanting oversize grafts. Weston et al [23]

found that a minimum mean wall shear stress rate occurs at a divergent geometry (ie from a small artery to a large graft or from a small graft to a large artery). They suggested that diameters of grafts should be matched in the pressurised state (ie similar to in vivo pressure) to prevent diameter mismatch upon implantation. Low shear stress rates have been shown to be associated with increased hyperplasia. Compliance and diameter mismatch will cause abnormal shear stress distributions, therefore it is important to match both of these factors. Nicolaides [5] showed the Poiseuille equation to be useful as a rough assessment to the onset of turbulent flow, by calculating the Reynold's number according to diameter and flow rates in different vessels. However, this approach is not really applicable to pulsatile flow scenarios and hence is only really a qualitative tool. It is interesting to note that despite the assumptions of steady laminar flow and an incompressible fluid in a straight vessel, there is a transition point at a 6mm vessel where the Reynold's number exceeds that for steady flow and becomes turbulent. Generally, Reynold's numbers above 2300 indicate turbulent flow, These calculations are based on the maximum flow rate ie peak systolic flow. Analysis of vascular haemodynamics is further complicated by the fact that the vascular tree tapers – not only in size but also in terms of mechanical properties [5]. Near to the heart, where the flow volume and pressure is high, blood vessels are generally more compliant and elastic [24,25,26]. This phenomenon is termed the *Windkessel* effect and serves to smooth the sharp pulsatile output of the heart. The origin of this term is from an 18th century device used in fire engines at the time. The Windkessel chamber served to smooth the spurting flow created by the hand-operated pump. Being half filled with air and half with water, the air portion served as an elastic "cushion", taking up the initial pressure spike and propagating a smooth flow as the air expanded back to normal state. Physiologically, the elasticity of the aorta acts in the same way, as a buffer to the systolic output of the heart. Since there is an aortic valve and the flow cannot be reversed, when the aorta returns to normal state, it propagates a forward flow. This can be demonstrated by observing the blood pressure curve: the pressure increases sharply to the maximum systolic value due to the output of the heart, then reducing at a slower rate to the diastolic value before repeating the cycle again. More distally, arteries tend to decrease in compliance and elasticity in order to prevent energy losses as blood flows to the periphery. The term *impedance* is used to describe this effect and is a measure of the resistance of the system to forward flow. It is dependent on the geometry of the vessels (ie. lumen area) as well as their compliance or modulus of elasticity (which is the inverse of compliance), as well as viscosity and inertia of the blood. Nicolaides [5] defines an input impedance as the ratio of the modulus of each pressure wave to the modulus of each pressure wave harmonic, and one is able to calculate this by the simultaneous measurement of pressure and flow. Since impedance

increases and compliance decreases toward the periphery, the pressure pulse wave shows a change in shape as one moves distally along the vascular tree (see figure 1.1). From being a triangular-shaped wave in the aorta, it is transformed into a sharper peak with a higher systolic pressure at the extremities. Conversely, the flow waveform shows a decrease in amplitude towards the peripheral vessels, and can be explained by the corresponding changes in the pressure waveform. Changes in the shape of the pressure waveform result in changes in the pressure differential for each pulse, and hence effects the amplitude of the volume flow curve.

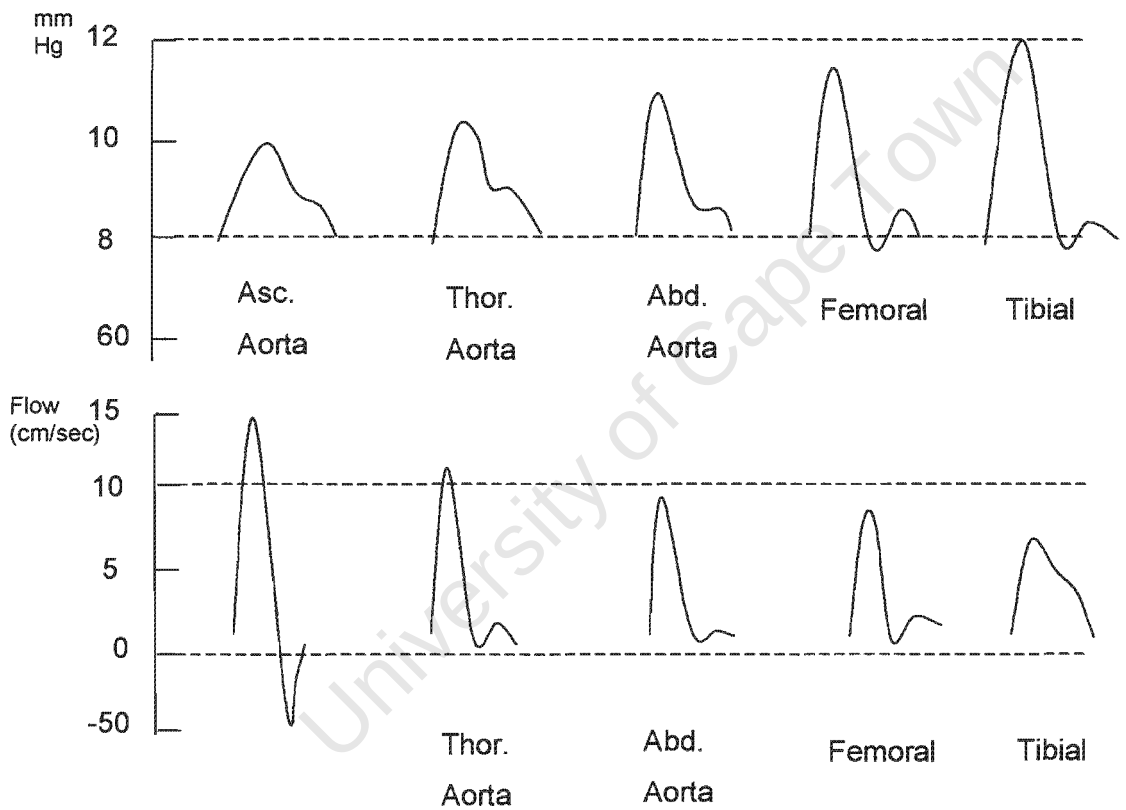

Figure 1.1: Transformation of the pressure pulse and flow waves in the arterial tree (Adapted from [5])

1.3. IMITATING THE PROPERTIES OF NATURAL VESSELS

Researchers have until recently been more concerned with the biocompatibility of a prosthesis, and have paid more attention in developing graft materials and structures that are accepted by the body. Less emphasis has been placed on matching the mechanical properties of the graft with the host vessel. Although material biocompatibility is important in the initial period of implant (as a minimal immune response is desired after implantation), the mismatch in mechanical properties will also ultimately result in failure of the graft. Medical researchers have realised the need to initially have a blood-compatible lumen on the internal surface of the graft. In this regard, much time has been spent on developing a graft that can quickly establish a layer of endothelial cells on the inside surface of the graft. As far as is known, the endothelial surface is the only truly thromboresistant surface, and even the best polymer surfaces still encounter deleterious protein adhesion. The issue of mechanical mismatch becomes more of a factor influencing patency at a later stage. This might be a gradual loss of compliance over a period of time, either due to tissue ingrowth or deterioration of the graft properties (especially in the case when the graft is made from a visco-elastic material, and the phenomenon of creep occurs. Some researchers have recognised that the larger the mismatch in compliance between artery and graft, the more pronounced the effect on patency [19,27,28]. This is understandable, since a material with a completely different stress response will have a direct effect on the blood haemodynamics. Stiff grafts cause a certain amount of impedance, and reduction of blood flow, which ultimately results in failure by thrombosis [8,29] It would be very difficult to imitate the anisotropic properties of an artery utilising one material. At best, some variation in structure might have some effect, but one would not be able to achieve difference in Elastic modulus between collagen and elastin for example ($E_{collagen}$=±1x10^3 MPa, $E_{elastin}$ = ±0.4 MPa)

1.3.1 The Physiological Structure of Blood Vessels

One can divide the blood vessels into two categories: veins and arteries. Veins act as a 'return' path from the organs back to the heart and are generally low-pressure vessels. Arteries distribute blood from the heart to the rest of the body and have to deal with relatively higher blood pressures which fluctuate in a cyclic manner. Due to these different roles, the tissue composition of veins and arteries differ considerably. There is also a distinct difference in composition of arteries depending on their size and location in the body. For instance, the aorta has a 1:10 wall thickness:diameter ratio and is composed mostly of elastic tissue and some smooth muscle,

whereas an artery of 4mm diameter has a 1mm wall thickness and the ratio of smooth muscle to elastic tissue is greater. Arteries further from the heart have a greater percentage of muscular tissue and are thicker-walled, while the larger vessels closer to the heart are thinner-walled and consist mainly of elastin and collagen. The blood vessel is composed of various layers of tissue, each with a different composition and a different function. The inner-most layer of the artery (intima) is comprised of an endothelial layer, essentially flat cells that act as an interface between the blood and serve a friction-reducing role. The medial layer is comprised of smooth muscle cells and elastin, the smooth muscle to provide the contraction of the vessel wall and the elastin to serve a structural purpose and cause the vessel to maintain its original shape. The outermost layer or adventitia is made up of collagen interspersed with elastin. Collagen is a stiff material compared with elastin and the two act in conjunction: elastin for distensibility and collagen as a limiter to excessive arterial expansion. Figure 1.2 below shows the cross-section of an artery and details the different structural components. Figure 1.3 is a simplified schematic of a vascular tree, showing the tapering in size of veins and arteries towards the periphery and the difference in compositions of veins and arteries at different positions.

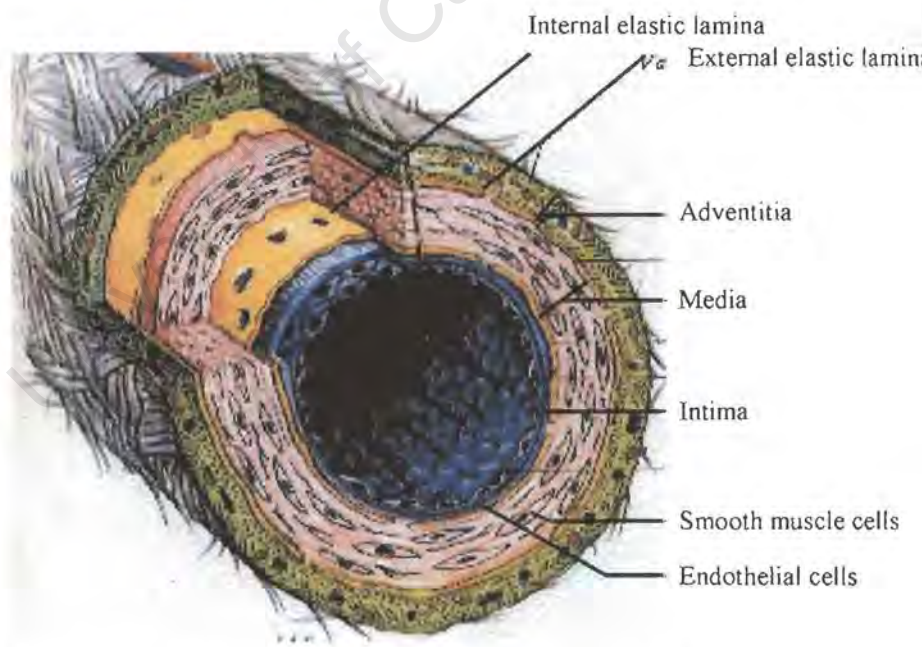

Figure 1.2: Schematic representation of the cross section of an artery.

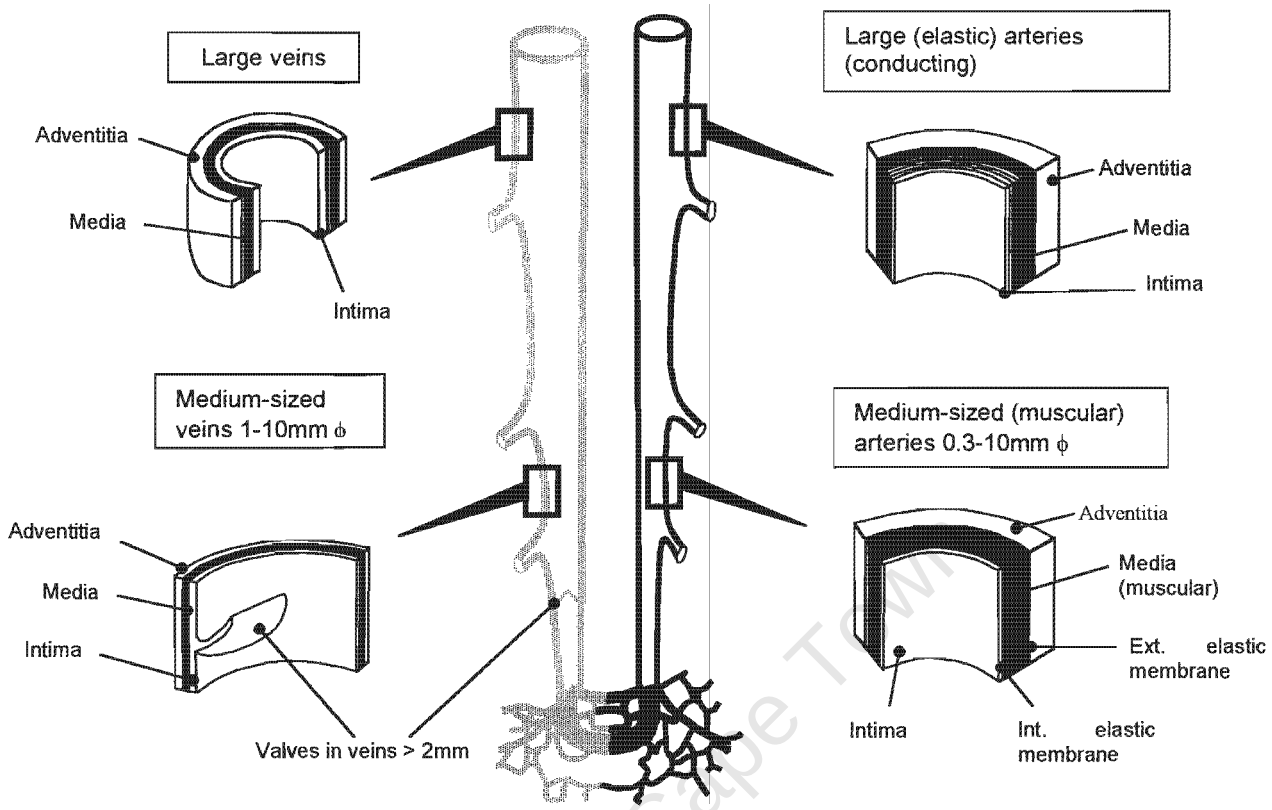

Figure 1.3: Variation of artery and vein composition in the vascular tree. (adapted from [137]).

1.3.2 The Mechanical Properties of Arterial Tissue

Numerous researchers have shown the stress-response of natural blood vessels to be non-linear in nature [17,18,19,30,31,32]. Generally, arteries show an increase in stiffness with an increase in internal pressure. Shadwick [24] measured the elastic properties of the arteries of several different species. When normalised with the mean arterial pressure found in each subject, the elastic moduli of arterial tissue is more or less equal, even when comparing different species. He further points out that arterial tissue is hence modular in nature and its composition will depend on the position in the arterial tree and the mean pressure. With increasing distance from the heart, the ratio of elastin to collagen changes from about 2:1 in the aortic arch to 1:2 in the abdominal aorta. Hence arteries closer to the heart are more elastic in nature, while those more distal are less so.

Fung et al. [33,34], sought to describe the properties of the different layers found in a blood vessel, and divided the blood vessel into 2 distinct layers: the intima-media and the adventitia (see table 1.1 below). By testing segments of arteries in bending-type experiments, he calculated the moduli of the two layers and determined the position of zero-stress in the artery wall (the location of the neutral axis). Although he shows the adventitial layer to have a much lower modulus than the intima-media layer, this is probably because the testing was conducted at low strains, and the influence of the stiff collagen in the adventitia would have been negligible.

Table 1.1: Properties of porcine aorta at different positions [31]

Vessel type (porcine)	Young's modulus: intima-media	Young's modulus: adventitia	Neutral axis location (% of total wall thickness from intimal surface)
Thoracic aorta	43.25 kPa	4.7 kPa	30 %
Ascending aorta	447.5 kPa	111.9 kPa	35 %
Descending aorta	247.8 kPa	68.7 kPa	35 %

1.3.3 The Response of Arteries to Stress

Peterson et al [30] analysed the in vivo response of arteries to pressurisation under various conditions. They refuted the theory that the smooth muscle content of the arteries assist in pressure pulse propagation. The synchronisation of contraction of the arteries with that of the heart would be far too complicated, as the pulse is a highly variable occurrence, and there is evidence to suggest that the elastic response of smooth muscle is far too slow to achieve this. No evidence has been found to support the theory of synchronous contraction. Generally, under small strain conditions, the artery response can be seen as elastic, and will be proportional to the elastic and viscosity moduli of the vessel.

1.3.4 Replicating the Compliance of Arteries

Gershon et al. [9,29], have manufactured grafts by a winding process, whereby an elastic fibre is embedded in a biodegradable polymer matrix to give the desired properties. The mechanical properties and compliance of the graft can be well controlled by adjustment of the winding angle

and fibre content, and depending on the constituent materials. As can be seen from figure 1.4 below, they found a maximum compliance (minimum elastic modulus, E) in the longitudinal direction to exist with a winding angle of 45 degrees. As they defined the winding angle to be measured from the longitudinal axis of the graft, this can be explained by the fact that at angles close to 90 degrees, the fibres lie closer together in the transverse direction and the polyurethane matrix will essentially 'glue' the fibres together. At angles closer to 0 degrees, the fibres become more aligned with the longitudinal direction, hence increasing stiffness in that direction.

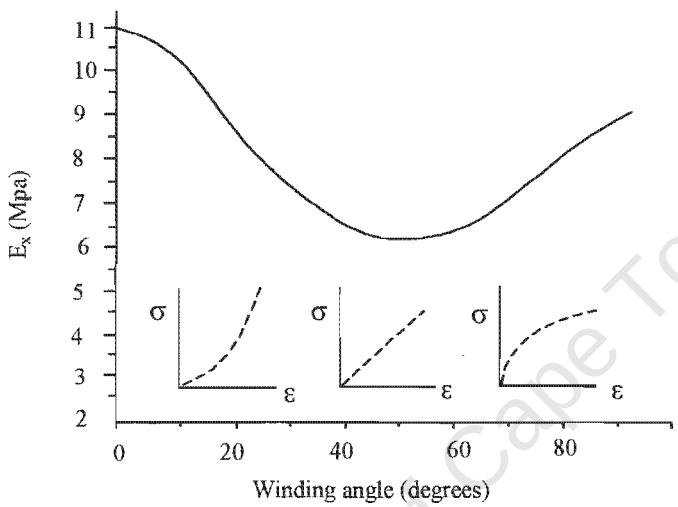

Figure 1.4: Graph of Young's modulus in the x-direction as a function of winding angle [9].

Figure 1.5 below shows also how fibre content affects the stiffness of the grafts in the longitudinal and transverse directions.

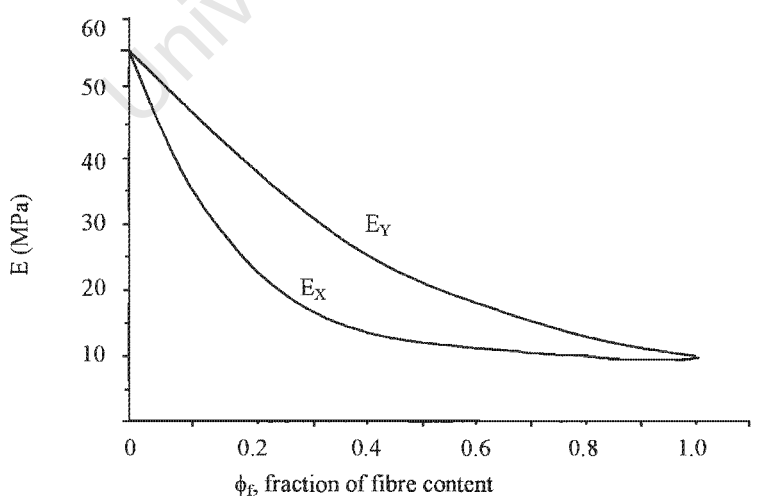

Figure 1.5: The effect of fibre content on Young's modulus (wind angle of ±73°), [9].

By this process, it is possible to manufacture a graft that has the anisotropic material properties of a real artery. The advantage of this is that is a very controllable process, and by using a biodegradable matrix, into which smooth muscle cells would grow, one can compensate for an increase in stiffness of the graft, which would happen in the case of using a purely porous, non-degradable graft. Gupta and Kasyanov [10] manufactured a graft by weaving 2 different fibres: a polyester fibre with a high modulus of elasticity to imitate collagen and a Lycra® fibre with a low modulus to imitate the properties of elastin. They were also able to introduce a certain amount of circumferential pre-stress by knitting the Lycra® fibre under some tension in this direction.

1.4 COMPLIANCE TESTING OF GRAFTS AND NATURAL VESSELS.

1. 4.1. Static and Dynamic Compliance Testing

Generally, there are two ways of characterising the compliance of a vessel: Statically and dynamically. Static compliance testing entails the stepwise, incremental increase in internal pressure and a corresponding diameter measurement for each step. The advantage of this method is that it is quite easy to generate a pressure-diameter relationship, and is useful when characterising compliance over a large pressure range. However it does not take into account the effect of strain rate on the graft response. This could have quite a large influence on the data obtained, especially if there is an appreciable delay between pressurisation and diameter measurement (a weak, visco-elastic material will creep under constant applied stress conditions, thus distorting the diameter measurement). The viscosity of the material will determine the rate of change of stress, so at higher strain rates or faster pressurisation within the vessel, a highly visco-elastic material will appear "stiffer', due to the slower strain response [30].

Dynamic compliance measurement conversely, is undertaken during pulsatile flow conditions, over a period of time. This means a more realistic response to natural conditions ie. the effect of strain rate on tissue response. In order to do pressure and diameter measurements, one has to have a suitable data capturing facility in order to accomplish this (a very fast capturing rate to generate accurate curves). Some researchers have shown compliance to be heart-rate dependent, ie. strain rate dependent [35]. Generally, at higher pulse rates (higher strain rates), the arteries show a decreased compliance. MacWilliams et al. [31] also showed that compliance varies within the pressure pulse and is hence pressure-dependent.

1.4.2 Methods of Measuring Compliance of Natural and Synthetic Vessels.

1.4.2.1 Measuring Compliance in Vitro

Numerous sources have cited the use of equipment to simulate the *in vivo* blood conditions ie. flow and pressure. There are several ways of producing a pulsatile fluid flow, and the facility to accurately recreate true conditions will depend on the design of the apparatus. There is always a difficulty associated with testing natural vessels in vitro: that is the vessel tissue degrades very quickly after being removed from the body (due to the lack of nourishment by the blood). Hence testing must be carried out as soon as possible after explant to prevent degradation (desiccation) of the material which in turn causes a change in the material properties. Also, to reproduce the physiological pressures and flow waveforms is quite a challenge because of the complexity of the vascular haemodynamics, and usually one is able to reproduce one but not the other simultaneously. Labadie et al. [36] built a perfusion system and tested canine carotid arteries as well as human saphenous vein portions, using a fluid-filled testing chamber maintained at a constant temperature and containing tissue culture medium. The pulsatile waveform was generated using a centrifugal pump and a computer-controlled gate valve which allowed accurate recreation of the pressure pulse.

Brant, Rodgers & Borovetz [37] utilised a similar system in testing canine vessels. In order to measure the diameter of the grafts during perfusion, both of these teams of researchers used a non-contact method, by using a laser-micrometer to monitor the changing diameter. The diameter was determined by the amount of light the graft blocks (see figure 1.6 below).

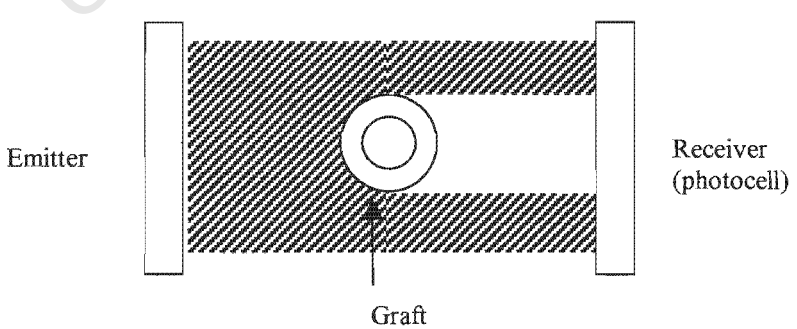

Figure 1.6: Principle of laser micrometer diameter measurement.

The advantage of this is that it is a non-contact method of measuring the diameter and hence there are no restrictive effects to the dilation of the tube and therefore no error introduced. However, some difficulty arises if the sample is submerged in water – this would have an effect on the diffraction of the beam as it would have to pass through a transparent window and then the fluid before it reaches the sample. Currently though, the effect can be compensated for by the use of custom built-electronics. Alternatively, the apparatus could be pre-calibrated by measuring rods of known diameter and calculating the percentage of error.

1.4.2.2 Reproduction of Physiological Flow and Pressure Waveforms

There have been numerous attempts to reproduce the physiological haemodynamics of the vascular tree. Law et al [38] made use of a modified peristaltic pump to create the desired flow waveforms. They claimed that the system was only able to replicate the flow waveform and not the pressure wave. Output flow rates can only be adjusted by changing the diameter of compression tubing used in the pump. A needle valve was used to adjust flow resistance in the circuit and since the pump was controlled by a stepping motor, different waveforms could be created by computer-controlling the stepper motor by means of a program. Electronic feedback was provided by monitoring the signal produced by the ultrasonic flow probe.

Other researchers have also made use of computer-controlled pumps to simulate physiological waveforms, for example Holdsworth et al [39] made use of a stepper-controlled pumping system in which a stepping motor was used to drive a reciprocating rack which operated 2 opposed cylinders. A spool valve was then used to redirect the flow in between strokes. The advantage of using this system is that it can produce negative flow, which is more difficult to achieve in a positive-displacement roller pumping system. Also, since the flow discharge of each cylinder is a discrete amount for each step of the motor, the flow waveform could be programmed easily. There was no need for a correction factor or feedback, since there was negligible attenuation and the system was shown to be stable over long periods of time. Law et al [38] also used a computer-controlled pump, but instead made use of a roller pump with a slight modification. They added an insert to allow for a more gradual release of the tube as the roller leaves the chamber, thus producing a smoother flow curve instead of the table-shaped curve normally produced by a 2-roller pump. To test the effect of shear stress on an endothelialised graft, Schima, Tsangers and Zilla [40] made use of a ventricle pumping system to pump fluid in a circulation loop. In principle, compressed air is used to drive the membrane in an artificial ventricle. Similar in operation to a heart, the use of 2 mechanical valves ensures correct flow direction. Two

Windkessel chambers were used to smooth the output pulse of the ventricle and to create the necessary back-pressure. The drawback of this system is that although the flow waveform can be quite accurately reproduced, it does not produce a suitable pressure waveform.

1.4.2.3 Measuring Compliance in Vivo

Recently, several techniques have been developed to measure compliance of natural vessels in vivo. Kidson and Abbott [17] measured the compliance of Dacron®, PTFE and vein grafts after being implanted in the femoral position of dogs. Simultaneous pressure and diameter readings were taken in situ after 2 weeks and again at 3 months to assess the change in compliance with time of implantation. To measure diameter in vivo, they used a specially built cantilever strain gauge device, which converted a diameter change into a voltage, which could then be measured. This technique was employed previously by Kidson and Baird [41] to compare the compliances of Dacron® grafts and mesh-covered umbilical grafts., and also by Murgo, Cox and Peterson [42] who measured diameter change of natural arteries only. This technique required some invasive surgery in order to expose the vessel. Another invasive technique requires the simultaneous recording of flow at 2 positions along a vessels length using ultrasound flow probes [31]. The difference in instantaneous flow rates is then used to calculate the corresponding change in cross-sectional area and hence the wall displacement. This method requires the assumption that the vessel remains at a constant length. Others have used non-invasive techniques using ultrasound images to track the change in arterial dimensions within the pressure pulse [43,44,45,46,47]. This technique makes use of the phenomenon of the different levels of sound absorption/reflection of different materials, and the interfaces between blood and vessel wall can hence be tracked.

1.4.3 Some Compliance of Natural and Synthetic Vascular Grafts.

Tables 1.2 and 1.3 below contain a collection of compliance values of synthetic grafts and natural arteries as measured by other researchers. These values will be used as reference values for the compliance values measured in this project. The variation in measured compliances for some of the vessels and grafts is notable, for example Teflon® (PTFE) grafts which have reported compliances of 1.63, 2.1 and 0.43%/100mm Hg. This indicates a broad range of compliance values, the differences in measured values most likely because of the dissimilar testing methods. Hence these values should not be taken as absolute and should be used merely used as a guide.

Table 1.2: Compliance values of natural vessels.

Ref. no.	Author	Vessel type	Animal model	Compliance measurement	Compliance (%/100mm Hg)
17	Kidson, Abbott	Femoral artery	Dog	Cantilever with strain gauge	7.4
17	"	Femoral vein	Dog	"	2.67
41	Baird, Kidson et al	Artery		"	12.7
41	"	vein graft		"	4.8
16	Kidson quoting Schultz	Artery	Human	-	2.2
61	Learoyd + Taylor	"	"	-	3.3
57	Rosset et al	Common carotid	Human	Ultrasound	6.6
57	"	Superficial fem.	"	"	1.8
28	Ballyk	Femoral artery	Human	-	5.87
28	"	Saphenous vein	"	-	4.4
18	Walden	Femoral artery	"	Cantilever with strain gauge	5.9
27	Kinley	Aorta	"	-	13.0

Table 1.3: Compliance values of synthetic grafts.

Ref. no.	Author	Graft type	Compliance measurement method	Compliance (%/100mm Hg)
17	Kidson, Abbott	Double-velour Dacron®	Cantilever with strain gauge	1.86
17	"	Expanded ptfe	"	1.63
41	Baird, Kidson et al	Dacron® graft	"	3.4
20	Giudiceandrea et al	Compliant polyurethane	Gamma imaging	12.3
20	"	ptfe	"	2.1
59	Chen et al	Porous segmented polyurethane	Video imaging	2.8 - 6.3
28	Ballyk et al. quoting work by Hastings	Dacron®	-	1.8
60	Martz et al	Microporous polyurethane-urea	Cantilever with strain gauge	4.11
60	"	Expanded ptfe	Cantilever with strain gauge	0.43

1.5 SUMMARY

One can conclude from the above literature that there are numerous factors that will determine whether a graft will remain patent or not. While grafts of natural tissue have better mechanical properties than synthetic grafts, they are not always available. Synthetic grafts have the problem of being under or over complaint and are less compatible in the body, causing thrombotic events and eventually occlusion. Improving the mechanical properties of synthetic grafts remains one of the challenges in vascular research. The following chapters describe an approach to improve the mechanical properties of an existing polyurethane graft and the development of a testing apparatus to determine the static and dynamic compliance of these grafts.

2. Modelling an Adventitially Reinforced Graft

2.1 INTRODUCTION

The adventitia is a natural composite structure, comprising mostly elastin and collagen as the mechanically significant components. Due to the different elastic properties of these components, the adventitia exhibits a distinctly non-linear behaviour (see Literature Review 1.3.2). Although there are some elastomeric materials that have similar non-linear stress-strain curves, modelling the elastic properties of the adventitia with a single synthetic material is difficult. In the natural vessel, elastin takes up the initial stress as the pressure in an artery increases. At higher blood pressures, the collagen comes into play and being much stiffer than elastin, limits further distension of the vessel wall. This chapter looks specifically at the mechanical properties of the adventitia and its elastin and collagen components, and discusses how these properties can be imitated using different materials. A mathematical approach is also described, which can be used as a qualitative tool to predict the effect on compliance of various types of reinforcement.

2.2 MECHANICAL PROPERTIES OF THE ADVENTITIA

Table 2.3 below shows some data for the mechanical properties of elastin and collagen. Fung et al [34] measured the Young's modulus of porcine thoracic, ascending and descending aortas and calculated the elastic modulus for the intima-media layer and the adventitial layer. Using bending-type experiments, he calculated that the neutral axis to be located between 30 and 35% of the total wall thickness from the intimal surface (using the assumption that the intima-media layer makes up for 50% of the total wall thickness).

Table 2.1: Properties of the aorta at different positions (Adapted from [33].)

Vessel type (porcine)	Young's modulus: intima-media	Young's modulus: adventitia	Neutral axis location (% of total wall thickness from intimal surface)
Thoracic aorta	43.25 kPa	4.7 kPa	30 %
Ascending aorta	447.5 kPa	111.9 kPa	35 %
Descending aorta	247.8 kPa	68.7 kPa	35 %

From these values we can see the differences in mechanical properties between the two layers of the aorta (in the zero stress state): the adventitia is less stiff than the intima-media layer. Also, the difference in modulus values between the different vessels indicates a difference in the composition of the vessels. The data in table 2.2 below indicates the differences in tissue composition of different arteries at different positions in the human body, while table 2.3 gives the elastic modulus and maximum elongation of elastin and collagen, as measured by Fung [34].

Table 2.2: Proportions of the various materials found in 3 artery types [33]

	Pulmonary artery	Thoracic artery	Plantar artery
Media	%	%	%
Smooth muscle	46.4 ± 7.7	33.5 ± 10.4	60.5 ± 6.5
Ground substance	17.2 ± 8.6	5.6 ± 6.7	26.4 ± 6.4
Elastin	9.0 ± 3.2	24.3 ± 7.7	1.3 ± 1.1
Collagen	27.4 ± 13.2	36.8 ± 10.2	11.9 ± 8.4
Adventitia			
Ground substance	25.1 ± 8.3	10.6 ± 10.4	24.7 ± 9.3
Fibroblasts	10.4 ± 6.1	9.4 ± 11.0	11.4 ± 2.6
Elastin	1.5 ± 1.5	2.4 ± 3.2	0
Collagen	63.0 ± 8.5	77.7 ± 14.1	63.9 ± 9.7

values in percentages

Table 2.3: Tensile properties of elastin and collagen [33]

	Young's modulus / Elastic modulus	Maximum elongation
Elastin	0.1-0.5 MPa	130 %
Collagen	3-9 GPa	2-4 %

2.2.1 The Mechanical Behaviour of Elastin

Elastin has been shown to have a variation in properties, depending on temperature and water content. Gosline and French [48] showed that elastin has the characteristics of an amorphous polymer and has a glass transition point that will vary depending on the water content and temperature at which hydration was carried out. (A glass transition temperature is the temperature at which a polymer will transform from exhibiting a brittle, linear tensile response to a plastic non-linear response). Gosline and French [48] further suggested that it is the unusual hydrophobic

nature of elastin that gives it a temperature-independent behaviour. When tested in an open system where elastin is allowed to absorb water, no glass transition occurs, since elastin swelling increases with decreasing temperature and this causes the glass transition temperature to shift. Debelle and Tamburro [49] sought to describe the function and performance of elastin based on its molecular structure and claim that the properties of elastin are complex due to the interaction with other molecules in the extracellular space. In its mature form, elastin is a very stable material that is most likely able to last the full lifetime of the host. In vivo, elastin absorbs water, despite itself already containing water of hydration. The elastin polymer is composed of several tropoelastin molecules covalently bound by cross-links. There is a lot of controversy as to the true structure of elastin, due to differing theories of polymer chemists, who view elastin as a polymer chain free to rotate and move; and protein chemists who advocate a crystallographic structure. Sherebrin, Song and Roach [32] tested the tensile properties of elastin from the thoracic aorta of dogs and sheep and plotted stress-strain curves for the longitudinal and circumferential directions, as well as the relationship of strain and Young's modulus (see figure 2.1 below). Note the non-linear stress-strain response of elastin, as well as the increase in elastic modulus with strain, in both the circumferential and longitudinal directions.

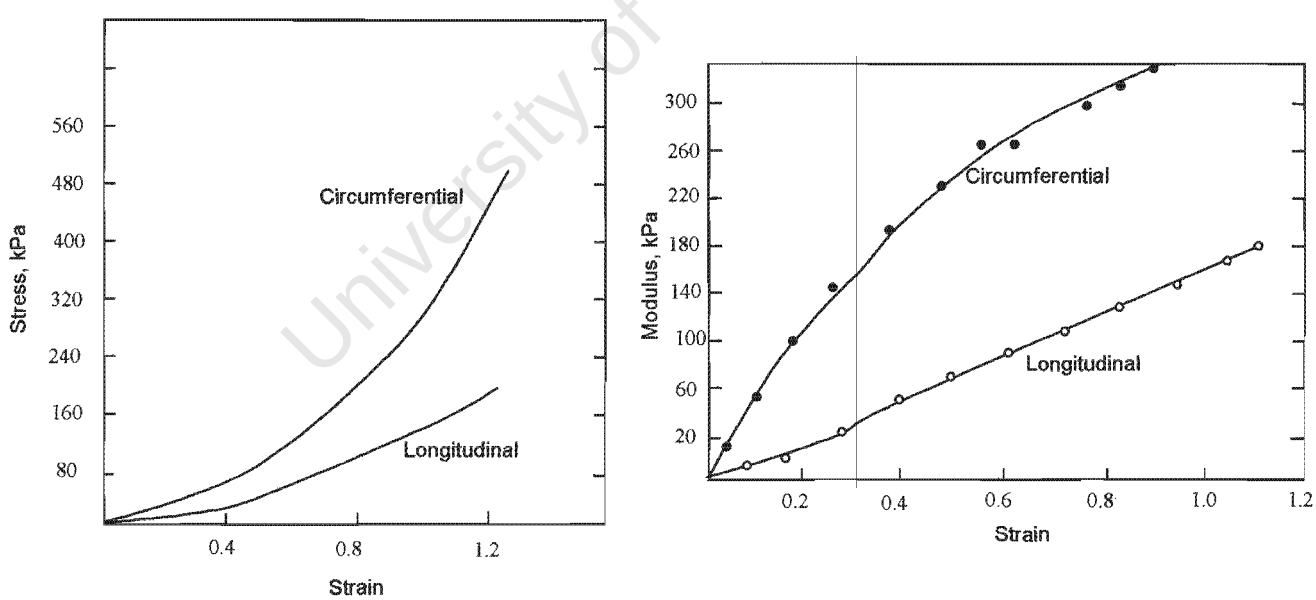

Figure 2.1: Tensile properties of elastin [32]

2.2.2 The Mechanical Behaviour of Collagen

It has been shown that in comparison with elastin, collagen is a much stiffer, less extensible material. In fact, the Young's modulus of collagen for a similar strain value is in the order of 1 x 10^4 Pa times greater than elastin. Also, the stress-strain curve for a collagen fibril is more linear in shape compared to elastin's j-shaped curve. Sasaki and Odajima [50] sought to describe the Young's modulus of collagen molecules by pulling samples of bovine achilles tendon in a tensile testing apparatus. To measure the modulus of single fibres, an x-ray diffraction technique was used to monitor the deformation of a small area of the crystal lattice (the angle of reflection of the x-ray beam is dependent on the distance between adjacent amino acids). They found the modulus to be in the region of 3 GPa. Harley et al [51] used a similar method of measuring the modulus of collagen excised from rat tail, by using the Brillouin effect (interference of incident and reflected laser light). They also studied the effect of different humidity contents on the modulus. At 0% humidity, they measured a modulus of 2.15 MPa, decreasing with an increasing water content.(1.47 MPa with 30% humidity). Fratzl, Rapp et al [52] characterised the mechanical behaviour of fibrillar rat tail collagen and described it with a 3-part curve (as shown in figure 2.2 below)

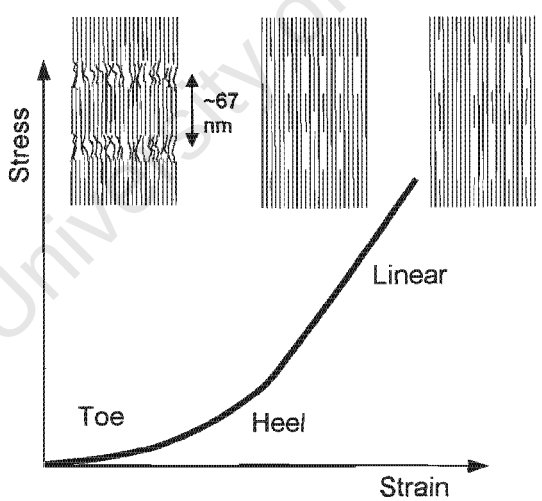

Figure 2.2: typical stress-strain curve of a rat tail tendon [52]

In region 1 (the 'toe'), low strains cause an un-crimping of the collagen fibrils at a macroscopic level. At higher strains in the heel region, molecules begin un-crimping and in the linear region there is most likely some molecular slippage as molecules glide over one another. Note the above

curve is indicative of the behaviour of a collagen tendon and hence describes the response of the collagen microstructure (ie fibrillar structure) and not the properties of a single collagen fibre.

2.3 NUMERICAL MODELS OF THE ADVENTITIA

Several researchers have attempted to model the adventitia using mathematical models. Bank et al. [53] used a modified Maxwell model to characterise the elastic properties of the human brachial artery in vivo. Essentially it uses three categories to describe the contribution of elastin, collagen and smooth muscle have to arterial mechanics. The first is elastin, acting in parallel, the second a parallel collagen component and thirdly, smooth muscle in series with collagen as the third parallel component (see figure 2.3 below).

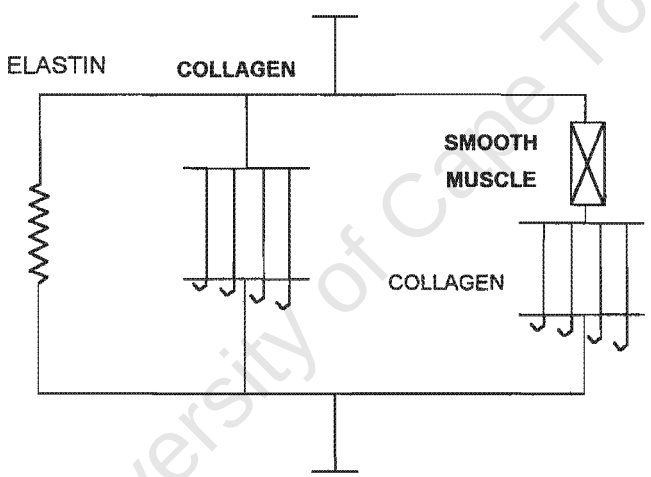

Figure 2.3: Modified Maxwell model for a human brachial artery [53].

Thus the total stresses in the wall (circumferential direction) will be a sum of the three individual components, ie.

$$\sigma_{total} = \sigma_{elastin} + \sigma_{C(P)} + \sigma_{SM+C(S)} \quad (2.1)$$

Where C(P) = collagen in parallel and C(S) = collagen in series, SM = smooth muscle. The collagen is represented by stiff springs, which only come into play at higher strains, while elastin bears all stresses at low strains. Using this approach, they calculated the elastic modulus for elastin being 0.3Mpa (3×10^6 dyne/cm^2), under the assumption that elastin remains linear-elastic at the pressures it was measured. They also found that at higher pressures (>50 mm Hg), elastin

and parallel collagen contributed a small amount to the total stress while the smooth muscle and series collagen provides the major portion of stiffness. Wuyts et al [54] used another structural model to describe the role of elastin collagen and smooth muscle in the arterial wall, although they only regarded the media as mechanically significant, the adventitia being of a 'loose' nature. The blood vessel is assumed to be a thick-walled cylinder of constant length, with a homogenous distribution of elastic membranes interconnected with smooth muscle and collagen. Other assumptions they make is that the elastin membranes within the media are linear-elastic in nature and that the vessel wall is incompressible and has a constant volume. The work of Carton et al [55], showed that elastic membranes may be treated as linear elastic in nature, but the tensile properties of pure elastin are not linear (they tested single elastin fibres in petri dishes).

2.4 MIMICKING THE MECHANICAL PROPERTIES OF THE ADVENTITIA BY USING DIFFERENT MATERIALS

Since the adventitia is comprised chiefly of two distinct materials: elastin and collagen, it makes sense to use materials with similar mechanical characteristics, in particular, the Young's modulus or elastic modulus. Since few materials are completely elastic, ie having a completely linear stress-strain curve, one cannot really apply a single value for the elastic modulus. Rather, one should apply the shape of the curve, or describe the Young's modulus as a function of strain. Below in figures 2.4 and 2.5 are tensile test graphs of two low-modulus elastane fibres (Lycra® and Dorlastan®) and two higher modulus fibres (Polyurethane and nylon), tested in the laboratory. Note in the elastane graphs the large amount of extension before break (curves on graph are shortened just before failure point). The thinner Lycra® fibre has over 600% elongation before break and the slightly thicker Dorlastan fibre has an elongation of 900%. In contrast, the stiffer polyurethane and nylon fibres break after much less extension and the stress-strain curves are more linear in shape.

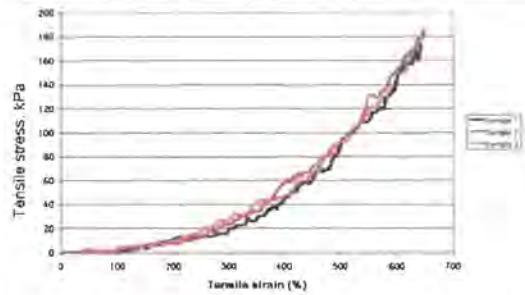

Stress-strain curves for 3 samples of 17 dtex Lycra® elastane fibre tested at 100mm/min strain rate.

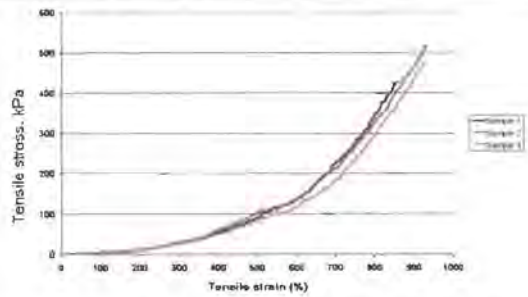

Stress-strain curves for 3 samples of 33 dtex 'Dorlastan®' elastane fibre tested at 100mm/min strain rate

Figure 2.4: Tensile test data of Lycra® and Dorlastan® fibres.

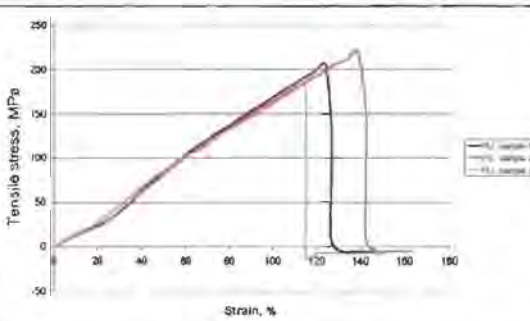

Stress-strain curves for 3 samples of 290µm polyurethane fibre tested at 100mm/min strain rate (tested in air).

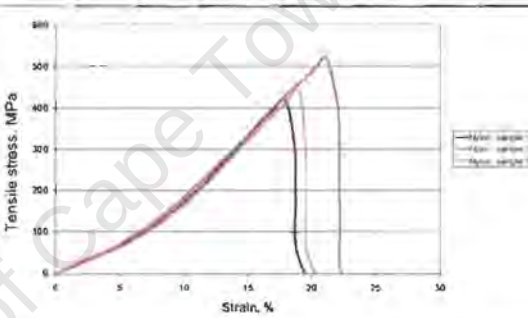

Stress-strain curves for 3 samples of 130µm nylon fibre tested at 100mm/min strain rate (tested in air).

Figure 2.5: Tensile test data of Polyurethane and nylon fibres.

2.5 PREDICTING THE EFFECT OF REINFORCING ON COMPLIANCE

2.5.1 Methods of Predicting Compliance Used by Other Researchers.

The effect of helical windings on the external surface of a cylinder may be empirically determined. Hellener, Cohn and Marom [8] showed the circumferential stiffness of a helically-wound filament graft to increase with a decrease in winding angle, where the angle is measured from the transverse axis. The obvious reason for this is that there are more windings per unit length of the graft, and hence there is more material to resist the circumferential distension. Gershon et al [9] used the following equation to predict the engineering compliance of a filament-wound graft material in the circumferential direction.

$$C_E = \frac{1}{E_h} = \frac{\cos^4 \phi}{E_L} + \frac{\sin^4 \phi}{E_T} + \frac{1}{4}\left(\frac{1}{G_{LT}} - \frac{2\nu_{LT}}{E_L}\right)\sin^2 2\phi \qquad (2.2)$$

Where ø is the winding angle measured from the circumferential direction and E, v and G the Young's modulus, Poisson's ratio and shear modulus; with the suffixes L and T representing the principal material axes (longitudinal and transverse). The medical compliance, which is equivalent to the definition in this project, is related to the engineering compliance by:

$$C_M = (2R_o / t)C_E \qquad (2.3)$$

Where t is the wall thickness of the graft and R_o is the internal radius of the graft. Plotting medical compliance as a function of wind angle, they found a maximum to exist for an angle of 45^0. Since this theory is for a single –material wound structure, it was decided to model the graft using a different approach.

2.5.2 Modelling the Graft as a Composite Filament-wound Structure

In this project, the graft was modelled as an open-ended tube reinforced with single windings of reinforcement at a certain pitch. If the reinforcement was applied under tension, there would be some initial pre-stresses introduced in the graft, but for the sake of simplification, this effect was ignored. Figure 2.6 below shows schematically how the graft was modelled. In this model, the effect of the latex inserts on the inside of the graft has also been included, since it was found that these had quite marked influence on the values obtained. As can be seen from figure 2.6, the reinforcing windings have been considered as separate rings and not as a continuous fibre reinforcement. This was for the sake of simplification of the mathematics. Realistically, this would have quite an effect on the predicted values. It is also assumed that upon pressurisation, the porous graft and fibre windings experience equal diametral strains, ie. there is no shear force at the interface of the windings and the graft. The elastic moduli of the porous graft and the fibre winding are assumed to remain linear over the applied physiological pressure range. This assumption is actually a realistic one, as proven by tensile tests conducted in the laboratory (measured elastic moduli from these tests were used in the calculations).

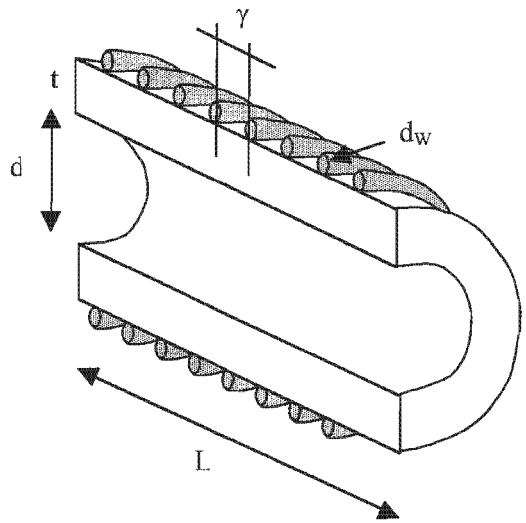

Figure 2.6: Model of the graft as a filament-wound structure.

Taking the graft in cross-section:

For equilibrium, the forces in the graft wall and the windings must equal the force projected on the inside of the graft (assuming there is no pre-tension in the windings).

Since force = pressure x area, this gives

pdl = force exerted by pressure on wall = force in graft wall + force in windings

$$pdL = 2\left(\sigma_w \cdot N \cdot \frac{\pi}{4} \cdot d_w^{\,2}\right) + 2 \cdot \sigma_g \cdot t \cdot L \tag{2.4}$$

where σ_w and σ_g are the stresses in the winding and the graft respectively, t is the thickness of the graft, N is the number of winds per length L and d_w is the diameter of the reinforcing filament.

The number of windings for a length of the graft, L can be written as: L/γ, where γ is the winding pitch, [2.4] can be written as:

$$pdL = 2\left(\sigma_w \cdot \frac{L}{\gamma} \cdot \frac{\pi}{4} \cdot d_w^{\,2}\right) + 2 \cdot \sigma_g \cdot t \cdot L \tag{2.5}$$

simplifying this we get:

$$pd = \left(\sigma_w \cdot \frac{\pi}{2\gamma} \cdot d_w^{2}\right) + 2 \cdot \sigma_g \cdot t \tag{2.6}$$

Now, assuming that when pressurised, the strain in the graft is equal to the strain in the windings, ie. there is no shearing between the winding and the graft outer surface:

$$\text{strain in windings} = \text{circumferential strain in graft wall}$$

$$\varepsilon_w = \frac{\sigma_w}{E_w} = \frac{1}{E_g}\left[\sigma_{gc} - \upsilon \cdot \sigma_{gl}\right] \tag{2.7}$$

Where E_g and E_w are the Young's moduli of the winding and porous graft respectively and ν is the Poisson's ratio for the graft (the ratio of axial to transverse strain). The value used for the porous graft was 0.3, calculated from mechanical tests by Yeoman [56]. The suffixes *gc* and *gl* denote the graft stresses in the circumferential and longitudinal directions.

σ_{gl} can be found from the equation for longitudinal stress in a cylinder:

$$\sigma_{gl} = \frac{pd}{4t} \tag{2.8}$$

where p is the internal pressure of the graft and d the internal diameter, t being the wall thickness. (2.7) then becomes:

$$\sigma_w = \frac{E_w}{E_g}\left[\sigma_{gc} - \upsilon \cdot \frac{pd}{4t}\right] \tag{2.9}$$

Substituting (2.9) into (2.6):

$$pd = \left(\frac{\pi}{2\gamma} \cdot d_w^{\,2}\right)\left[\frac{E_w}{E_g}\left(\sigma_{gc} - \upsilon\frac{pd}{4t}\right)\right] + 2 \cdot \sigma_{gc} \cdot t \tag{2.10}$$

solving for σ_{gc} we get:

$$\sigma_{gc} = \left[\frac{pd}{\left(\frac{E_w}{E_g} \cdot \frac{\pi}{2\gamma} \cdot d_w^{\,2}\right)} + \upsilon\frac{pd}{4t}\right] \Bigg/ \left[1 + \frac{2t}{\left(\frac{E_w}{E_g} \cdot \frac{\pi}{2\gamma} \cdot d_w^{\,2}\right)}\right] \tag{2.11}$$

Which can be simplified by substituting a constant 'a' for the term: $\left(\frac{E_w}{E_g}\cdot\frac{\pi}{2\gamma}\cdot d_w^{\,2}\right)$

Thus (2.11) becomes

$$\sigma_{gc}=\frac{pd}{2t+a}+\upsilon\cdot\left(\frac{pd}{4t}\right)\cdot\left(\frac{a}{2t+a}\right) \tag{2.12}$$

For any given internal pressure p one can then calculate a value for σ_{gc} and then substitute back into equation (2.7) to solve for σ_w.

One can then find the resulting strain in the winding, which will equal the strain in the graft from the relationship (assuming equal strains in the graft and the winding):

$$\varepsilon_w=\frac{\sigma_w}{E_w} \tag{2.13}$$

And from this, one can calculate the compliance of the reinforced graft.

$$\text{circumferential strain}=\varepsilon=\frac{\Delta\text{circumference}}{\text{original circumference}}=\frac{\Delta d}{d_o} \tag{2.14}$$

Therefore:

$$\Delta d=\varepsilon_w\cdot d_o$$

And compliance is then:

$$\%C/100mmHg=\frac{\Delta d}{d_o}\cdot 100\cdot\frac{1}{\Delta P}\cdot 100mmHg \tag{2.15}$$

(Remembering to use the original internal diameter when calculating the compliance).

Alternatively, one could calculate compliance as a function of all the variables using one equation:

$$\%C/100mm\,Hg = \frac{1334000}{E_g}\left[\frac{\frac{d_g}{\frac{E_w}{E_g}\cdot\frac{\pi}{2\gamma}\cdot d_w{}^2}+\upsilon\frac{d_g}{4t_g}}{1+\frac{2t_g}{\frac{E_w}{E_g}\cdot\frac{\pi}{2\gamma}\cdot d_w{}^2}}-0.1.\frac{d_g}{t_g}\right] \tag{2.16}$$

or more simply:

$$\%C/100mmHg = \frac{1334000}{E_g}\left[\frac{d_g}{a+2t_g}+\upsilon\left(\frac{d_g}{4t_g}\right)\cdot\left(\frac{a}{a+2t_g}\right)-0.1\frac{d_g}{t_g}\right] \tag{2.17}$$

Where: E_w and E_g are the Young's moduli of the winding fibre and graft material respectively, as measured from data recorded from tests on the Instron tensile tester (see 3.1).γ is the winding pitch (in mm), d_g is the internal diameter of the graft (in mm), t_g is the thickness of the graft wall (in mm), d_w is the diameter of the reinforcing fibre (in mm) and ν is Poisson's ratio. The factor 'a' is the same used previously to simplify equation (2.11).

Note the compliance calculated from equation (2.17) is independent of pressure (there is no pressure term). This means that the compliance of the graft is the same irrespective of internal pressure. The reason for this is that the elastic moduli of the reinforcing and graft are assumed to remain constant. In reality, they will more likely exhibit a non-linear stress response and the graft will decrease in compliance with increasing pressure. One could substitute a non-linear function for the elastic modulus, and since this would mean that the modulus would be pressure-dependent, then the predicted compliance would be pressure-dependent also.

2.6 SUMMARY

While it is necessary to be able to predict the effect a certain type of reinforcement will have on the mechanical properties of graft, these mathematical findings will always need to be confirmed empirically. By making certain assumptions to simplify calculations, one cannot accurately predict what the end compliance will be, and therefore these equations can only be used as a qualitative tool. The non-linearity of the polymer materials used in the porous graft and reinforcement will cause compliance to be non-linear, especially at higher pressures. When calculating a theoretical compliance it was assumed that for the strains involved, the modulus of the graft materials remains constant.

3. Materials and Methods I: Manufacturing the Adventitially Reinforced Graft

The grafts tested in this project were essentially composite in nature, comprised of a porous inner tube (media) and a type of external reinforcing (adventitia). The porous salt-cast and bead-cast grafts were manufactured first and then reinforced externally with the fibre materials using an automated winding apparatus.

3.1 MATERIALS

3.1.1 The Porous Media

The porous media was manufactured from a medical-grade segmented polyurethane, supplied by Medtronic Inc. USA.

3.1.2 The Synthetic Adventitia

Since the natural adventitia is comprised of two distinct fibrous elements (collagen and elastin), it was decided to imitate the mechanical properties of this layer by using two different types of fibres with different elastic moduli. Namely, a stiff, high modulus fibre to imitate the non-extendable collagen and a weaker, low modulus fibre to imitate the elastin. For this purpose, a fine elastic monofilament, a 33 dtex elastane fibre (Dorlastan®) from Bayer was used to simulate the elastin and a stiff nylon monofilament was used for the collagen. An extruded polyurethane monofilament was also used to reinforce grafts, this fibre having a lower elastic modulus than the nylon fibre. A stiff polyester multifilament (shown in figure 3.1 below) was also considered to replicate the collagen, but was discarded because of the large diameter and associated difficulty in applying it to the exterior of the graft. Two other elastane filaments were considered: a 17 dtex Lycra® fibre from Dupont and a 22 dtex Dorlastan® fibre from Bayer. The larger 33 dtex fibre was chosen however because it was a larger diameter and easier to work with. The polyurethane and nylon fibres were both comparatively much thicker than the elastane fibre. The stiff fibre reinforcement also gives the graft some kink and crush-resistance, which is important if the graft is to be implanted over a joint where bending occurs.

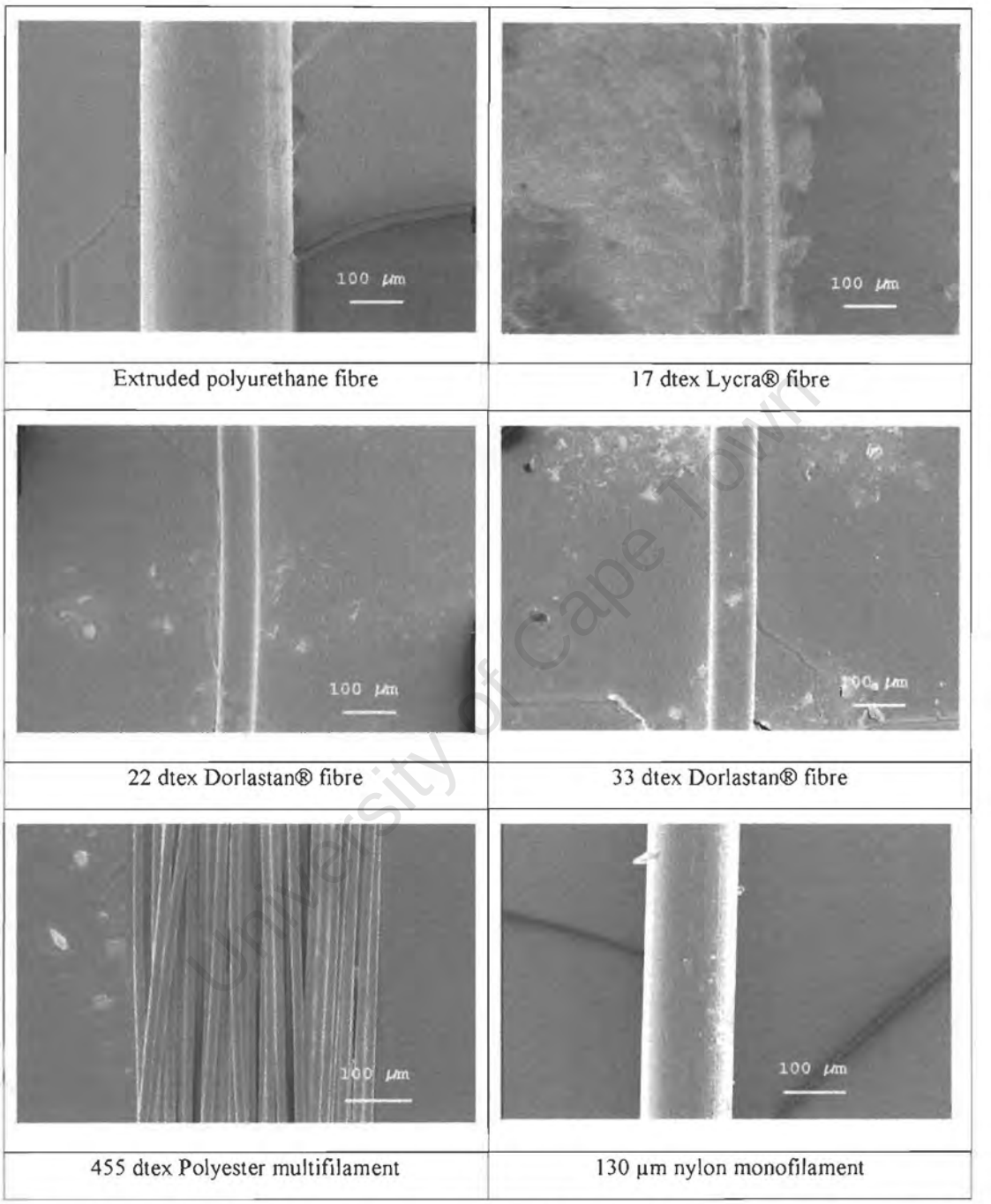

Extruded polyurethane fibre	17 dtex Lycra® fibre
22 dtex Dorlastan® fibre	33 dtex Dorlastan® fibre
455 dtex Polyester multifilament	130 µm nylon monofilament

Figure 3.1: Scanning electron micrographs of the fibres used to manufacture the synthetic adventitia

Table 3.1: Linear densities and diameters of the monofilament fibres

Fibre (monofilament)	dtex/ linear density	Measured diameter (μm)
Polyurethane	541g/10000m (est.)	288.7
17 dtex Lycra®	17g/10000m	48.7
22 dtex Dorlastan®	22 g/10000m	67.9
33 dtex Dorlastan®	33 g/10000m	82.6
nylon	140g/10000m (est.)	130.0

3.2 MANUFACTURING TECHNIQUES

3.2.1 The Porous Graft (Media)

Grafts with two different types of porosities were produced for testing: grafts manufactured by a rolling process with a salt as the pore-former, and grafts manufactured by a casting process with gelatin microspheres as the pore former.

3.2.1.1 Rolled Salt-cast Grafts

A paste of polyurethane solution plus salt (sodium hydrogen carbonate) was prepared. The polyurethane solution itself was a mixture of the pure polymer and a solvent, in this case NMP (1-Methyl-2-Pyrrolidinone) in a ratio of 20% polymer and 80% solvent. The salt was dried and sieved and particles in a size range of 90-106 μm were used. The paste was mixed in a ratio of 2:1 salt:solution which gave a salt:polymer ratio of 10:1. Once the paste was prepared, it was placed inside a large disposable-type syringe. Six millimetre diameter stainless steel mandrels of length ±200mm were prepared with 2 ring –shaped Teflon® spacers at each end (these are required to give an even wall thickness of 1mm during the rolling process). The paste was then squeezed from the syringe onto the mandrel and the mandrel rolled back and forth to distribute the paste evenly around the diameter. The rolled grafts were then placed in an incubator at 37 deg. C and 100% humidity for ±12 hrs to cure (curing happens by a precipitation process, whereby, the solvent in the polymer paste is replaced by a non-solvent, in this case water). After incubation, the grafts were then placed in cold water and cured for a further 2 days, changing the water 3-4 times

in this period. The washing process dissolves all the salt particles in the paste, leaving a non-defined sponge-like microstructure. The cured grafts were then dried in air and cut to the desired length when needed for testing. The porous structure is shown in figure 3.2 below.

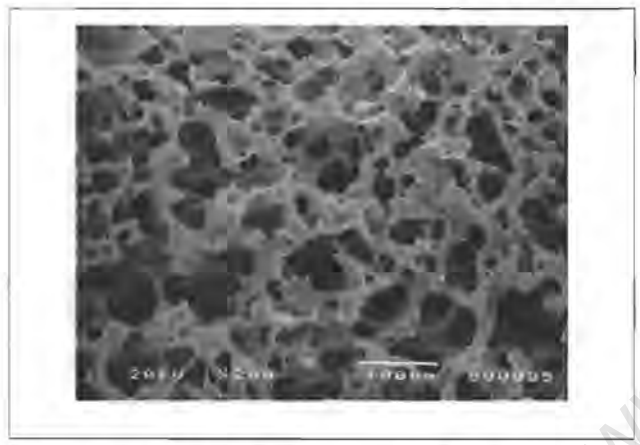

Figure 3.2: Scanning electron micrograph of the salt-cast structure

3.2.1.2 Bead-cast Grafts

With this method, grafts were formed by casting the NMP-polymer solution into an annular mould. The mould was pre-filled with 100μm gelatin microspheres, the pore-forming agent. The moulding device consisted of a manifold, into which glass tubes were inserted to form the outer graft surface. Down the middle of each of these, a stainless-steel mandrel that forms the inner diameter of the graft, was inserted. By the simultaneous application of a vacuum to the bottom manifold and pressurised air to the top of the mould, the solution was drawn down the length of the tubular mould. After the solution has travelled the full length of the mould, the mould-mandrel-graft assembly was removed from the casting manifold and placed in pure ethanol to cure (the reason for this is that the ethanol prevented the gelatin beads from swelling while still curing the polymer). Subsequently, the gelatin microspheres were extracted by placing the grafts in hot water (up to ±60 deg. C). Thus the end product was a porous tubular article, of length approximately 160 mm long). The grafts were then dried and were ready for further processing. A picture of the casting apparatus and micrograph of the final porous structure is shown in figure 3.3 and 3.4 below. The bead-cast grafts had a final diameter of 7.5mm cast from 8mm glass tubes – this could be the result of some shrinkage during extraction of the gelatin microspheres when the graft is heated. In comparison, the salt-cast grafts had a diameter of 8.3mm. When calculating compliance, this difference in graft size was corrected for.

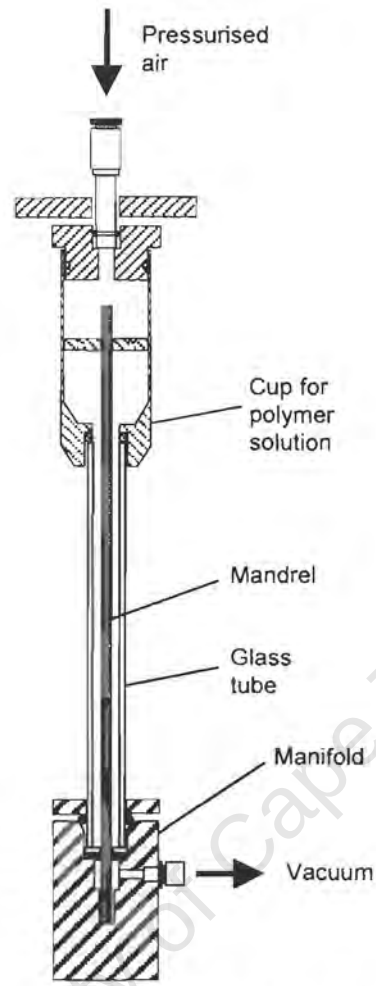

Figure 3.3: Schematic drawing of a cross-section through the vacuum-pressure casting device.

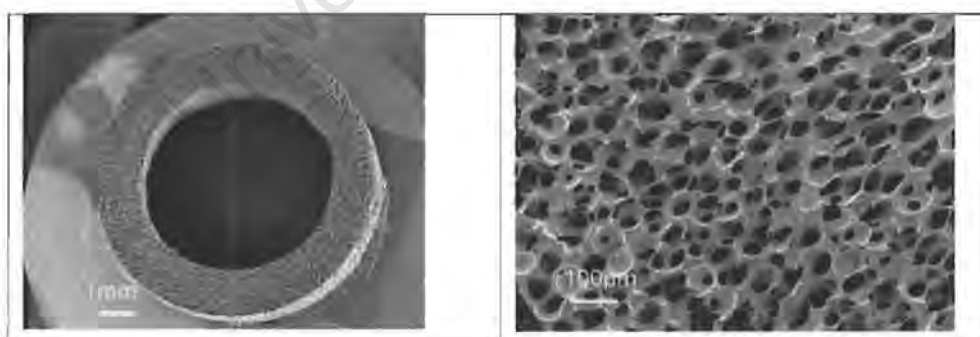

Cross section through vacuum-pressure cast graft	Detail of the gelatin-microsphere-cast structure

Figure 3.4: Detail of the cross-section of a gelatin-microsphere (bead-cast) graft structure, inside graft diameter: 6mm.

3.2.2 Manufacturing the Artificial Adventitia

The adventitial fibres were applied by helical winding and bonded to the external surface of the graft with polyurethane solution. For this purpose, an automated winding apparatus was designed and built. The porous grafts were inserted over a mandrel and the mandrel then positioned horizontally, with one end locating in a collett which was driven by a micro-stepping motor and the other end supported in a spring-loaded live centre (a free-rotating centralising device). A second micro-stepping motor controlled the motion of the applicator device, essentially a syringe filled with polyurethane solution through which the fibre passed before being applied to the graft surface. The applicator was driven by a lead screw parallel to the axis of the mandrel (see figure 3.5 below). By separately controlling the speed of rotation of the mandrel and the movement of the applicator, one could produce various winding patterns on the surface of the graft. This was achieved by custom-written software by which one could program the winding speed, winding angle (and hence wind gap), and also the number of traverses. Thus, the mechanical properties of the adventitial layer could be quite easily controlled. The winding angle, which also determined the gap between adjacent fibres, determined the end flexibility of a graft. As the winding gap decreases, the kink resistance of the graft improves but because there are more windings per length, but the radial compliance decreases.

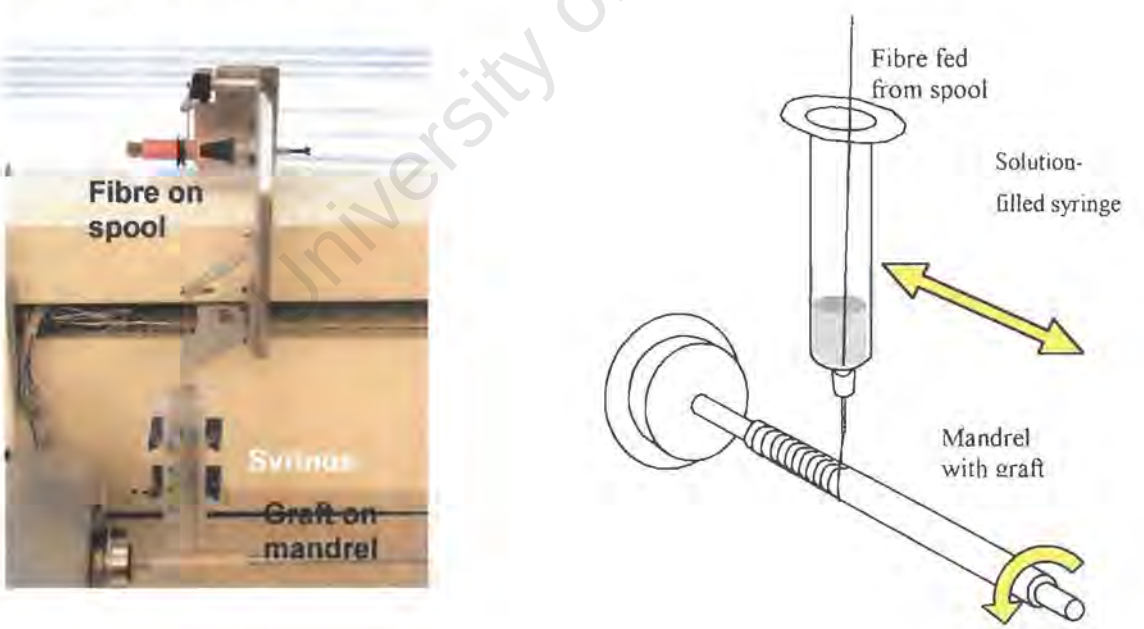

Figure 3.5: Detail of the winding apparatus used to reinforce the grafts.

Initially there were problems finding the correct polyurethane solution which would not destroy the fibre during winding (some solvents of the polyurethane also happened to be solvents of the polymer fibres as well). It was decided to use a solution with THF (tetrahydrafuran) as the solvent. A 10% mixture of polymer to solvent (by weight) was prepared. This solvent did not dissolve the Dorlastan® or nylon fibres. Importantly, the viscosity of this solution was low enough not to cause too much friction on the fibre as it passed through the solution. A viscous solution results in the fibre 'cutting' into the graft because of too much tension. Some electron micrographs of sections of the reinforced grafts are shown in figure 3.6 below.

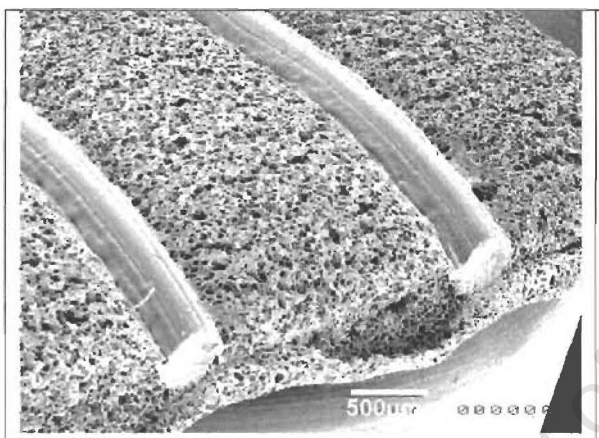

Salt-cast graft reinforced with 290µm polyurethane fibre at 2.5mm pitch

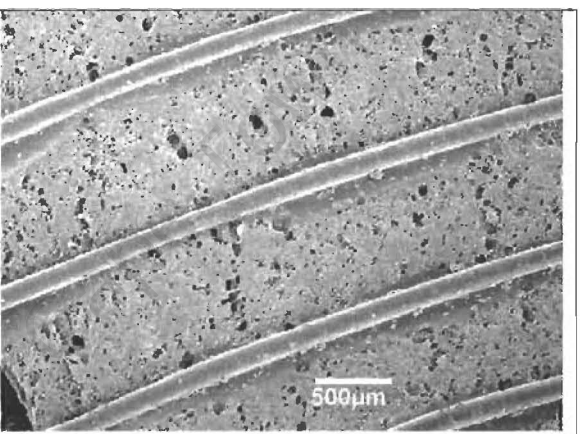

Salt-cast graft reinforced with 130µm nylon monofilament at 1mm pitch.

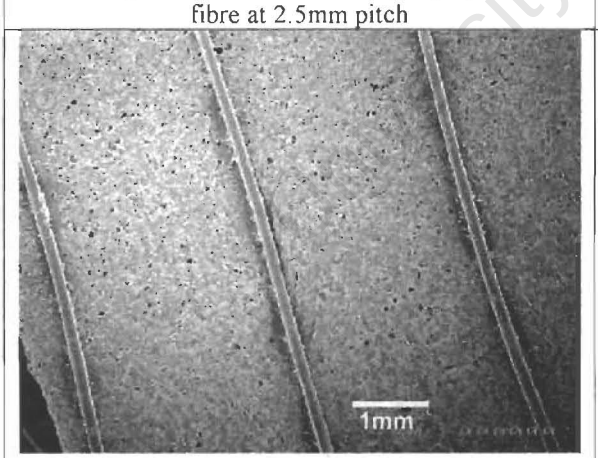

Salt-cast graft reinforced with 130µm nylon monofilament at 2.5mm pitch.

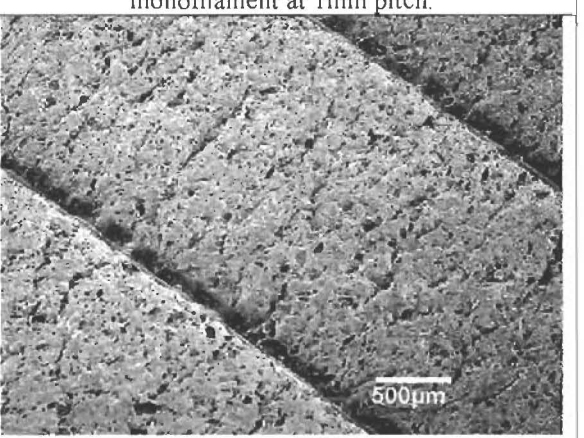

Salt-cast graft reinforced with 33dtex (80µm) Dorlastan® at 2.5mm pitch (single wrapping)

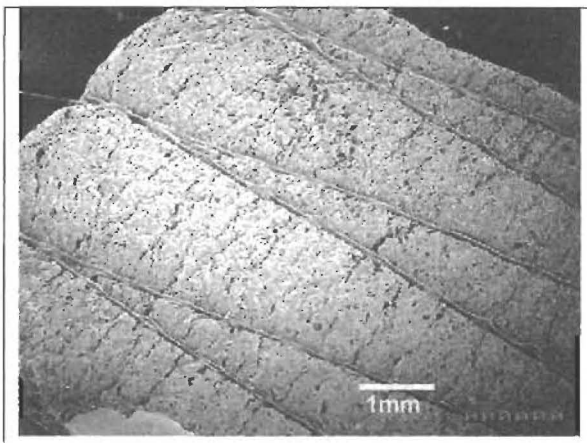

Salt-cast graft reinforced with 33dtex (80μm) Dorlastan® at 2.5mm pitch (double wrapping)

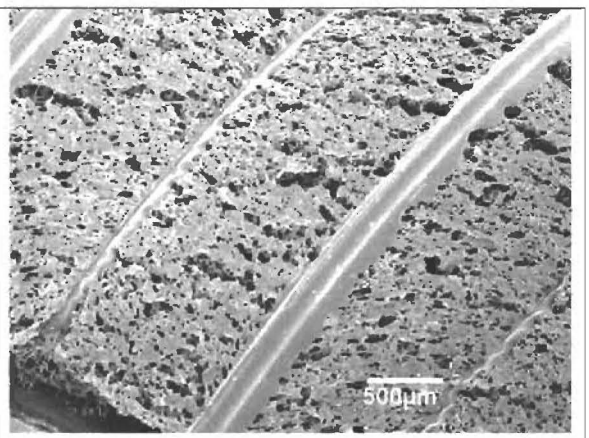

Salt-cast graft reinforced with 33dtex (80μm) Dorlastan® at 2.5mm pitch (single wrapping) and 130μm nylon at 2.5mm pitch.

Figure 3.6: Scanning electron micrographs of the exterior surfaces of the reinforced porous grafts.

After being wrapped with the particular reinforcing, the grafts were allowed to dry (the THF solvent in the polyurethane solution requires evaporation in order for the polyurethane to cure). Once dry the grafts were then ready for testing.

4. Materials and Methods II: Testing Materials and Methods

The mechanical properties of both the porous graft materials and the reinforcing materials were first determined on a tensile testing apparatus. Grafts manufactured from these materials were then tested on the custom-built compliance testing apparatus. Details of the testing apparatus and methods are described in the following pages. Methods of graft manufacture are contained in the chapter 4. Where applicable, the grafts and their constituent materials were tested in accordance with recommendations in the AAMI (Association for the advancement of Medical Instrumentation) standards for testing of vascular prostheses [135].

4.1 UNIAXIAL TENSILE TESTING

Tensile testing is a proven method of providing mechanical data on a particular material. From a stress-strain curve generated by the test, one can determine several properties of the material (see figure 4.1 below). The slope of the 'A' region of the curve will give the elastic modulus of the material, or the stiffness. In a completely elastic material, any deformation the material undergoes is entirely reversible, that is to say that if the stress were removed, the test specimen would return to its original state.

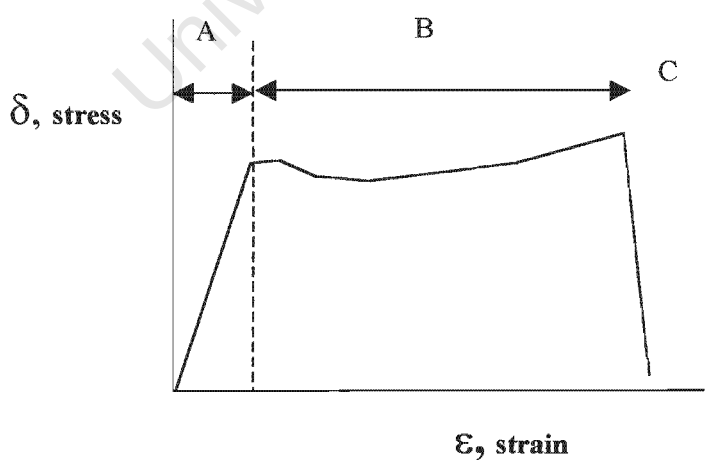

Figure 4.1: Example of a typical stress-strain curve for a semi-crystalline amorphous polymer.

At the dotted line, where there is an inflection in the curve, the material yields, or the secondary bonds between adjacent chain molecules are overcome and the material begins to undergo irreversible plastic deformation (or 'necking'). In polymers, the long chain molecules begin unravelling and the specimen will elongate. At 'C' the material reaches its ultimate tensile strength and the specimen breaks as the primary covalent bonds are broken. In polymers, the shape of the stress-strain curve is quite temperature-dependent: at lower temperatures, a polymer will exhibit a more brittle nature and might show little or no plastic deformation before breaking. At higher temperatures, the activation energy required to break the secondary bonds between molecules is lower and the material will yield at a lower stress. The mechanical properties of a plastic are determined by the length and shape of the long chain molecules found in them, as well as the type of secondary bonds between adjacent molecules. For instance, a cross-linked rubber has strong secondary bonds between chains that allow the material to return to its original shape after being stretched (see figure 4.2 below). When determining the properties of a composite structure, it is important to consider the mechanical properties of the constituent materials, as well as their interaction between one another and their arrangement within the structure.

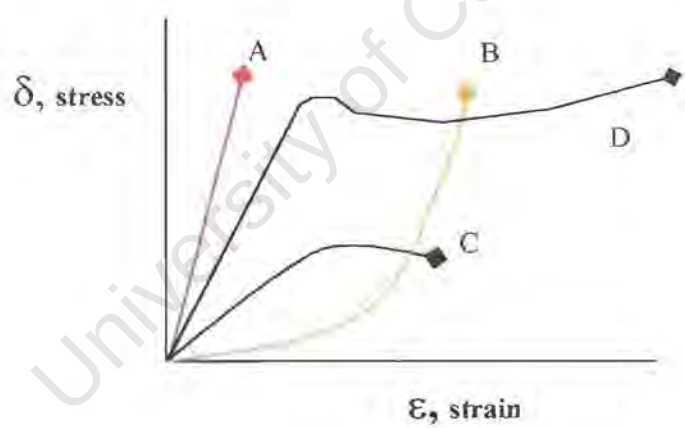

Figure 4.2: Some typical stress strain curves for some polymers: A – hard brittle polymer, B – cross-linked rubber, C – soft thermoplastic polymer, D- semi-crystalline polymer.

In figure 4.3 below is a tensile test graph showing the stress response of 3 of the polymer fibres tested in this project: a nylon fibre, a polyurethane fibre and an elastane fibre (Dorlastan®).

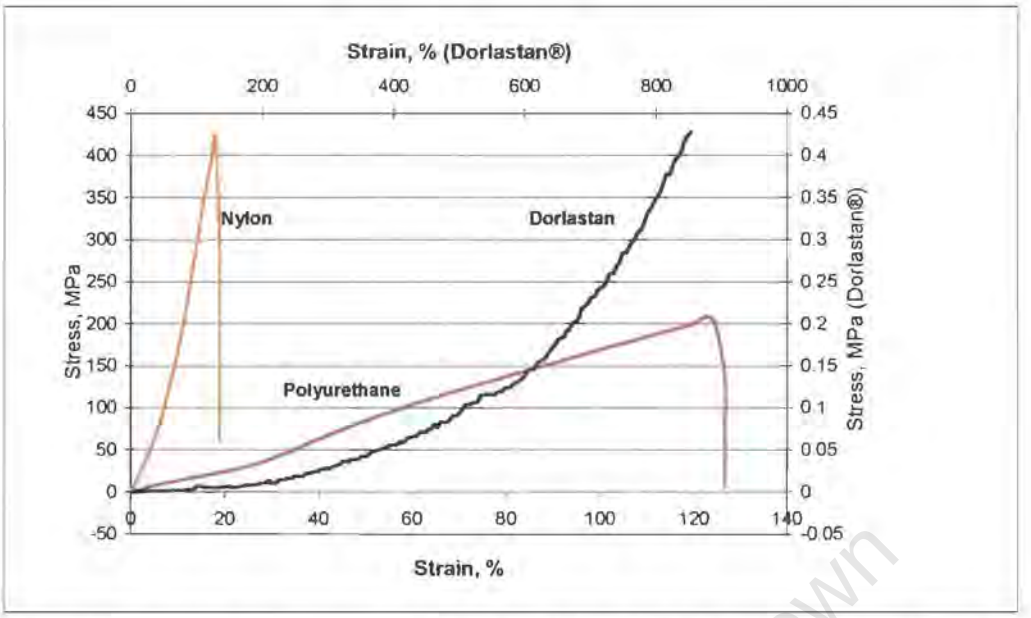

Figure 4.3: Stress-strain curves of 3 polymer fibres tested: nylon, polyurethane and Dorlastan®.

The terms "visco-elasticity" and "visco-plasticity" are used to describe the degree of recoverability of a material when it is stressed and then the stress removed. For example a visco-elastic material will take more time to return to its original dimensions than an elastic material. A visco-plastic material will only partly recover some of the deformation induced by an applied stress. These phenomena are exhibited by the response of a material to stress. The energy losses (hysteresis) due to visco-elasticity or visco-plasticity are determined by first loading the material and then unloading it. The amount of hysteresis is determined by the area enclosed by the two curves (see figure 4.4 below). The term "creep" refers to the gradual deformation of a material under a constantly applied stress. This is an important consideration for materials under cyclic loading conditions (an oscillating stress), and is particularly applicable to vascular graft materials, which undergo many such cycles. Should the graft be made of a visco-elastic or visco-plastic material, the diameter would increase gradually over time until the graft no longer functions properly.

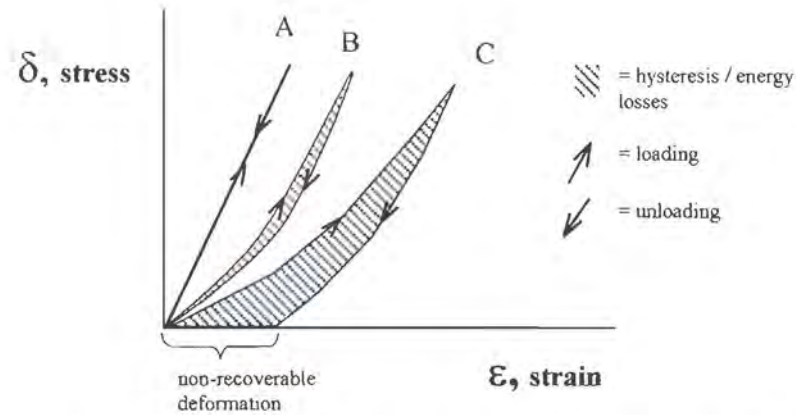

Figure 4.4: Loading-unloading curves for: A: a completely elastic material, B: a visco-elastic material with low hysteresis losses and C: a visco-plastic material with higher hysteresis losses and only partial dimensional recovery.

4.1.1 Tensile Testing Equipment

Testing was conducted on an *Instron* tensile testing machine, model 5544 using a load cell of 500N. The test data was recorded on a PC running the Merlin controller software. A removeable water-bath, fitted to the testing table of the Instron, allowed for testing at elevated temperatures (37 deg. C).

Figure 4.5: Model 5544 Instron tensile tester
(Shown here with water bath for testing at elevated temperatures)

4.1.2 Samples and Specimen Dimensions

The different material components of the grafts were tested individually to assess their stress-strain characteristics. Samples of the porous polyurethane, which formed the body of the graft as well as the reinforcing agents, were tested.

4.1.2.1 Porous Materials (grafts)

Rectangular samples were cut from porous polyurethane salt-cast and bead-cast grafts (see chapter 4: Graft manufacture). Since the grafts were tubular, samples in the longitudinal and circumferential direction were tested to ascertain any difference in tensile strength due to direction. For the porous graft samples, strips of 10mm wide were cut in the longitudinal and circumferential directions of the grafts, such that the gauge length was 10mm in all tests. The gauge length in this case is defined as the distance between the testing jaws.

4.1.2.2 Fibres

Several reinforcing fibres were evaluated: a solid polyurethane monofilament, (290μm diameter), 3 types of elastic monofilament (a 17dtex/48μm Lycra® filament from Dupont and 2 Dorlastan® fibres from Bayer, being 22dtex/67μm and 33 dtex/82μm. respectively. A stiff nylon monofilament fibre was also tested. For the fibre samples, specimens of equal length were tested, using a gauge length of 35mm in all the tests.

4.1.3 Tensile Test Method

Samples were secured firmly in the jaws of the tensile tester. Testing was performed at a strain rate of 100mm/min for all porous graft and fibre samples, as prescribed by the AAMI standards. Realistically, the grafts would experience a higher strain rate (closer to 350mm/min when tested at 120 bpm). Also, it should be pointed out that although the fibres were tested up to high strains, once applied to the graft they would most likely experience strains of at most 20%. The software used to capture the data from the Instron made use of a constant volume assumption in order to calculate true stress and true strain. Therefore, measurements of the specimen were taken before testing, ie. diameter, width, gauge length etc. A constant volume assumption means that the Poisson's ratio is 0.5(this means that the ratio of longitudinal strain:transverse strain for any given

stress is 0.5). While this assumption is acceptable for the solid materials (ie. the fibres), it is not accurate for the porous graft materials which will have a Poisson's ratio closer to 0.3 [56]. The data, in a RAW ASCII text format was then manipulated using Excel spreadsheet software. Where possible, all tests were conducted in water at 37 deg. C to simulate physiological temperature, the exception being the elastane fibres which were found to be too fine to be clamped in the test jaws fitted with the water bath. These tests were instead performed in air at room temperature with another set of jaws.

4.2 COMPLIANCE TESTING

In order to establish the compliance of vascular prostheses, it is necessary to have an apparatus capable of applying an internal pressure to the graft and a means of measuring the change in the external diameter of the graft associated with the pressure change. There are two ways of establishing compliance: Dynamically and statically. In this project, both methods have been employed to fully characterise the properties of the grafts. It should be noted that results compared in the literature might differ, due to the differing methods of compliance testing (ie the type of apparatus used, the method of measuring the diameter etc.). For the compliance measurement in this project, a testing apparatus was specifically designed and built.

4.2.1 AAMI Requirements for Compliance Testing

The following are some of the requirements and recommendations for the compliance testing apparatus and procedure.

4.2.1.1 Testing Apparatus

The AAMI standards specify an apparatus that is capable of producing a reproducible pressure pulse similar to physiological conditions (in the case of dynamic testing), to the interior of the prosthesis under constant length (isometric) or constant axial tension (isotonic) conditions. Also, the testing should be carried out at 37 deg. C. If a balloon is to be inserted into the graft to prevent leakage, then it should have a diameter at 120mm Hg of at least 1.05 times the unpressurized internal diameter of the graft. The apparatus should also include a means of measuring pressure to an accuracy of 2mm Hg, as well as a diameter-measuring device capable of measuring to an

accuracy of ±0.02mm. The device should also be able to take diameter measurements at various positions along the prosthesis length.

4.2.1.2 Testing Procedure

The length of the test specimen should not be less than ten times the unpressurized diameter. If isotonic testing is performed (constant tension), a longitudinal tension of between 30-60 g should be applied to the specimen. The testing rate should be between 50 and 70 beats per minute, and to assess the frictional effects of the system, testing should be performed at 3 different pressure ranges: 50-90, 80-120 and 110-150 mm Hg (in the case of dynamic testing).

4.2.1.3 Expression of Results

Once the diameter change has been calculated or measured, the compliance of the specimen should be expressed as a percentage change in diameter per 100 mm Hg (%/100mm Hg).

4.2.2 Design and Set-up of the Compliance Testing Apparatus

In this project, it was necessary test the grafts both statically (increasing the internal pressure incrementally), and dynamically, whereby the grafts were subjected to an internal pulsatile pressure. Thus it was necessary to have an apparatus that could be used both for static and dynamic testing, and also be capable of simulating a realistic physiological environment (in particular temperature, which should be similar to physiological temperature). For dynamic testing it was necessary to have a flow circuit which would reproduce a sharp systolic increase in pressure, as well as allowing adjustment of the diastolic and systolic pressures and the number of pulses per minute. Two different types of pumping units were evaluated to reproduce this pulsatile flow. Other components in the flow circuit are also discussed below. (See figure 4.13 for details of the flow circuit).

4.2.2.1 Pumping Units

a.) Ventricle–pumping Device:

A ventricle-pumping system, similar to the one used by Schima, Tsangaris and Zilla [40], was evaluated. Two Windkessel chambers were also used for pulse smoothing and to create the necessary back -pressure. While this apparatus provided quite a good flow waveform, it was more difficult to reproduce the desired pressure curve. The advantage of this device was that it was possible to adjust the pulse rate, the systolic time as well as the rate of pressure increase on the systolic curve. The apparatus made use of a type of artificial heart, which contained 2 chambers separated by a flexible membrane, one air-filled into which the compressed air from the driving unit was pulsed, the other water-filled and forming part of the fluid circuit. Two mechanical valves were used to ensure uni-directional flow (see figure 4.6 below). It was found to be important to maintain an adequate vertical geometry, and to have some head of pressure to ensure the proper opening and closing of the inlet valve on the heart. There was some concern that fluttering of either of these valves might also cause some irregularities in the flow.

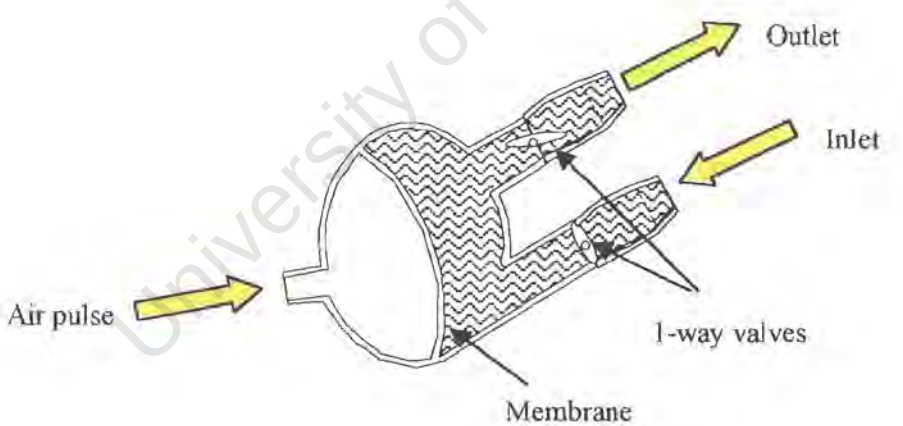

Figure 4.6: schematic drawing of the ventricle pump

See figure 4.8 for an example of the pressure waveform achieved with the ventricle pump.

b.) Modified Peristaltic Roller Pump

After attempting to produce a suitable pressure waveform with the ventricle pumping device, a Sarns peristaltic roller pump was connected to the circuit to see if a better waveform could be achieved. After some testing and the addition of an insert in the pumping chamber, an acceptable pressure curve was obtained (see figure 4.7 below). It was found that the shape and amplitude of the curve was quite dependent of the speed of rotation of the pump as well as the pinch gap of the rollers (see "Reproduction of the pulsatile waveform"). Unfortunately, at low revolutions, the shape of the pressure wave deteriorated, (see Addendum I, graph 'a' p123), hence testing was performed at 60 rpm which gave a pulse rate of 120 beats per minute (since there are 2 rollers and therefore 2 pulses per revolution). The front portion of the insert created a sharp increase in pressure, similar to a systolic pulse, while the tapered end of the insert gave a more gradual decrease in pressure back down to the diastolic value. Graph 'b' of figure 4.8 below is an example of the pressure waveform achieved using the roller pumping device.

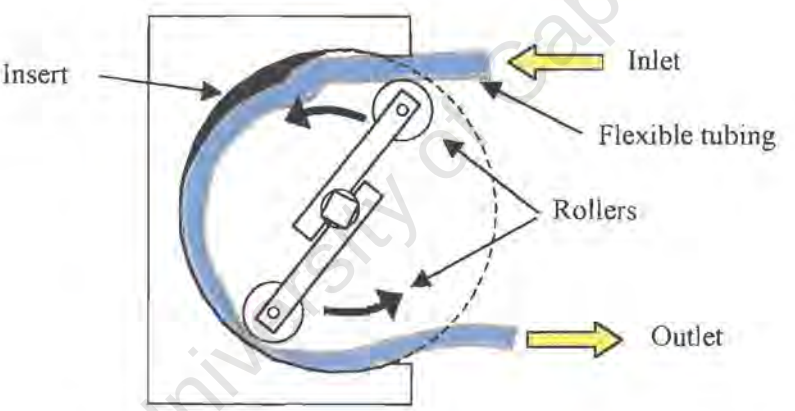

Figure 4.7: Schematic drawing of the modified roller pump

Below are two examples of the pressure and flow waveforms achieved with the ventricle pumping device and the roller pump. The modified roller pump was chosen as the preferred system because the pressure waveform it produced was closer to a physiological blood pressure waveform.

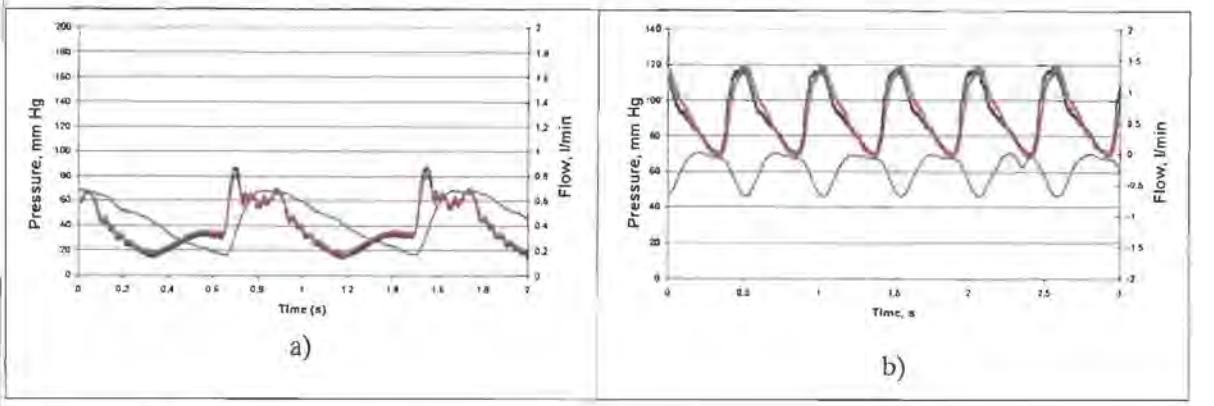

Figure 4.8: Two examples of pressure and flow waveforms achieved with the two types of driving units; a: ventricle pump, b: roller pump

Proximal pressure
Distal pressure
Flow

4.2.2.2 The Testing Chamber

A specialised testing chamber was purpose designed and built (see figure 4.9 and 4.10 below). A removable specimen holder allowed for easy change of specimens. Two different size nozzles allowed for the testing of different diameter grafts (namely 4 and 6mm internal diameter grafts). Since it was necessary to test at 37^0 C, the chamber needed to be able to contain a fluid that could be temperature-controlled. Thus the perspex-sided chamber enclosed an aluminum heat exchanger at the base (G), through which heated water was pumped from a Neslab RTE-300 water cooler/heater. This ensured that the water of the chamber was not disturbed during testing, which would possibly cause errors in the diameter measurement of the grafts. The left end of the specimen holder was adjustable by means of a nut and a lead screw (A), while the fitting at the right end of the holder was free to 'float' axially, or be clamped during testing. This end of the holder housed an air bearing (E) which allowed for lengthening of the graft during testing (this would be in the case of isotonic testing, whereby the graft is placed under a certain axial tension and allowed to lengthen under an applied pressure). Should one wish to perform isometric testing, (whereby the length of the graft is fixed during testing), then the right hand shaft may also be clamped by means of a clamping ring.

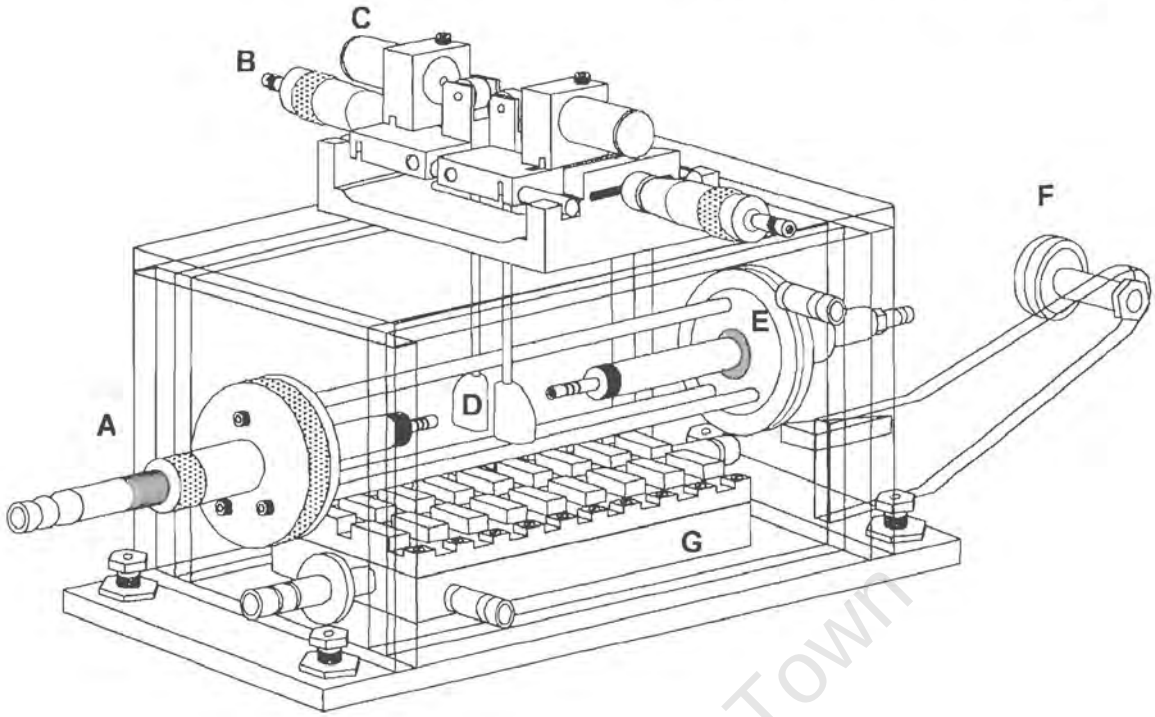

Figure 4.9: The compliance testing chamber; A: adjustment screw, B: Micrometer adjustment screw, C: LVDT, D: Pendulum, E: Air bearing, F: Tensioning pulley, G: Heat exchanger

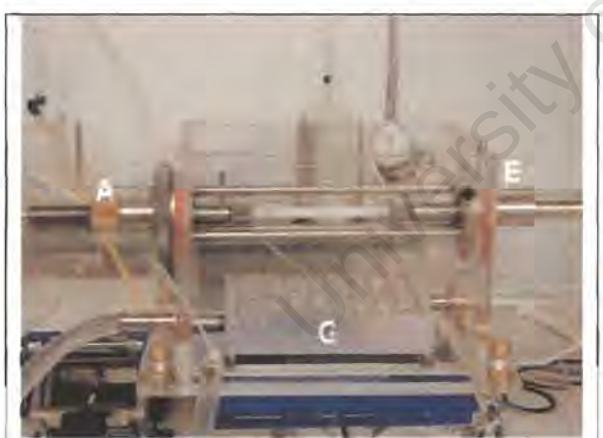

Detail of the testing chamber with the lid and diameter measuring apparatus removed: A: adjustment screw, E: air bearing, G: heat exchanger.

Detail of the diameter measurement and LVDT setup: B: micrometer adjustment screw, C: LVDT.

Figure 4.10: Details of the compliance-testing chamber

4.2.2.3 The Windkessel Chambers

The 2 Windkessel chambers in the circuit imitated the impedance of the vascular system, and in particular, the elastic effect of the aorta. Thus, they had the effect of smoothing the pulse wave

emitted by the pumping device. In the circulatory system, this pulse damping effect is achieved by the elasticity of the aorta, which acts as an expansion chamber and takes up a large percentage of the ventricular outflow. The return of the aorta to its natural state causes propagation of the flow in a smooth manner, in essence acting as a pump itself. This effect is continuous throughout the vascular system towards the periphery, but it has been found that the 'stiffness' of the arteries increases towards the periphery in order to maintain the correct blood flow velocity and to minimise energy losses. Figure 4.11 below gives depicts a glass Windkessel chamber as used in the fluid circuit. The Windkessel chamber on the inlet or proximal side of the graft allowed one to dampen the systolic pulse. The greater the amount of air in the top of the chamber, the more dampened was the pulse. By adjusting the level in the second chamber, placed distal of the graft, the amount of back-pressure in the system could be varied. However, it was found unnecessary to do so and this chamber was kept full during all tests.

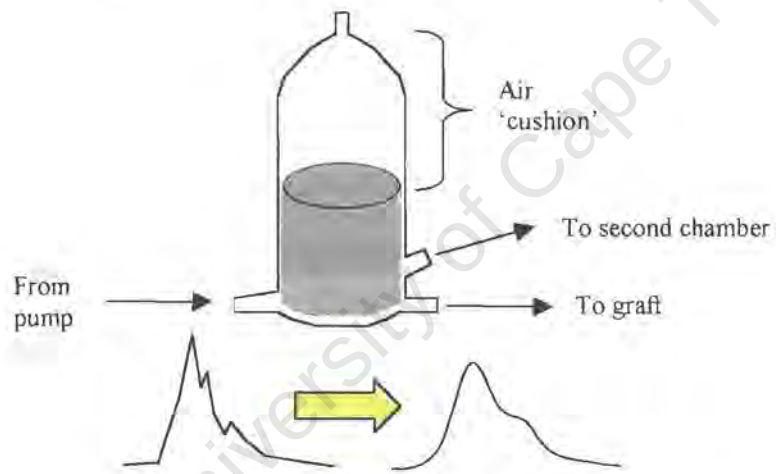

Figure 4.11: Function of the Windkessel chamber

4.2.2.4 Monitoring of Pressure, Flow and Diameter

a) Pressure

Pressure readings were taken simultaneously at positions just before and just after the graft. For this, two disposable type pressure transducers were used. These in turn were linked to a Triton physiological monitoring system that relayed the signal from the transducers to the analogue-digital interface card at the computer. This voltage received

at the card was then converted into a waveform via data-capturing software (Waveview, ver. 1.26).

b) Diameter Measurement

The diameter measurement of the grafts was achieved by two linear variable displacement transducers (LVDT's), mounted on top of the lid that encloses the testing chamber. Two opposing pendulums made contact with either side of the graft and followed the movement of the graft walls. The pendulums pivoted on low friction bearings and by means of a small linkage, were coupled to the armatures of the transducers, as shown in figure 4.12 below. The principle of operation of the LVDT's is the movement of an armature inside a magnetic field. The movement causes a voltage drop in the surrounding coil. The voltage output is proportional to the amount of movement and can thus be measured. In this case, the voltage output was fed directly to an Analogue to Digital card. The advantage of this method is that any non-homogeneity in the graft wall thicknesses may be detected. In other words, if one transducer is deflected more than the other for any particular sampling, then that wall is most likely thinner than the other at that point. The resulting voltage traces were then displayed graphically by means of data acquisition software (Waveview version 1.04). The amount of movement was amplified mechanically by the ratio of the linkage mechanism, producing an amplification of 1.5 times. Also, the LVDT voltage was multiplied electronically by a factor of 10 to allow easier reading of the diameter displacement (the amount of signal gain could be adjusted in the Waveview software).

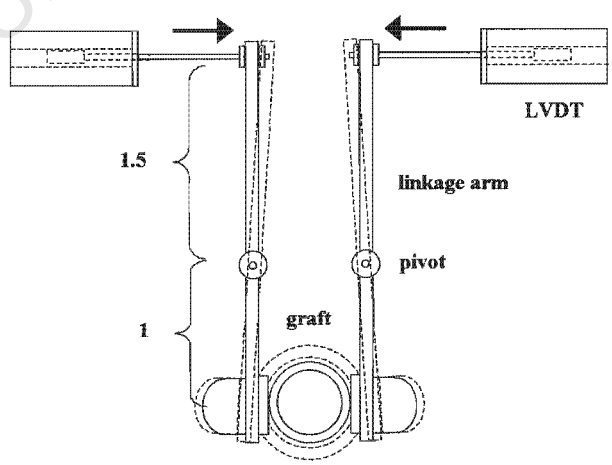

Figure 4.12: Detail of the diameter-measuring apparatus.

4.2.3 Operation of the Fluid Circuit

For compliance testing, it was necessary to adjust several variables in order to get the desired pressure and flow. It was necessary that one be able to adjust the diastolic pressure (or datum pressure), as well as the amplitude of the pulse (diastolic-systolic). See figure 4.13 for a schematic of the fluid circuit.

4.2.3.1 Reproduction of the Physiological Waveform

A great deal of testing and adjustment was required before a satisfactory pressure waveform was achieved. The waveforms were very dependent on the type of driving unit used. In the case of the ventricle pump it was found that the flow profile was quite adjustable, but it was difficult to achieve a simultaneously acceptable pressure waveform. Also, it was thought that the presence of 2 one-way valves at the ventricle might cause some flow irregularities in the system. It was also found that the levels of each of the Windkessel chambers had a marked effect on the shape of the pressure wave. Other factors such as stiffness of the tubing in the flow circuit and continuity (ie sharp diameter changes) had a lesser effect on the waveform. Eventually it was decided to use the modified roller pump, the reason being that it simultaneously produced quite acceptable pressure and flow waveforms. While the roller pump normally produces a sinusoidal pressure waveform, it was deemed necessary to add an insert to provide a more realistic systolic pressure increase and systolic pressure decay, such that the grafts experienced a more realistic pressure profile. In Addendum I are some examples of waveforms obtained with different driving units and with different circuit conditions (Windkessel levels, pinch valve closure etc.)

4.2.3.2 Adjustment of the Diastolic or Datum Pressure

In the case of the system employed in this project, namely the modified roller pump, the diastolic pressure was varied by an elevated reservoir on the inlet side of the pump. Due to the lack of vertical space, a static head of pressure could not be used in the laboratory (2.5m of height would have been need to create the necessary pressures). Instead, a sealed reservoir was built, in which the internal pressure could be adjusted. This was achieved by compressed air, fed into the top of the reservoir. The air pressure in the top portion of the reservoir could be adjusted by a fine pressure-regulating valve. The lower portion of the reservoir was filled with water, which fed into the inlet side of the roller pump by means of a connecting pipe. The pressurised reservoir was

refilled by another open reservoir at a higher level, into which the return pipe of the fluid circuit fed. After testing, the pressure reservoir could be refilled by gravity from the open reservoir. By adjusting the air pressure regulator, one could achieve very fine variations in the diastolic or datum pressures in the circuit (see Addendum I for details of this apparatus).

4.2.3.3 Adjustment of the Pressure and Flow Amplitude

There were several variables that could be adjusted to affect the peak amplitude. Firstly, the pinch of the rollers in the pumping region had an effect on the flow output. At maximum pinch (ie the flexible tube is completely compressed in the pumping chamber), one could achieve a maximum flow. As one decreased the amount of pinch, the flexible tube did not completely seal and the pump became less efficient, and accordingly the pressure and flow amplitude decreased. The level of the first Windkessel chamber also affected the pulse amplitude, as mentioned earlier. The greater the amount of air in the first chamber, the more the damping of the pressure peak and hence the more the amplitude decreases. In the end it was found that the amplitude of the pressure curve could be adjusted by pinch valve B, placed distal of the graft (on the tube returning to the filling reservoir). Increasing the pinch on the tube effectively increases the amount of back-pressure and causes the pulse amplitude to increase (and hence increase the systolic pressure). See also Addendum I for details of the different waveforms.

Figure 4.13: Schematic of the compliance testing apparatus.

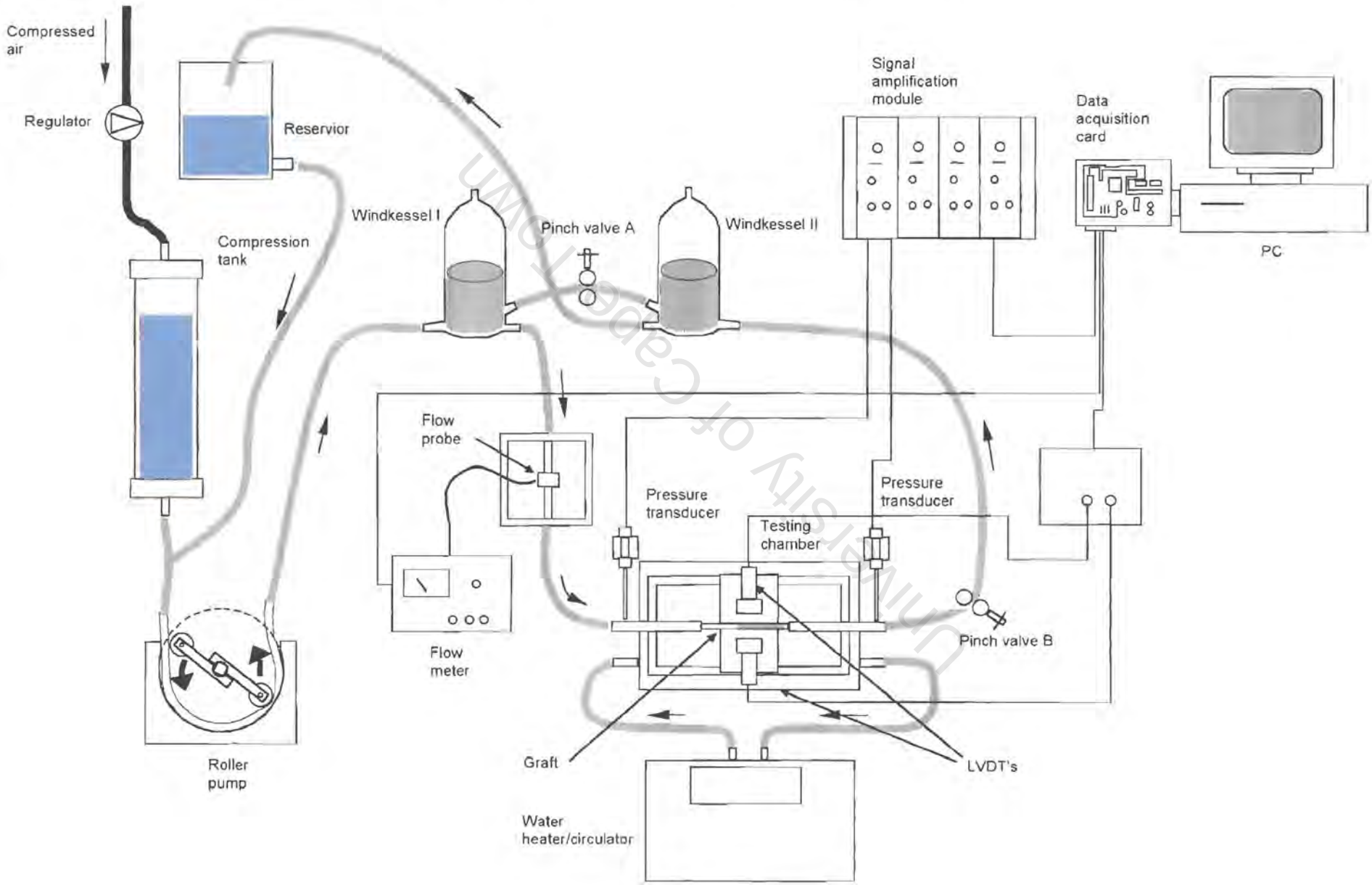

4.2.4 Compliance Testing Samples

4.2.4.1 Porcine Aorta

Two samples of porcine aorta were tested statically and dynamically as a means of correlating our data with other researchers who tested natural tissue. Latex inserts were used due to the presence of small lateral vessels off the aorta that would have resulted in leakage during testing. Two samples of aorta were taken from juvenile pigs. Unfortunately, the femoral arteries were too small to test on the rig and samples of aorta had to be used instead. Testing was conducted in buffered saline solution at 37 deg. C. Some modifications to the test fittings were required since the aorta samples had a tapered diameter, varying from 6mm internal diameter to about 9mm internal diameter. Since the diameter measurement was midway on the graft length, the internal diameter was taken to be 7.5mm.

4.2.4.2 Latex Inserts

The latex inserts manufactured by Roynhardt, Johannesburg were tested separately to determine their specific compliance. The reason for this was to ascertain the effect of the latex during the dynamic testing. Two samples of 90mm were cut from each of 3 lengths 200mm long to see if there were any variations in quality along the supplied 200mm lengths. The results however do not support any large variation on properties along the length. Samples were only tested statically, as dynamic testing caused the pendulums to 'bounce' off the walls of the graft due to the latex being very elastic.

4.2.4.3 Salt-cast Grafts

Salt-cast grafts with several types of reinforcing were tested. Below in table 4.1 is a list of the different types tested. The details of how the salt-cast grafts were manufactured are in section 3.2 in the previous chapter.

Table 4.1 List of the different types of salt-cast grafts tested.

1	Non-reinforced salt-cast graft	5	Salt-cast graft reinforced with single wrapping of nylon monofilament at 1mm winding gap.
2	Salt-cast graft reinforced with single wrapping of polyurethane monofilament at 2.5mm winding gap	6	Salt-cast graft reinforced with single wrapping of nylon monofilament at 2.5mm winding gap.
3	Salt-cast graft reinforced with single wrapping of 33 dtex Dorlastan® at 2.5mm winding gap.	7	Salt-cast graft reinforced with single wrapping of nylon monofilament at 5mm winding gap.
4	Salt-cast graft reinforced with double wrapping of 33 dtex Dorlastan® at 2.5mm winding gap.	8	Salt-cast graft reinforced with double wrapping of 33 dtex Dorlastan® at 2.5mm pitch and single loose wrapping of nylon monofilament at 5mm winding gap.

4.2.4.4 Bead-cast grafts

Bead-cast grafts with several types of reinforcing were tested. Below in table 4.2 is a list of the different types tested. The reason for testing these grafts was to compare the compliance of grafts made with the bead-cast method to those made with the salt-cast method. The details of how the bead-cast grafts were manufactured are in section 3.2 in the previous chapter.

Table 4.2 List of the different types of bead-cast grafts tested.

1	Non-reinforced bead-cast graft	3	Bead-cast graft reinforced with single wrapping of 33 dtex Dorlastan® monofilament at 1mm winding gap.
2	Bead-cast graft reinforced with single wrapping of polyurethane monofilament at 2.5mm winding gap	4	Bead-cast graft reinforced with single wrapping of 33 dtex Dorlastan® monofilament at 2.5mm winding gap plus single wrapping of nylon monofilament at 2.5mm winding gap.

4.2.4.5 Commercial 4mm Teflon® grafts

Teflon® grafts with an internal diameter of 4mm were tested to correlate the compliance values obtained on this apparatus with those values quoted in literature. It was not necessary to use latex inserts with these grafts, as they did not leak when pressurised internally.

4.2.5 Compliance Testing Methods

4.2.5.1 Sample Preparation

Sample preparation for static and dynamic compliance tests were the same. Three samples of each graft type were tested to confirm repeatability. Graft samples of length 90mm were used. Thin-walled latex inserts were used on the inside of the graft to prevent leakage. Testing adapters were inserted 15mm into each end of the graft, thus leaving a length of 60mm to be tested. The graft with adapters were pre-assembled before being inserted into the testing chamber (quick-fitting adapters were used, so that samples could be quickly interchanged).

4.2.5.2 Dynamic Compliance Testing

The grafts samples were subjected to 2 dynamic tests: one conducted at a pressure range of 80-120 mm Hg and another conducted at 180-220mm Hg, the one at the elevated range being to compensate for the effect of the latex inserts. The testing was carried out in accordance to recommended AAMI standards for testing of vascular prostheses, 1994 revision, section 8.10 (see 4.2.1 above). After insertion of the graft into the testing chamber, the graft was axially tensioned with 150g and then the ends fixed (the testing bath was pre-heated to 37 deg. C before inserting the graft). The internal pressure was then increased to roughly the diastolic value required (either 80 or 180mm Hg) in the fluid circuit by adjusting the air regulator. The pinch valve B was then opened and the roller pump switched on. It was necessary to monitor the pressure waveforms while adjusting the regulator and pinch valve B until the desired waveform was achieved ie. a pressure range of 80-120mm Hg or 180-220mm Hg. Sampling of 3-5 seconds were taken and from this data, three consecutive pressure and diameter waves were extracted for analysis. The mean internal pressure was calculated by averaging the pressures of the proximal and distal pressure transducers.

4.2.5.3 Calculation of Dynamic Compliance

Dynamic compliance was calculated by measuring the pressure differentials of three consecutive pulses and measuring the corresponding diameter changes by summing the measurements from the transducers. Values quoted are therefore diameter compliances and are given as a percentage change in diameter per100mm Hg. Some researchers quote compliance as a volume compliance [46,107,120], but diameter and volume compliance are not equivocal (see section 4.2.4 below). Compliance values for both the 80-120mm Hg and 180-220mm Hg ranges were calculated. Figure 4.14 below shows graphically how the dynamic compliance was calculated from the pressure and diameter traces. Compliance was then calculated from the equation:

$$C_{static} = \frac{\Delta d}{d_o} \times 100 \cdot \frac{1}{\Delta P} \times 100 \text{ mm Hg} \qquad (4.1)$$

Where: Δd = diameter change, d_o = original internal diameter, ΔP = pressure differential (max test pressure – min test pressure)

Results are then expressed as % diameter change per 100mm Hg (%/100mm Hg).

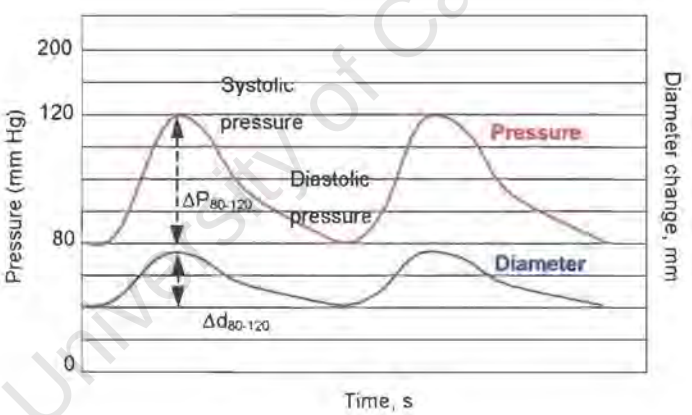

Figure 4.14: Method of calculating dynamic compliance (shown here over 80-120mm Hg range).

4.2.5.4 Static Compliance Testing

For static testing, the same apparatus was used, but pinch valves A and B were shut, thus excluding the rest of the pulsatile circuit so that only the testing chamber was used. An adjustable syringe was used to pump finite amounts of fluid (in this case water) into the graft. The graft was axially tensioned as in the dynamic tests. Only one pressure transducer was used to record

pressure, while the diameter measuring method remained the same as for dynamic testing. Pressure and diameter recordings were taken for each pressure increment. It should be noted that the grafts were first primed with a pressure of 40mm Hg, and the first measurement taken at this pressure. The reason for this was to overcome the external pressure on the graft caused by the hydrostatic pressure when immersed in the testing chamber. This caused the graft walls to collapse when the internal pressure of the graft was zero and resulted in some erroneous diameter measurements.

4.2.5.5 Calculation of Static Compliance

For each pressure increment, a reading was taken. From these, a curve of pressure vs. diameter change was plotted. In the case of a linear plot, the slope of the line would give the compliance of that particular graft. Compliance over the 80-120mm Hg range was calculated as well as the compliance over the 40-200mm Hg range (the grafts were primed with 40mm Hg to overcome the effects of hydrostatic pressure in the testing reservoir) - see figure 4.15 below. The static compliance was calculated on diameter change by using the equation (4.1) also. Compliance values were quoted the same as for dynamic compliance, being %/100mm Hg.

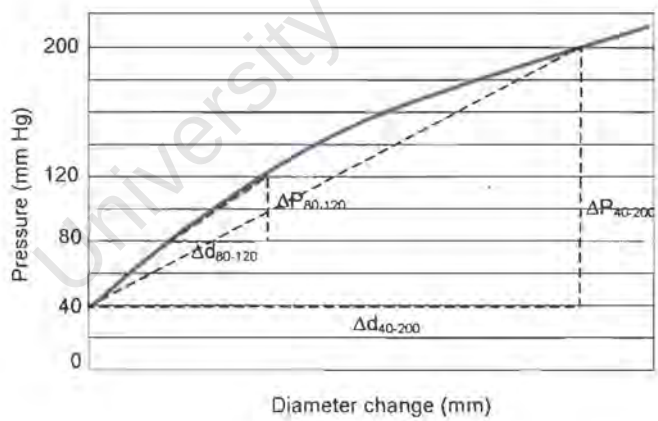

Figure 4.15: Method of calculating static compliance over the 80-120mm Hg and 40-200mm Hg range.

Note that since the gradient of the straight line drawn between the points on the pressure-diameter curve will give the compliance. As can be seen, the slope of the line drawn between 40 and 200mm Hg is less than that for the line drawn between 80 and 120mm Hg. Hence this compliance

value will always be lower for this shape of curve. The important compliance value is the one calculated between 80 and120mm Hg since this is the value most often quoted.

4.2.6 Calculating Diameter Compliance

Compliance of vascular grafts is usually quoted in percentage change in diameter or radius per unit increase in pressure. In this project, compliance in all cases has been calculated as % diameter change per 100mm mercury. Some researchers use change in volume to calculate compliance and give values in terms of percentage volume compliance. It should be noted that volume and diameter compliance are not equivocal, as the following derivation will show, the volume compliance is approximately twice the diameter compliance.

For example: A graft with an internal diameter of 6mm shows a diameter increase of 0.3mm for a 100mm Hg pressure increase.

The **Volume compliance** can be calculated from the following equation:

$$\%\mathbf{C}_v = \frac{\Delta V}{V_o} \cdot \frac{1}{\Delta P} \cdot 100 \tag{4.2}$$

Where V_o is the original volume and ΔV is the change in internal volume of the graft due to the pressure increase. These can be calculated from the equation for volume:

$$\mathbf{V} = \frac{\pi}{4} \cdot d^2 \cdot l \tag{4.3}$$

Where d and l are the internal diameter and length respectively.

Therefore, ΔV may be calculated as such:

$$\Delta \mathbf{V} = \frac{\pi}{4} \cdot d_1^2 \cdot l_1 - \frac{\pi}{4} \cdot d_o^2 \cdot l_o \tag{4.4}$$

Where d_o, l_o and d_1, l_1 are the original diameter and length and pressurised diameter and length respectively.

One can assume a minimal change in length due to the pressurisation, thus equation (4.1) may be simplified as:

$$\%\mathbf{C}_v = \frac{d_1^2 - d_o^2}{d_o^2} \cdot \frac{1}{\Delta P} \cdot 100 \tag{4.5}$$

Now the term $d_1 = d_o + \Delta d$, therefore (4.5) becomes:

$$\%C_v = \frac{(d_o + \Delta d)^2 - d_o^2}{d_o^2} \cdot \frac{1}{\Delta P} \cdot 100 \tag{4.6}$$

Which can be simplified and rewritten as :

$$\%C_v = \frac{2d_o \cdot \Delta d + \Delta d^2}{d_o^2} \cdot \frac{1}{\Delta P} \cdot 100 \tag{4.7}$$

Or:

$$\%C_v = \left(\frac{2\Delta d}{d_o} + \frac{\Delta d^2}{d_o^2} \right) \cdot \frac{1}{\Delta P} \cdot 100 \tag{4.8}$$

Now, for $\Delta d << d_o$, the term $\frac{\Delta d^2}{d_o^2}$ becomes very small and one can assume it to be negligible, hence (4.7) becomes:

$$\%C_v = \left(\frac{2\Delta d}{d_o} \right) \cdot \frac{1}{\Delta P} \cdot 100 \approx 2 \cdot C_d \tag{4.9}$$

Thus the volume compliance is roughly equal to twice the volume compliance.
Compliance values in this project were however calculated using the diameter compliance equation.

4.2.7 Compensation for the Effect of the Latex Liners

Since latex inserts were used to line the inside of the grafts and prevent leakage during pressurisation, they would have had an effect on the compliance values obtained, despite having a higher compliance than the grafts. To overcome this problem, the grafts were tested dynamically at an elevated pressure range in order that the graft experiences the desired physiological pressure range (80-120mm Hg). Dynatek-Dalta Scientific Instruments USA, a company that specifically

tests the compliance of various commercially available grafts, used such a method to calculate the compliance. In order that the graft experiences a physiological pressure range of 80-120 mm Hg, the pressure is increased to compensate for the effects of the latex, for example 110-160mm Hg. To calculate this compensated range, a latex insert is first tested separately and then a graft lined with the latex insert, generating two static curves. The latex curve is subtracted from the latex+graft curve and the points are found where the difference between the curves is 80mm and 120mm Hg respectively. These pressure values (P_{DIA}, P_{SYS}) are then the values at which the graft should be tested dynamically so that it experiences the physiological pressures desired. (See figure 4.16 below)

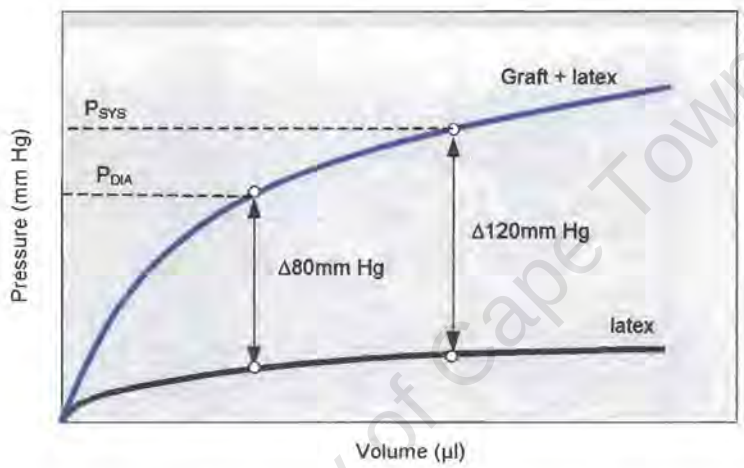

Figure 4.16: Graphical method of subtracting of the effect of the latex (as used by Dynatek-Dalta, USA.)

In this project, a similar approach was applied. The latex inserts (from Roynhardt Jhb.) were tested statically first and an average compliance calculated. Each of the graft types were then tested statically with the latex inserts and static curves generated. For each graft tested, the average latex curve was plotted with the average static curve of the graft+latex tests. Using best-fit equations to model the static curves, the latex curve was subtracted from the graft+latex curve and the equation was solved for pressure differences of 80 and 120mm Hg. These points were then substituted back into the graft+latex equation to find the required testing pressures. Unfortunately this method was not completely satisfactory due to the fact that the Roynhardt latex inserts used were slightly thicker-walled and thus less compliant than those used by Dynatek. This meant that the inserts had a higher influence on the compliance of the non-reinforced grafts. Ideally, the latex inserts should have as small a wall thickness as possible, in order not to have too

much effect on the compliance calculations. However, the only graft type for which this approach was not applicable was the non-reinforced salt-cast grafts. (See figure 4.17 below). After testing a number of graft types statically with the latex inserts, it was found that in order to compensate for the effects of the latex, a dynamic testing range of around 180-220mm Hg was required. This was found to be the average amount of compensation required for the grafts to experience the 80-120mm Hg physiological range. Therefore all the grafts were tested at this range to give more realistic compliance values. An example of how the compensated pressure range is calculated is shown below.

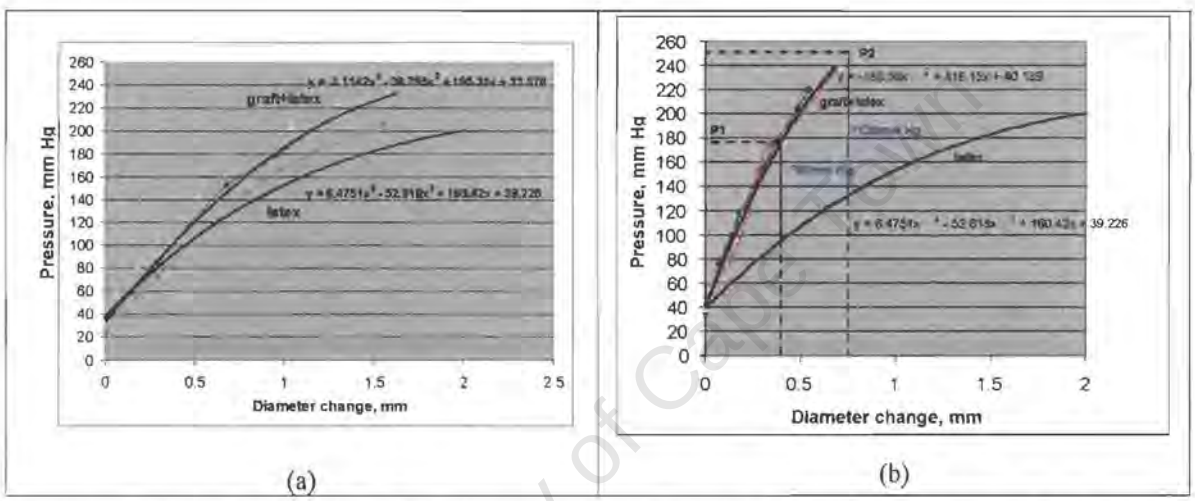

Figure 4.17: Comparison of the static compliance curves for the non-reinforced salt-cast grafts and the latex (a) and the PU-reinforced salt-cast grafts with the latex (b). Note that in the case of the non-reinforced graft, the subtraction method is not applicable due to the fact that the two curves are too close together. This means that pressure differences of 80 and 120mm Hg occur only at much higher pressures and graft diameters at these pressures could not be measured on the rig.

Best-fit equation for the latex inserts (Roynhardt latex, wall thickness ±240μm).

$$y = 6.4751x^3 - 52.818x^2 + 160.42x + 40 \quad (4.10)$$

Best-fit equation of a PU-reinforced salt graft with latex insert (average curve).

$$y = 132.6x^3 - 246.82x^2 + 432.59x + 40 \quad (4.11)$$

Subtraction equation (graft+latex)-(latex) ie. (4.11-4.10).

$$y = 126.1249x^3 - 194.002x^2 + 272.17x \quad (4.12)$$

Solving for y=80 and y=120mm Hg from eqn. 3.10 we get pressures of 179.1 and 245.3mm Hg respectively. These are then the adjusted pressures at which the graft should be tested dynamically in order to subject the graft to a realistic 80-120mm Hg pressure excursion. Note it was decided to test at 180-220mm Hg as opposed to 180-240mm Hg because this was the average compensated range for the all the grafts tested. (See also Addendum III for detailed static compliance curves compared with the plotted static compliance of the latex inserts). Carmines et al. [117] used a similar approach by analytically correcting for the effect of the latex. They did this by applying a best-fit exponential equation to model the stress-strain curves of the latex separately and together with the graft. This equation was then used to solve for the average circumferential and axial stress in the graft wall (in this case they were testing human and pig carotid arteries).

4.3 CREEP TESTING (EXTENDED DYNAMIC COMPLIANCE TESTING)

These tests were conducted to simulate the physiological conditions experienced by a graft over an extended period of time. Four graft types were tested: a non-reinforced salt-cast graft, a graft reinforced with a double winding of Dorlastan® monofilament and a bead-cast graft reinforced with Dorlastan® at 2.5mm pitch and a bead-cast graft with nylon at 2.5mm pitch. The purpose of testing a non-reinforced graft was to affirm the need for an adventitial reinforcement. The reinforced grafts were tested to see what the effect of reinforcement on durability of the grafts would be.

4.3.1 Method

The graft samples were tested dynamically as described in the methods above (see 4.2.4.2, Dynamic compliance testing). Dynamic testing was carried out at an applied pressure range of 80-120mm Hg. The pinch valve distal of the graft (pinch valve 'B') was closed to prevent emptying of the reservoir. Testing was not carried out at the compensated range because this would have resulted in systolic pressure being too high due to the pinch valve being closed. Data capturings were taken at times of t=0, t=10, 20, 30, 60, 120 minutes, 4 hours and 20 hours respectively. The compliance for each capturing was calculated from the amplitude of the Proximal and distal pressure curves and the diameter curve measured by the displacement transducers. Compliances

were compared to the original compliance (at t=0) and the change in external diameter was also compared to the original diameter. All tests were carried out at 37 deg. C.

4.4 BURST TESTING

Burst testing is a method of testing the graft to failure and is therefore useful in determining the maximum internal pressure a graft can take.

4.4.1 Burst Testing Apparatus

For this test, the same holding chamber was used as for the compliance testing. The rest of the flow circuit was excluded by the pinch valve on the distal end of the graft (pinch valve 'B'). One of the pressure transducers used in the compliance testing was connected to the distal end of the graft, allowing pressure measurements to be taken. Data from the pressure transducer was captured using the same A/D card and data acquisition software (Waveview).

4.4.2 AAMI Requirements for the Burst Test

According to the AAMI standards, the burst test apparatus should include a means of applying a steadily increasing fluid or gas pressure to the interior of the test sample. It should also have a means of measuring and recording the pressure to greater than that required to burst the sample. The rate of pressure increase should be expressed in kilopascals per second (kPa/s), and the bursting pressure in kilopascals.

4.4.3 Method

The graft was inserted into the holder and secured at an axial tension of 200g. A priming pressure of 40mm Hg was applied to the inside of the graft to prevent collapse of the graft wall. Sampling was started at 40mm Hg. Pressure was increased by means of the pressure regulator used for the pressure reservoir. The rate of pressure increase was judged by monitoring a pressure gauge attached to the distal side of the graft. This rate was kept equal for all grafts tested.

4.5 SUTURE PULL-OUT TEST

The suture pull-out test is a good test to determine the suture retention of the graft and thus how close to the end of the graft the surgeon may suture without failure of the graft. Both non-reinforced and reinforced grafts were tested.

4.5.4 Method and Apparatus

For this test, the Instron tensile tester was also used. The graft was clamped in the bottom jaw while a half-loop of suture was clamped in the top one and pulled out of the graft. The suture passed once through the graft and formed a half-loop, such that it included at least two windings of the fibre reinforcement in the case of the reinforced grafts). The sample was then tested at the prescribed strain rate of 150mm/min(see figure 4.18 below), and the force required to pull the suture through the graft wall or cause the wall to fail, was recorded.

4.5.5 AAMI Requirements for the Suture Pull-out Test

The standards advocate the use of a suitable tensile testing apparatus with a load cell and jaws suitable for gripping the specimen. In the case of reinforced grafts, the reinforcement should only be included in the test if it is to be included in the anastomosis. The grafts may either be tested cut obliquely to the longitudinal axis or normal to the axis. Strain rates of 150±50mm/min are prescribed.

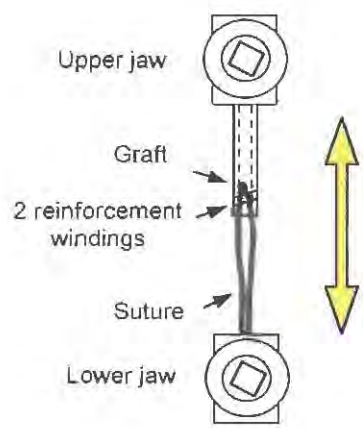

Figure 4.18: Method of performing the suture pull-out test

5. Results & Discussion:

5.1. UNIAXIAL TENSILE TEST RESULTS

5.1.1 Fibre Testing

Tensile testing was carried out to establish the mechanical properties of the materials used in graft manufacture ie. the reinforcing fibres as well as the porous graft material. The reason for testing at 37 degrees was to duplicate the physiological conditions and therefore subject the graft materials to realistic in-vivo conditions. Three samples of each fibre material were tested and an average modulus calculated for each. It should be noted that moduli were calculated over linear regions of the curve: in the case of the nylon fibres it is the 0-5% strain region, the PU fibres over the 0-30% strain. The moduli of the elastane fibres were calculated from 0-100 and 0-200% strain, being much more extensible fibres. Unfortunately it was impossible to test the elastane fibres (Lycra®, Dorlastan®) in the water bath as these were too fine.

5.1.1.1 Nylon and Polyurethane Fibres Tested at 100mm/min.

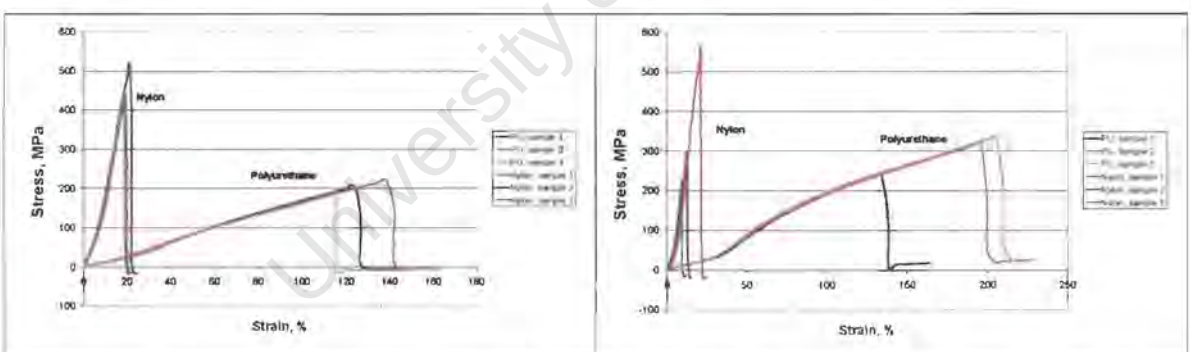

3 samples of nylon and polyurethane fibres tested in air.	3 samples of nylon and polyurethane fibres tested in water at 37 deg. C.

Figure 5.1: Tensile test curves of polyurethane and nylon monofilaments at room temperature in air and at 37 deg. C in water.

As can be seen from the above graphs, temperature definitely has an effect on the stiffness of the materials. All fibres show a decreased modulus (stiffness) at higher temperatures. The reason for this is that, the materials all being polymeric in nature, show an increase in the polymer-molecule mobility and a weakening of the secondary bonds. Therefore the materials appear less stiff at

elevated temperatures. The polyurethane samples show a higher elongation at the elevated temperature, most likely also because of increased molecular mobility. The polyurethane samples also break at higher stresses, perhaps because of water absorption effects.

5.1.1.2 Elastane fibre tensile tests at 100mm/min room temp, (air tested).

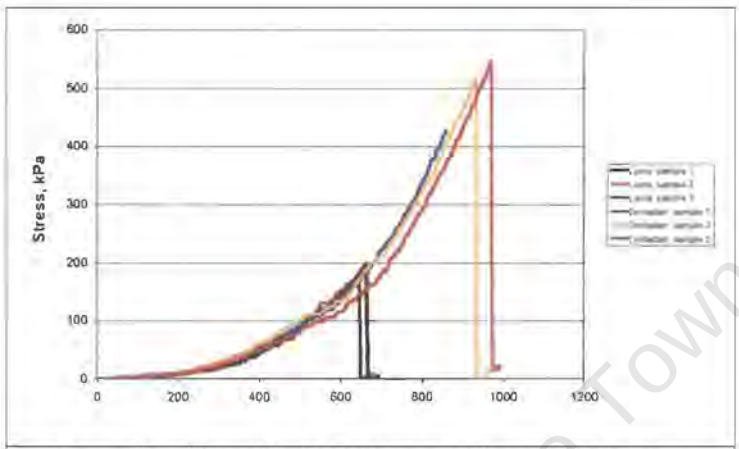

3 samples of Lycra® and Dorlastan® fibres tested at room temperature in air.

Figure 5.2: Tensile test curves of Lycra® and Dorlastan® monofilaments tested at room temperature in air.

Table 5.1: Measured elastic moduli of the polymer fibres tested.

Fibre	Young's modulus, (GPa)	
	Room temp., air	37 deg. C, water bath
PU (0-30% strain)	0.1501 ± 0.012	0.1215 ±0.001
nylon (0-5% strain)	1.396 ± 0.082	1.561 ± 0.224

Fibre	Young's modulus, (MPa)	
	0-100% strain	0-200% strain
Lycra®	1.859 ± 0.975*	4.752 ± 0.605*
Dorlastan®	3.411 ± 0.630*	4.90 ± 0.324*

* Lycra® and Dorlastan® fibres tested at room temperature in air only.

One can see from the stiff fibre tensile tests that the nylon was much less extensible than the PU, since the nylon had much higher modulus compared to the PU. The nylon showed a higher standard deviation when tested in water, and was also stiffer, most likely due to the fact that nylon absorbs water and this will affect the tensile properties. However, the presence of defects in the individual samples might also affect measurements. The elastane fibres tested (Lycra® and Dorlastan®) both showed a typical j-shaped curve, the modulus increasing in an almost

exponential way with strain. The 33 dtex Dorlastan® fibre was chosen for the reinforcement because it was a more robust fibre than the very fine Lycra® samples. The graphical comparison of the moduli of the stiff fibres and elastane fibres is shown in figure 5.3 below.

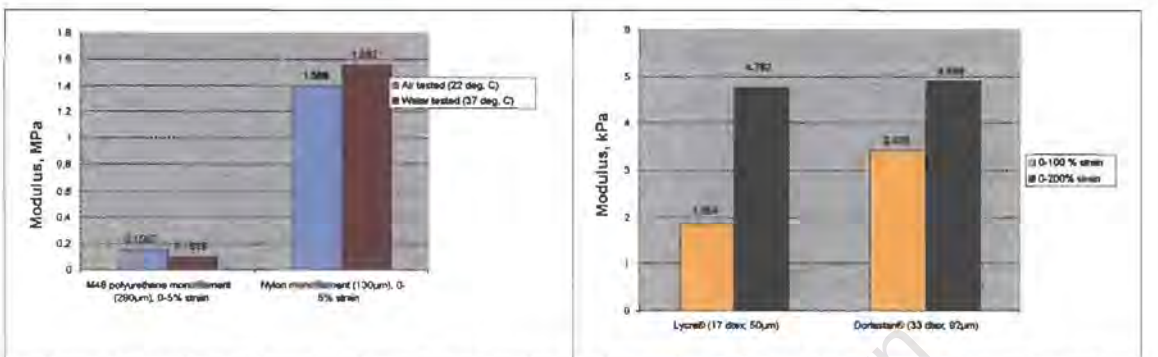

Young's moduli of the stiff fibres (PU, nylon) tested at room temperature and 37 deg. C.	Young's moduli of the elastane fibres (Lycra®, Dorlastan®) tested at room temperature in air.

Figure 5.3: Graphical comparison of the elastic moduli of the polymer fibres tested.

5.1.2 Porous Graft Testing

Samples of the non-reinforced porous salt-cast grafts and bead-cast grafts were tested to determine the Young's modulus of elasticity and to see if these values correlate with the compliance values obtained. Three circumferential samples and three longitudinal samples were cut from each graft and tested (figure 5.4). All tests were conducted at 37 deg. C in a heated water bath.

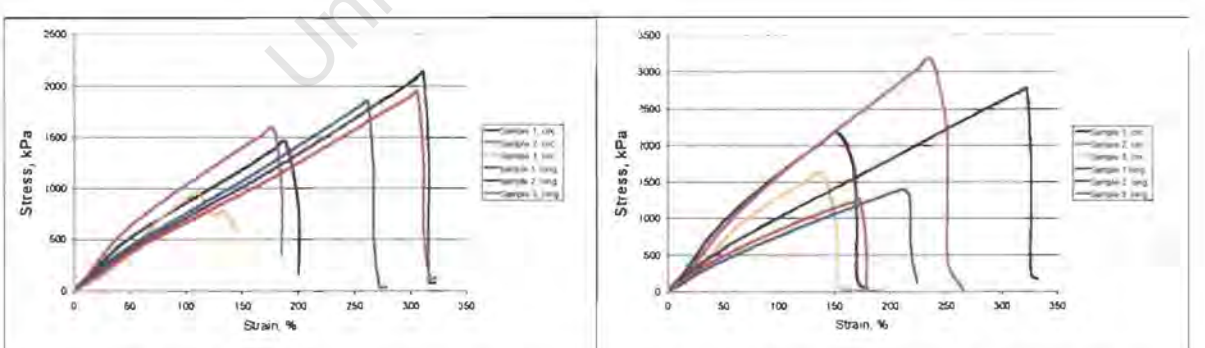

3 samples of salt-cast grafts tested in the circumferential and longitudinal directions.	3 samples of bead-cast grafts tested in the circumferential and longitudinal directions.

Figure 5.4: Tensile test curves of the porous graft samples tested longitudinally and circumferentially in water at 37 deg. C.

Table 5.2: Measured elastic moduli of the porous graft samples tested in water at 37 deg. C.

Graft type	Young's modulus, (MPa), 0-30% strain		Young's modulus, (MPa), 30% strain - break	
	Circumferential	Longitudinal	Circumferential	Longitudinal
Salt-cast	1.255 ± 0.187	0.851 ± 0.099	0.788 ± 0.142	0.650 ± 0.03
Bead-cast	1.681 ± 0.327	1.090 ± 0.184	1.118 ± 0.123	0.681 ± 0.109

From table 5.2 the moduli measurements show the grafts made by bead-casting to be generally stiffer than the salt grafts. The reason for this was most likely the different pore structure: the bead-cast grafts having a more regular structure than the salt-cast graft. Also one can see that the circumferential moduli are slightly higher than the longitudinal moduli in both the salt-cast and the bead-cast grafts. It is difficult to account for this effect in the bead-cast grafts, since the structure is fairly homogenous. The salt-cast grafts are however rolled and often 'weld-lines' are introduced into the grafts where the polymer paste wraps around the mandrel. For the circumferential testing, the samples were cut such that no weld lines were lying in the test region. However for the longitudinal samples it is difficult to avoid these and this would account for some weaknesses in the sample, hence giving a lower modulus. The variability in the curves and the failure stresses for both the salt-cast and the bead-cast grafts could indicate some non-homogeneity of the porous structure which could be due to manufacturing techniques, but differences between the samples could also influence results, ie. the presence of flaws etc.

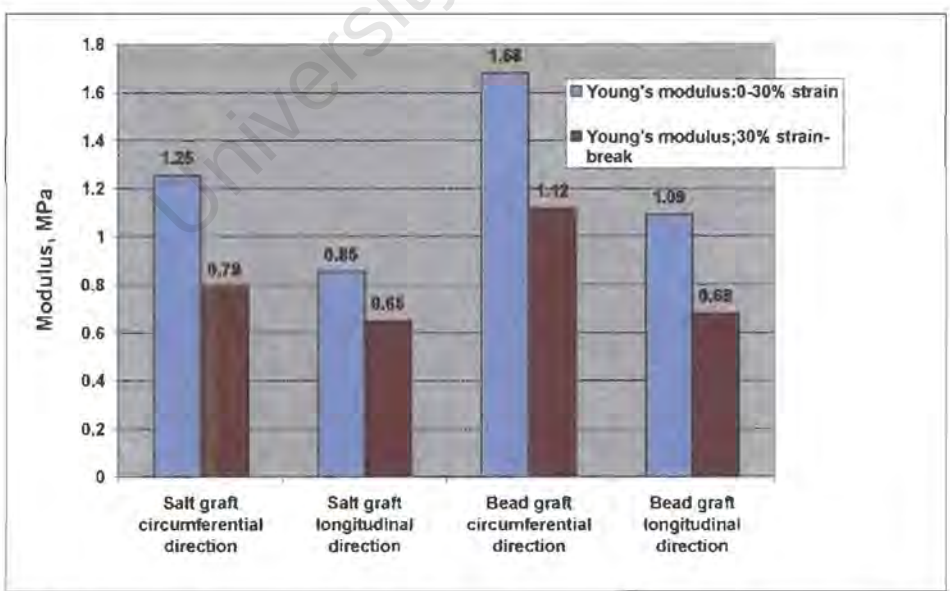

Figure 5.5: Average Young's moduli values of three samples of salt-cast and bead-cast grafts tested circumferentially and longitudinally at 37 deg, C

5.2. COMPLIANCE TESTING

The compliance values quoted in the following sections are all diameter compliances and calculated using an internal diameter of 6mm for both the salt- and bead-cast porous grafts. Where possible, calculated values are compared to those found in literature.

5.2.1 Compliance of Natural Vessels: Porcine Aorta

Dynamic and static testing of two samples of juvenile porcine aorta showed the natural tissue to be quite compliant, as expected. Testing methods for the natural tissue was identical to the method used for the porous grafts. The results are shown in Figure 5.6 and table 5.3 below.

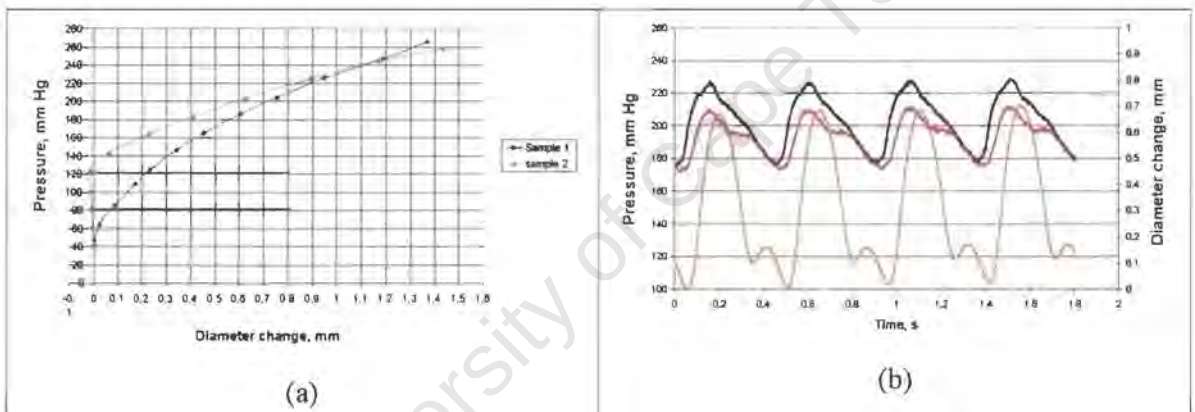

Static compliance curves of 2 samples of porcine aorta. (sample 2 excluded)	Dynamic compliance test of a sample of porcine aorta tested at the 180-220mm Hg range.

Figure 5.6: Static compliance curves of two samples of porcine aorta and a dynamic measurement of one of the samples.

In figure 5.6 (a), sample 2 initially shows a slight decrease in diameter with pressure, which is difficult to explain, but the diameter begins to increase after 120mm Hg. This could be attributed to the diameter size mismatch between the latex inserts and the aorta, so the latex takes up the initial pressures. Also, the aorta was tapered. Unfortunately, the samples could not be tested without the latex inserts due to the presence of small side vessels off the aorta which would have caused leaking during testing.

Table 5.3: Measured static and dynamic compliances of the porcine aorta.

Static compliance (%/100mm Hg)		Dynamic compliance (%/100mm Hg)	
80-120mm Hg	**40-200mm Hg**	**80-120mm Hg**	**180-220mm Hg**
5.0*	7.21 ± 1.07	8.62 ±3.31	25.75 ± 2.83

*Compliance calculated from one sample only

As can be seen from the results, the dynamic compliance in the 180-220mm Hg range is quite high compared to the other results. This could be due to the elasticity of the aorta, the rapid distension of the wall due to the pressure pulse causing the pendulums to 'bounce' slightly, thus increasing the diameter reading. However, Kinley [27] quotes a volume compliance of 26.8% (about 13% diameter change) for a human aorta, although the work does not say whether it is static or dynamic compliance.

5.2.2 Static Compliance of Latex Inserts

Six samples of latex inserts were tested to ascertain their static compliance. The value of 14.24% calculated over the 80-120mm Hg is quite high compared to the grafts, but is only half of the compliance value of the inserts used by Dynatek (see 5.2.6), which had a compliance of 28.52% when tested. Thus one can assume their inserts to be much thinner-walled than the ones used in this project. The static compliances are shown in table 5.4 below.

Table 5.4: Static compliance of the latex inserts.

Static compliance	
80-120mm Hg (%/100mm Hg)	**40-200 mm Hg (%/100mm Hg)**
14.24 ± 2.42	19.89 ± 3.55

5.2.3 Salt-cast Grafts

Salt-cast grafts with a variety of reinforcement were tested statically on the rig. Three samples of each graft type were tested. Table 5.5 and figure 5.7 below gives the results and standard deviations for the three samples tested.

Table 5.5: Static and dynamic compliance measurements of the different types of salt-cast grafts tested.

Graft type	Static compliance, %/100mm Hg		Dynamic compliance, %/100mm	
	80-120mm Hg	40-200 mm Hg	80-120mm Hg	180-220mm Hg
Non-reinforced salt-cast graft	9.21 ± 0.84	12.38 ± 1.66	5.36 ± 0.46	5.88 ± 0.16
Salt-cast graft + PU monofilament at 2.5mm pitch	4.18 ±0.19	4.99 ±0.25	4.43 ±2.66	3.86 ± 1.85
Salt-cast graft + Dorlastan® monofilament at 2.5mm pitch (single wind)	8.47 ± 1.68	9.74 ± 2.22	6.51 ±0.96	7.72 ±1.26
Salt-cast graft + Dorlastan® monofilament at 2.5mm pitch (double wind)	7.77 ± 0.63	9.20 ± 0.46	7.08 ± 1.46	9.50 ± 1.36
Salt-cast graft + nylon monofilament at 1mm pitch (single wind)	1.76 ± 0.48	1.84 ± 0.53	1.98 ± 0.96	1.80 ± 0.28
Salt-cast graft + nylon monofilament at 2.5mm pitch (single wind)	3.46 ± 1.37	3.72 ± 0.84	2.53 ± 1.48	2.72 ± 0.59
Salt-cast graft + nylon monofilament at 5mm pitch (single wind)	4.84 ± 0.24	5.76 ± 1.52	3.22 ± 1.13	3.61 ± 0.28
Salt-cast graft + double Dorlastan® reinforcement at 2.5mm pitch + loose nylon monofilament at 5mm pitch	6.06 ± 0.74	6.62 ± 1.33	3.71 ± 1.07	5.14 ± 2.16

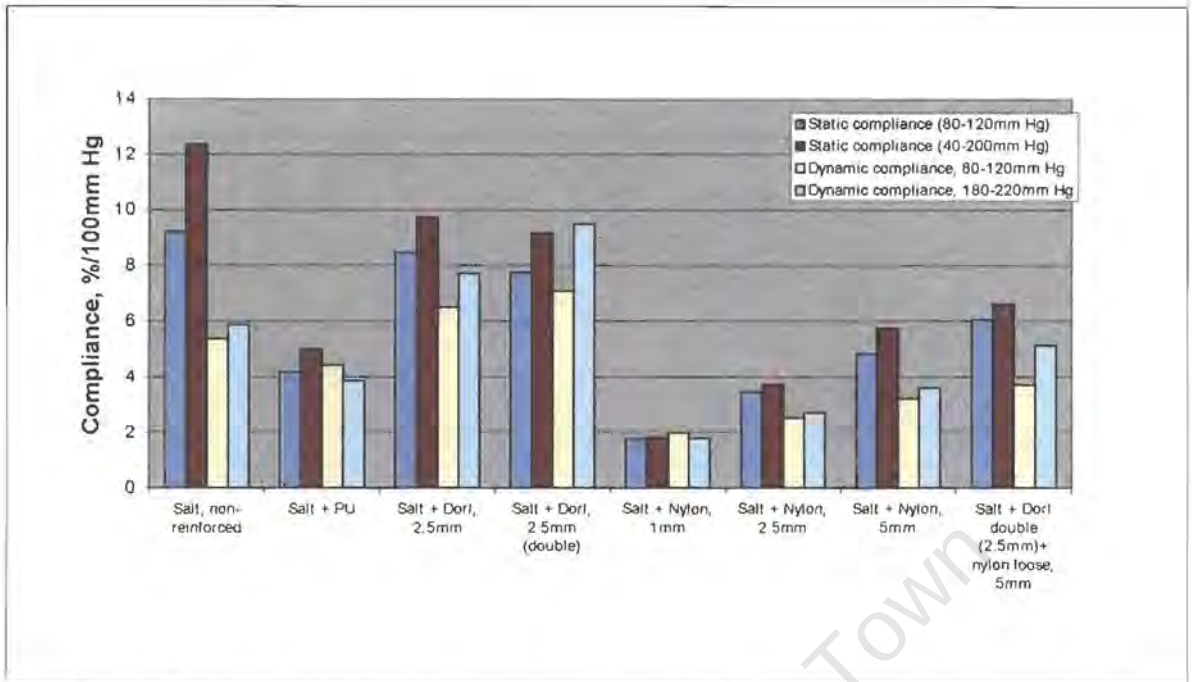

Figure 5.7: Static and dynamic compliance values of the various salt-cast grafts tested

The non-reinforced grafts had the highest static compliance when compared to the reinforced grafts. However, dynamic compliances were actually lower than the Dorlastan® reinforced samples. A possible explanation for this could be that the winding of the elastane filament on the grafts actually weakened them due to the winding solvent eating into the graft, and the filament itself being very weak did not significantly strengthen the graft. The grafts with the double-winding of Dorlastan® also had a higher static compliance than the singly reinforced grafts, which possibly supports this theory as more solvent would have been applied to the graft, therefore weakening it further. The least compliant grafts were the nylon-reinforced grafts, understandably since nylon was the stiffest reinforcing material. Compliance increases almost linearly with an increase in winding gap for the nylon-reinforced samples. In most cases, the dynamic compliance values were lower than the static ones, as predicted. Being visco-elastic, the grafts will appear stiffer because of the higher strain rates experienced during dynamic testing.

5.2.4 Bead-cast Grafts

Some reinforced bead-cast grafts were also tested for purpose of comparison with the salt-cast grafts. Three samples of each graft type were tested. Table 5.6 and figure 5.8 below gives the results and standard deviations for the three samples tested.

Table 5.6: Static and dynamic compliance measurements of the different bead-cast grafts tested.

Graft type	Static compliance, %/100mm Hg		Dynamic compliance, %/100mm	
	80-120mm Hg	40-200mm Hg	80-120mm Hg	180-220mm Hg
Bead-cast graft, non-reinforced	5.21 ± 0.91	5.87 ± 1.68	5.03 ± 0.06	6.02 ± 0.31
Bead-cast graft + PU monofilament at 2.5mm pitch	4.57 ± 0.92	4.92 ± 0.69	1.83 ± 0.30	2.62 ± 0.85
Bead-cast graft + Dorlastan® monofilament at 1mm pitch (single wind)	7.47 ± 3.65	7.13 ± 0.68	4.60 ± 0.33	4.95 ± 0.62
Bead-cast graft + single Dorlastan® reinforcement at 2.5mm pitch + nylon monofilament at 2.5mm pitch	3.25 ± 1.50	2.96 ± 1.49	1.83 ± 0.79	2.69 ± 0.64

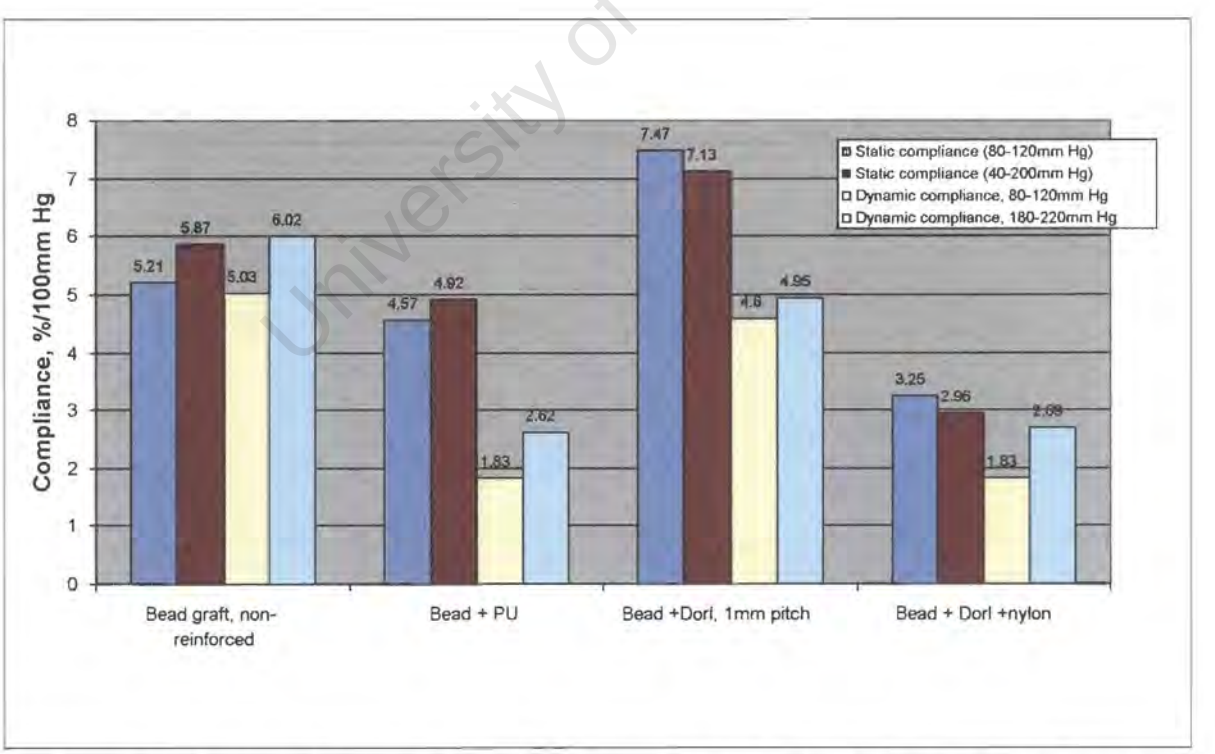

Figure 5.8: Static and dynamic compliance values of the various bead-cast grafts tested. (values in %/100mm Hg)

As with the salt-cast grafts, the bead-cast grafts reinforced with nylon had the lowest compliance as expected (the last set shown in the graph above, with a combination reinforcement of nylon and Dorlastan®. Interestingly, the grafts reinforced purely with Dorlastan also had a higher static compliance than the non-reinforced grafts. The compliance of the non-reinforced grafts was quite close to the 5.87% compliance quoted by Ballyk [28] for human femoral arteries (which are of similar diameter the grafts manufactured in this work). However, this value would probably increase with time after implantation. As with the salt-cast grafts, the values measured for dynamic compliance were generally lower than those measured for static compliance.

5.2.5 Teflon® Commercial Grafts (4mm internal diameter)

Teflon® grafts with a 4mm internal diameter were tested as a means of comparing the compliance values obtained by our apparatus with those obtained by other researchers for this type of graft. Only static compliance testing was measured, since the Teflon® was a very stiff material and the wall displacement under dynamic conditions was very small and could not be measured on the apparatus.

Table 5.7: Static compliance measurements of the commercial Teflon® grafts tested.

Static Compliance	
80-120mm Hg (%/100mm Hg)	**40-200mm Hg (%/100mm Hg)**
3.58 ± 0.94	2.66 ± 0.29

5.2.6 Grafts Tested by Dynatek Dalta® Scientific Instruments, USA.

For the sake of comparison, three graft types were sent to Dynatek Dalta Scientific Instruments, Galena, Missouri, USA. A non-reinforced salt-cast graft, a non-reinforced bead-cast graft and a Salt-cast graft reinforced with nylon at a 2.5mm pitch were sent. They tested only one sample of each graft type, dynamically at 72 beats per minute. Latex inserts were used during testing to prevent leakage. They also supplied dynamic compliance data of the latex inserts. The results supplied were compensated (the effect of the latex had been subtracted) and hence are compared to the dynamic values tested at the elevated pressure range. See table 5.8 and figure5.9 below.

Table 5.8: Compliance values of some of the grafts as measured by Dynatek Dalta USA compared to the dynamic values obtained on the apparatus.

Graft type	Dynatek dynamic radial compliance - %/100mm Hg	Measured dynamic compliance (180-220mm Hg range). - %/100mm Hg.
Non-reinforced salt-cast graft	4.06	5.88 ± 0.46
Non-reinforced bead-cast graft	1.73	6.02 ± 0.06
Salt-cast graft reinforced with nylon at 2.5mm pitch.	4.76	2.72 ± 1.48
Latex insert (Dynatek latex).	28.52	14.24 ± 2.42 *

* Static compliance measured from 80-120mm Hg.

It should be noted that the Dynatek results supplied to us were quoted as a radial compliance and are calculated based on a change in internal volume. The values quoted above however, have been converted to a diameter compliance as used for all the compliance values quoted in this work.

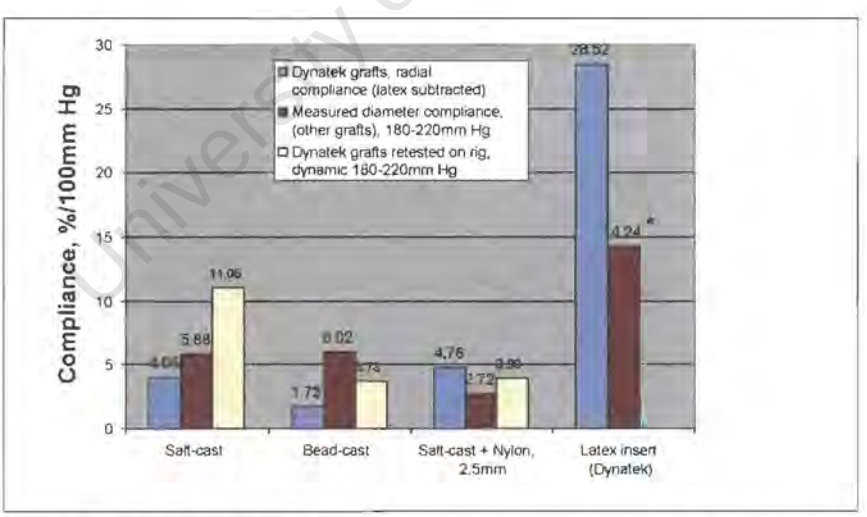

Figure 5.9: Dynatek Dalta® dynamic compliance results compared to the dynamic values measured on the rig.

One can see that the Dynatek results for the salt- and bead-cast grafts are lower than the values measured in this report for the same graft types. They record a higher compliance for the reinforced graft than for the non-reinforced grafts that is quite inexplicable. The compliance of

their latex inserts is quite high (28.52%/100 mm Hg) compared to the measured static values of the Roynhardt inserts used in this project. Unfortunately, these inserts could not be tested dynamically with our method since the latex caused the pendulums to 'bounce' off the graft during dynamic testing, resulting in an erroneous diameter measurement. However, Dynatek latex inserts were tested statically on the rig and compared to the Roynhardt inserts. The Dynatek inserts were more compliant (25.83%/100mm Hg compared to 14.17%/100mm Hg) – see figure 5.10 below. This difference in the compliance of the inserts suggests that their compliance values should be higher, but this is not the case. The difference in their values could be attributed to the fact that they only tested one graft of each type due to the high cost of testing, whereas 3 of each type were tested in this report. Once returned to us, the 3 grafts were re-tested on the compliance rig (see graph above). The retest values were somewhat higher for the non-reinforced salt-cast graft and the nylon-reinforced graft than the values recorded previously for these graft types. This could be attributed to a deterioration in material properties between one test and the next (due to pre-test axial tensioning), or it could just be a more compliant graft and is not representative of an average of a few samples. The non-reinforced bead graft is the stiffest with a compliance of 3.73%/100 mm Hg when tested dynamically in the 180-220mm Hg range, surprisingly stiffer than the reinforced graft. The fact that they record a higher compliance for the reinforced salt graft than for the non-reinforced one is difficult to explain and could have something to do with the way the latex effect is subtracted. Otherwise, their method for calculating compliance is essentially the same, the only difference being that they use a change in internal volume of the graft to calculate compliance.

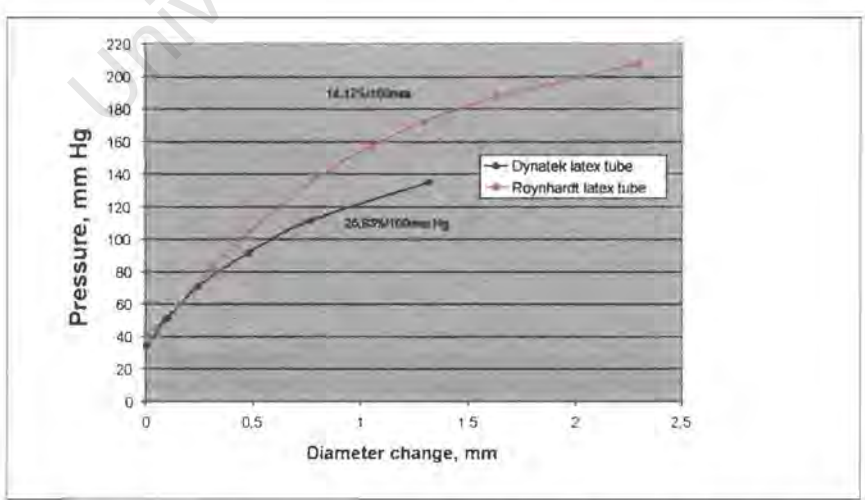

Figure 5.10: Static compliance curves of Dynatek and Roynhardt latex inserts.

5.2.7 Predicted and Measured Compliance:

Predicted theoretical compliance was compared to the static compliance measured over the 80-120mm Hg range, as these are the more accurate compliance values. Using the equations in chapter 2, compliance values were predicted for the reinforced graft to ascertain if one could calculate what the effect of reinforcement would be on the distension of the grafts under pressure. The graft was modelled as a thin-walled cylinder reinforced with single windings at a certain pitch. Hence the number of windings is taken into account when calculating the stiffness of the graft. The material properties used (Young's modulus), were calculated from the stress-strain curves generated by the tensile testing of the porous graft and the fibres. This theory makes use of the equations for thin-walled cylinders:

$$\sigma_h = \frac{pd}{2t} \qquad \sigma_l = \frac{pd}{4t}$$

where σ_h and σ_l are the stresses in the hoop (circumferential) and longitudinal directions respectively and p, d and t are the pressure, internal diameter and wall thickness. This theory assumes that there is no variation of stresses across the wall thickness of the graft. In reality, the stresses in a cylinder wall are always higher at the inside of the wall than the outside, and there is a non-linear stress distribution across the thickness of the wall. Also, the presence of any axial pre-tension on the graft has been ignored. The Young's modulus values obtained from the tensile tests were also assumed to remain constant. Figure 5.11 below depicts the predicted and measured compliance values for several grafts and shows the effect of winding pitch on compliance. The compliance for grafts with latex inserts has also been modelled and one can see that for reinforced grafts, the effect of the latex is less. That is to say, the stronger the reinforcement, the less significant is the effect of the insert on compliance.

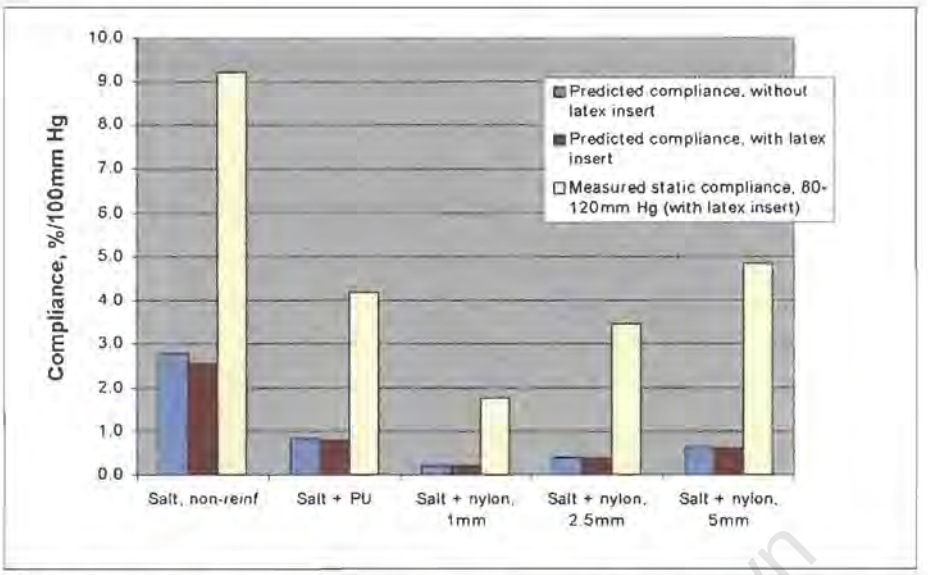

Figure 5.11: Predicted and measured (static, 80-120mm Hg) compliance values of some of the salt-cast grafts.

Although the predicted values are much lower than the measured ones, there is some a correlation between graft stiffness and reinforcing material (the nylon is stiffer than the PU fibre). The effect of winding pitch on compliance may be noted by the grafts reinforced with nylon at 1, 2.5 and 5mm pitches. Hence one can still use the theory as a qualitative tool to see the effect of reinforcing material and structure on compliance. The difference in the values could be most likely attributed to the assumptions made: non-compression of the graft wall, no pre-tension on the windings, and constant material properties. Possibly, the fact that the reinforcing winds were modelled as single and separate rings as opposed to a continuous winding, will be the major contributor to the difference in predicted and measured compliances. A graft with a continuous winding will intuitively be more compliant than one reinforced with separate rings.

5.2.8 Comparison of the Compliance Values of the Reinforced Porous Polyurethane Grafts to Natural and other Synthetic Vessels.

For comparison of the compliance of these grafts with compliance values in other literature, only the static compliance values have been used. The reason for this is that the measured dynamic values are in most cases lower due to the visco-elastic effects of the porous graft material, as well as the fact that dynamic compliance can be shown to be pressure and testing-rate dependent. They are therefore not indicative of a true compliance. Thus static compliances over the 80-120mm Hg physiological range have been used for comparison. Dynamic and static compliance

measurements were collected from several researchers who measured the compliance of some synthetic arterial grafts and also vessels from human and animal models (see "Literature Review", 1.4.3). Rosset et al. [57] found the dynamic compliance of human carotid arteries to be 6.6%, while Ballyk et al. [28], quoted work by Hastings, who published a value of 5.87% for a human femoral artery. Walden [18] measured the compliance of human femoral arteries with a cantilever strain-gauge and found the value to be 5.9%/100mm Hg.

In this project, a static compliance of 3.58%/100mm Hg was measured for the 4mm diameter Teflon® grafts (Dynamic testing yielded very little movement of the graft wall and was below the detectable limit of the apparatus). Other researchers recorded values of 1.63, 2.1 and 0.43% for expanded Teflon® (18,56,58), while Dacron® grafts varied from 1.8%/100mm Hg to 3.4% (18, 28, 38). Guidiceandrea et al. [58] tested a compliant polyurethane graft and recorded a compliance of 12.3%/100mm Hg, which is more comparable to the compliance of the latex tubes measured in this project (14.24% static compliance, 80-120mm Hg range). Others testing polyurethane grafts recorded values of 2.8-6.3%/100mm Hg (Chen et al, 59) and 4.11% (Martz et al, 60). The non-reinforced salt and bead-cast grafts showed static compliances of 9.21 and 5.21%/100mm Hg respectively (at the 80-120mmHg range), indicating the bead-cast structure to be much stiffer than the salt-cast structure. The least compliant graft was the salt-cast graft reinforced with nylon monofilament at a 1mm pitch (1.76%/100mm Hg – static compliance, 80-120mm Hg range). The grafts with possibly the closest-matching static compliance (taking 6%/100mm Hg to be the target compliance), were salt-cast grafts reinforced with a double wrapping of Dorlastan® at 2.5mm pitch and loose wrapping of nylon at 5mm pitch. These had an average static compliance of 6.06%/100mm Hg respectively over the 80-120mm Hg testing range. The other graft type which had a near-matching static compliance were the salt-cast grafts reinforced with a double wrapping of Dorlastan® at 2.5mm pitch (7.77%/100mm Hg). For the salt-cast grafts reinforced with nylon, there seems to be a progression of increasing compliance with winding gap. The grafts with a 1mm winding gap having the least compliance (1.76%) while the grafts reinforced at the 2.5mm pitch had a higher compliance of 3.46% and the grafts at 5mm gap having the highest compliance with a value of 4.84%/100mm Hg over the static 80-120mm Hg range. Therefore, a graft reinforced at an even larger winding gap (perhaps 7mm) could have an even closer compliance to 6%. Figure 5.12 below shows a comparison of the static compliance plots for some of the reinforced grafts compared to the porcine aorta plot. Note that the porcine aorta curve falls in between the non-reinforced salt-cast and non-reinforced bead-cast plots. This gives an indication that salt-cast graft compliance is slightly higher than natural aortic tissue, while the bead-cast graft is slightly less compliant.

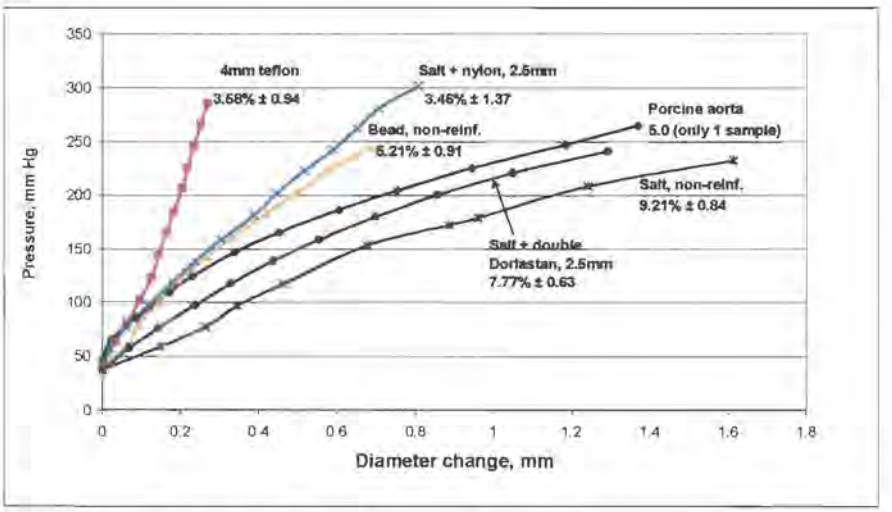

Figure 5.12: Static compliance curves of some of the grafts tested compared to the porcine aorta and 4mm commercial Teflon® grafts.

Note the plot for the salt-cast graft reinforced with a double winding of Dorlastan® has a closer static compliance plot to the porcine aorta sample, and being above the non-reinforced plot indicates it to be slightly stiffer than this graft type.

5.2.9 Notes on Static Compliance Testing

For static testing, it was found necessary to prime the grafts with about 40mm Hg in order to prevent any irregularities in the graft shape from influencing the readings. For most graft types the static results were quite reproducible from one sample to the next, with some exceptions, which could be attributed to differences in quality of the porous grafts (often some defects are introduced during manufacture of the grafts). These differences were particularly noticeable in the bead-cast grafts, with some large variation in the shape of the static curves. This could be attributed to some non-homogeneity in the cast structure. During casting, there are several factors that could influence the flow of polymer through the column of beads (see 3.2 "Manufacturing techniques"). For example the packing of the beads in the column might not be optimal and might result in some variations of homogeneity. However, only the best graft samples were chosen for testing. Despite this there are always some defects. Another factor that could affect the compliance results is the quality of the latex liners. From the static testing of these tubes one can see that there is some variation in the pressure-diameter response of the liners. Since these were made by a dipping process, there is always a chance of the wall thickness not always being the same for different tubes. Static compliance was calculated over the 80-120mm Hg range, as well

as over the total applied pressure range. In all graft types, the total compliance values were higher than those in the 80-120mm range, indicating that the grafts appear stiffer or less compliant at lower pressure values. This is corroborated by the static compliance curves, which show a decreasing gradient with increasing diameter. One would expect the opposite to occur. Most probably, a stiffening of the graft wall might occur at much higher pressures (ie. above 300 or 400mm Hg), but the apparatus would not have been able to measure above such pressures, since the linear variable displacement transducers (LVDT) were only capable of measuring up to a certain diameter. It should be pointed out that for the static tests, the pressure was increased to the maximum measurable diameter. For the non-reinforced grafts and those reinforced with Dorlastan®, this maximum pressure was usually around 200-260mm Hg, while those grafts with stronger reinforcing (nylon, PU) were tested to higher pressures (up to 300 mm Hg). If it had been possible to test up to higher pressures, perhaps a change in the shape of the pressure-diameter curve might have occurred, and indeed this is expected, particularly in the case of the reinforced grafts. Figure 5.13 below shows a graphical comparison of the static compliance values measured for the various salt-cast and bead-cast grafts.

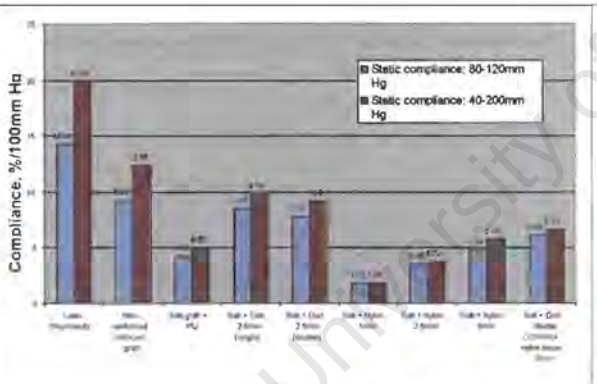

Static compliance values of latex tubes, salt-cast grafts.

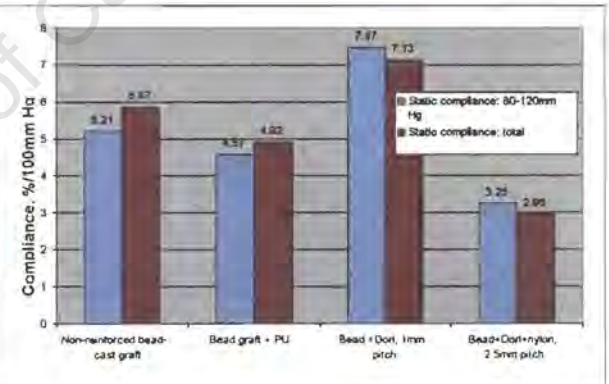

Static compliance values of bead-cast grafts.

Figure 5.13: Static compliance values of latex inserts, salt-cast and bead-cast grafts

5.2.10 Notes on Dynamic Compliance Testing

Dynamic compliance testing was carried out on the grafts at two pressure ranges: 80-120mm Hg range and 180-220mm. Reproducing the exact diastolic and systolic pressures for consecutive tests was found to be quite demanding, since the pressure regulator for the pressure vessel and the pinch valve had to be re-adjusted for each test. Also, since the pressure vessel acts essentially as a

reservoir, and there is no return flow into it, one has a limited volume to pump through the graft. This means a reduced testing time is available and adjustment of the diastolic and systolic pressures has to be done within this time, until the correct pressure curve is obtained (see 4.2.2.2 "Operation of the fluid circuit"). It was found however, that the shape of the pressure curve was quite reproducible for consecutive tests, even though the diastolic and systolic pressures might vary by up to 10-15 mm Hg between tests. For most graft types, compliance values were slightly higher in the 180-220mm Hg range compared to the 80-120mm Hg range (see figure 5.14 below). Again, as with the static tests, one would expect this to be the opposite, and especially the reinforced grafts should show a decrease in compliance with pressure. For comparative purposes, the values at the higher pressure range were used, since the effect of the latex liners is being compensated for. Mid-graft pressure was calculated by averaging the peak proximal and distal pressure values, obtained from each of the two pressure transducers. Because of the distension of the graft during a pulse, the pulse distal of the graft is always characteristically dampened and is always lower than the systolic pulse. When adjusting the pressure regulator and pinch valve, it was necessary to adjust the curves according to the average pressure, ie a point between the systolic and diastolic pressure traces. The dynamic compliance is therefore calculated mid-graft since the diameter measurement is also taken at this position.

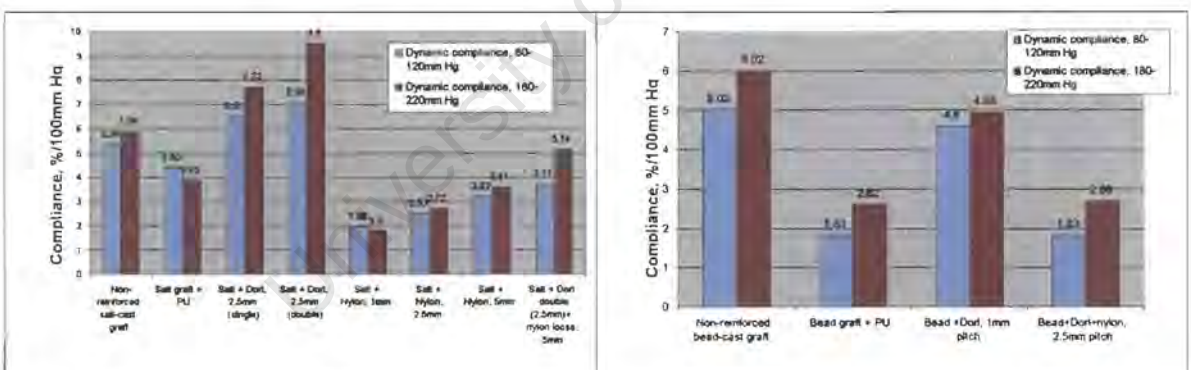

Dynamic compliance of salt-cast grafts. | Dynamic compliance of bead-cast grafts.

Figure 5.14: Dynamic compliance values of salt-cast and bead-cast grafts.

Figure 5.15 below show different diameter traces for some of the grafts tested compared to the dynamic tests conducted on the porcine aorta samples. Note how stiff the 4mm commercial Teflon® grafts are compared to the aorta, indicated by the small amplitude of the diameter waveform.

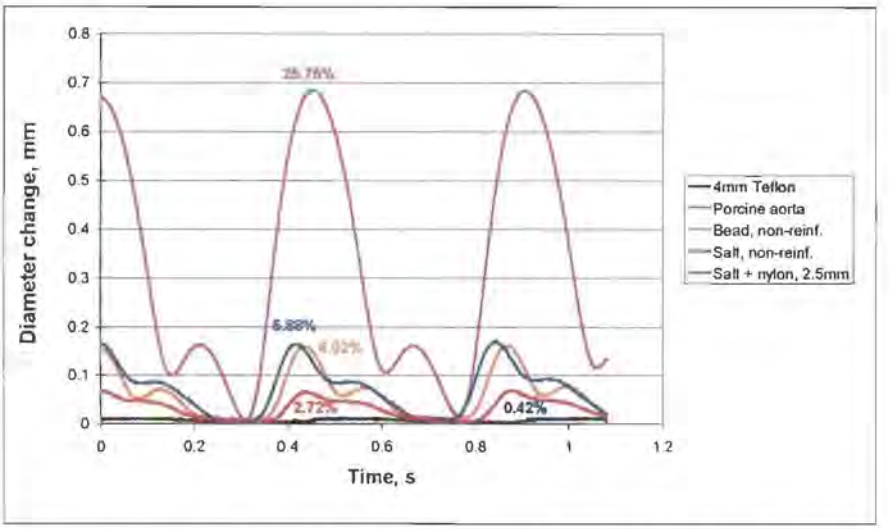

Figure 5.15: Diameter curves from the dynamic tests of some of the grafts tested compared to the Porcine aorta and 4mm commercial Teflon® grafts (Dynamic tests conducted at the elevated 180-220mmHg range).

The visco-elasticity of the grafts is also demonstrated by the time lag of the pressure and diameter curves. The diameter curve always lags slightly behind the pressure curve due to stress-time effects. A perfectly elastic material would respond immediately to an increase in pressure, and it was evident that the more compliant grafts also followed the pressure curve closely, whereas the less compliant grafts tended to exhibit a smaller-amplitude diameter curve. The more compliant graft is distinguished by its large-amplitude diameter curve (for comparison see figure 5.17).

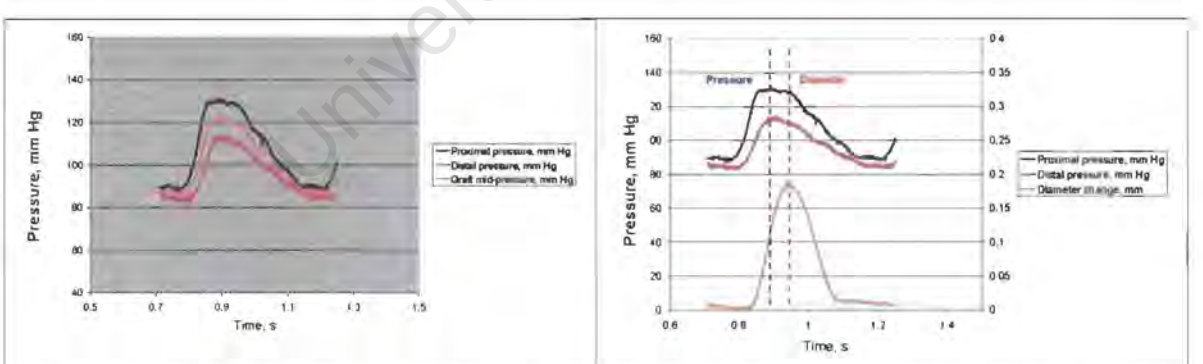

Extrapolation of the mid-graft pressure from the proximal and distal pressure curves

The time lag of the diameter curve in relation to the pressure curves

Figure 5.16: Calculation of the mid-graft pressure and time lag of the pressure and diameter waveforms.

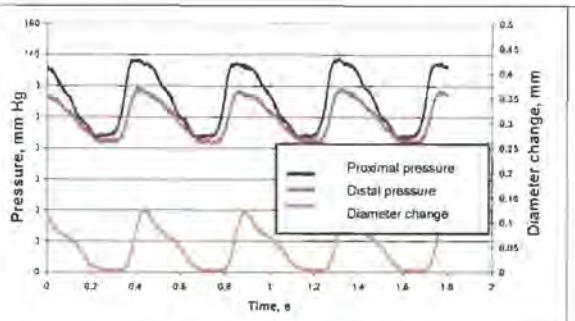

6mm non-reinforced salt-cast graft tested dynamically at the 80-120mm Hg range (proximal, distal pressure in blue, pink, diameter in yellow)

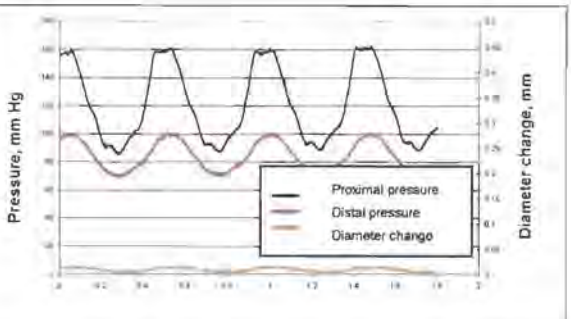

4mm Teflon® commercial graft tested at 80-120mm Hg range

Figure 5.17: Comparison of dynamic compliance curves of a non-reinforced salt-cast graft and a commercial 4mm Teflon® graft.

The effect of testing rate on compliance was evaluated on only one set of grafts: the non-reinforced salt-cast grafts. Although one would expect a decrease in compliance at higher testing rates because of the visco-elastic behaviour of the grafts, there is actually an increase in compliance, as demonstrated in figure 5.18. Conti, Strope et al [45] tested the effect of testing rate on compliance of latex tubes and found a decrease in compliance with increased testing rates, although it should be pointed out that they tested up to much higher frequencies (72 – 2700 bpm). Despite this, they show a decrease in compliance in the samples tested at 72bpm and 400 bpm. The compliance decreases further up to a rate of 1600bpm and then increases again. The possible cause of this, suggested by Conti and Strope [45], could be a harmonic oscillation in the system ie. there might be some resonance at certain frequencies that coincide with the natural frequency of the graft being tested. This could explain for a decrease and then increase in compliance. Of course this would depend on the graft material. The apparent increase in compliance of the salt-cast grafts could be explained by the inertia of the diameter measuring system. The two pendulums which make contact with the graft wall are fairly heavy, and at higher testing rates, the fast-moving pulse passing through the graft could cause the pendulum to 'bounce' off the side of the graft wall. This would cause it to move to a larger diameter and would account for an increase in the transducer reading. This effect could be slightly reduced by increasing the angle at which the pendulums made contact with the graft (by winding the micrometer screws in), thereby improving the response of the pendulums. Ideally, one requires a non-contact measuring system, whereby the measuring device does not interfere with the graft wall movement.

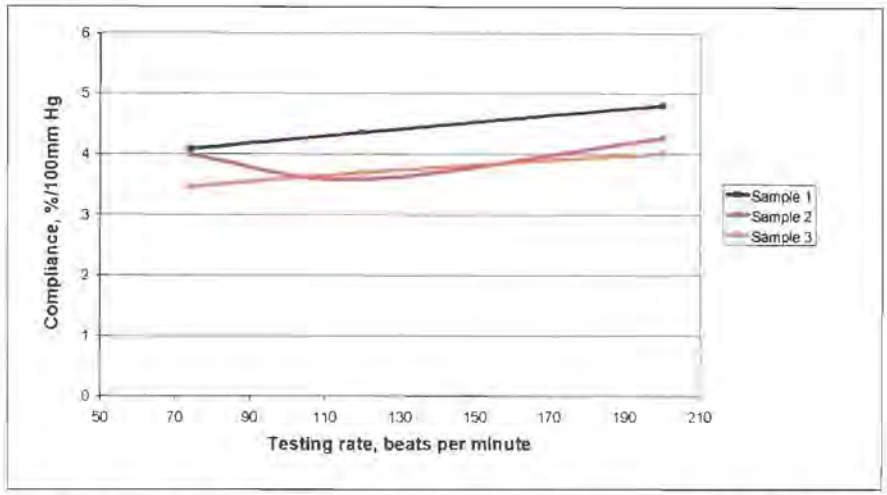

Figure 5.18: The effect of testing rate on compliance of salt-cast grafts with no reinforcement.

5.2.11 The Effect of Reinforcing Structure on Compliance (wind angle, number of windings).

The effect of winding angle (winding gap/pitch) on compliance was determined by the set of nylon-reinforced salt-cast grafts. Grafts were reinforced with wind gaps of 1, 2.5 and 5mm respectively. The results show a definite increase in compliance with larger winding gap, although it is not quite proportional (see figure 5.19 below). Obviously, a smaller wind gap means more reinforcing winds per length of the graft and this would increase the graft stiffness, hence decreasing compliance. Grafts reinforced at a larger wind gap than 5mm might have an even closer-matching compliance to the 6% of a human femoral artery. Salt-cast grafts were also reinforced with single and double traverses of Dorlastan® 33 dtex monofilament, at a single winding pitch value (2.5mm). If one looks at the results, there is not much difference between the compliance values of the single and double-wound grafts. The static compliance values over the 80-120mm Hg range were quite close (8.47% and 7.77% respectively), but slightly stiffer than the non-reinforced salt-cast grafts which had compliance of 9.21%. The reason for the values being close could be that the Dorlastan® was a very fine fibre and thus did not have much effect on the stiffness of the graft. That is to say that there might have been comparatively little effect on compliance by double-winding (see figure 5.19 below).

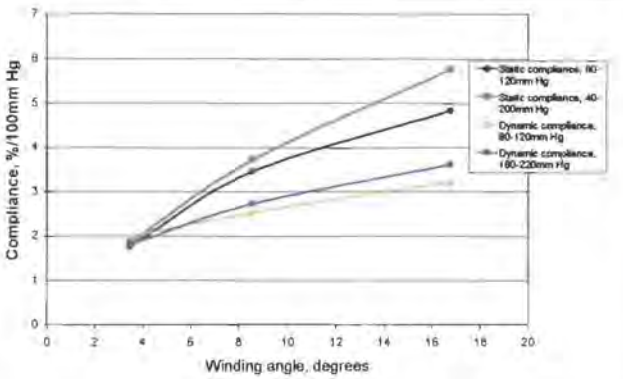

A plot of compliance vs. winding angle for the nylon-reinforced salt-cast grafts, showing a definite increase in compliance with winding angle.

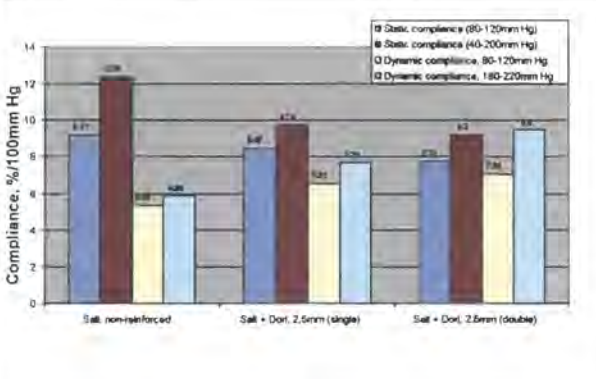

Static and dynamic compliance values of non-reinforced, single- and double-wound Dorlastan reinforced salt-cast grafts

Figure 5.19: Variance of compliance with winding angle and comparison of the compliance values of non-reinforced, single-and double- wound Dorlastan® reinforced salt-cast grafts.

5.2.12 The Effect of Reinforcing Material on Compliance

As shown by the uniaxial tensile tests, the nylon fibre is stiffer than the polyurethane fibre. The compliance values of the grafts reinforced with these two fibres reflect this difference in elastic modulus. The salt-cast grafts reinforced with PU had a higher compliance (were less stiff) than those reinforced with nylon (both at the same wind pitch:2.5mm), The salt-cast grafts with nylon at 2.5mm had an average static compliance of 3.46%/100mm Hg (in the 80-120mm Hg range), while the salt grafts with PU had a value of 4.18% for the same test (see figure 5.20 below). The dynamic tests also yielded lower compliance values for the nylon grafts. The Dorlastan® reinforcing had a comparatively small effect on compliance, the single- and double- reinforced salt-cast grafts showing static compliances over the 80-120mm range of 8.47% and 7.77% respectively compared to the 9.21% of non-reinforced grafts. The reason for this was that the elastane fibre was much weaker than the nylon and PU fibres, and was also much smaller in diameter. For Dorlastan® to have more effect on compliance, a thicker fibre would have to be used, or alternatively more windings applied to the graft.

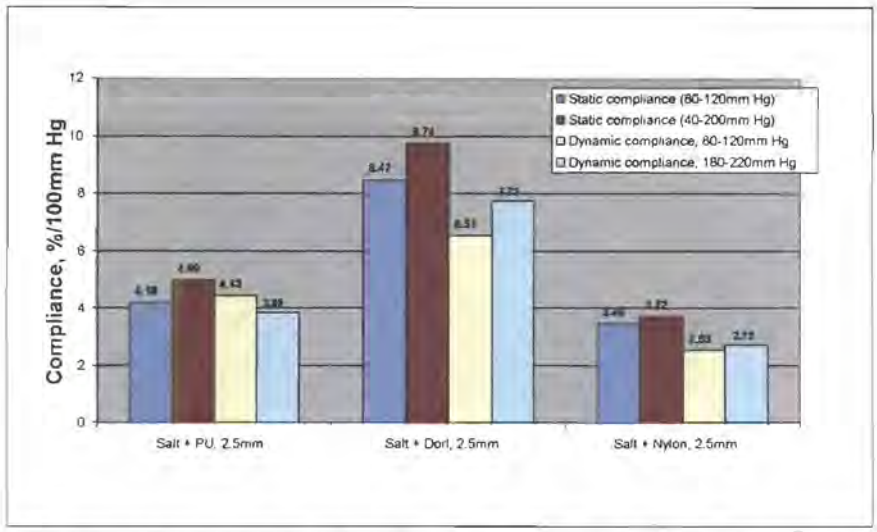

Figure 5.20: Compliance values of grafts reinforced with PU, Dorlastan® and nylon

5.2.13 The Variation of Compliance with Pressure

From the static compliance curves generated, it is evident by the shape of the curve that the rate of diameter change increases with pressure. That is to say, by plotting diameter as a function of pressure, the gradient of the curve increases with pressure. This means that compliance actually increases with pressure. This was evident in all the grafts tested. As mentioned earlier, the static testing was only performed up to about a maximum of 300mm Hg, so what happens after that cannot be ascertained. One would expect that the compliance begins to decrease at a certain pressure level. From two sets of grafts, the pressure-diameter curve was plotted. From the sample judged to be the average of the three tested, a best-fit second-order polynomial was plotted. The first derivative of this curve was taken to give the compliance as a function of pressure. See figure 5.21 below for details.

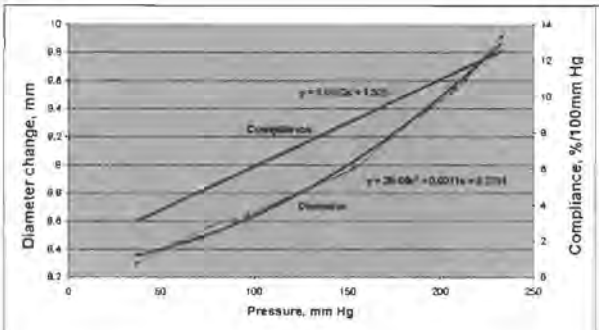

Non-reinforced salt-cast graft: diameter vs pressure and compliance vs. pressure.

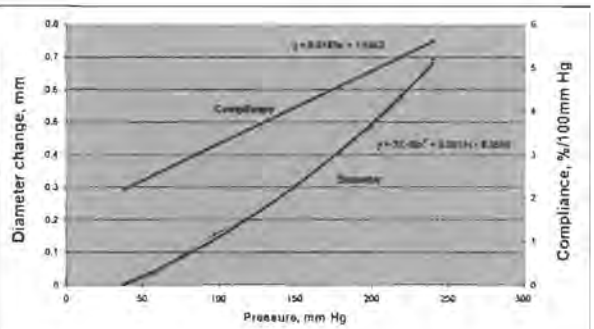

PU-reinforced salt-cast graft: diameter vs pressure and compliance vs. pressure.

Figure 5.21: Variation of diameter with pressure and compliance vs. pressure for non-reinforced and PU-reinforced salt-cast grafts.

Note that the gradient of the compliance plot is higher for the non-reinforced graft than the reinforced one. This means that the compliance of the reinforced graft increases more slowly than the non reinforced one, as expected, indicating greater stiffness.

5.2.14 Compliance of the Combination-reinforced Grafts

To improve the compliance of salt- and bead-cast grafts, they were first reinforced with single materials (PU, nylon, Dorlastan®), and then with a combination of Dorlastan® monofilament and nylon. The reason for using a combination of materials was to try and replicate the response of a natural adventitia, which has two distinctly different material components. The bead cast grafts were reinforced with a single wind of Dorlastan® at a 2.5mm pitch and a single wind of nylon also, at the same pitch. The nylon winding bisected the Dorlastan® winding and both fibres were secured to the graft surface by 'gluing' them with polyurethane solvent. The salt grafts were reinforced in a similar manner, but instead having 2 traverses of Dorlastan at 2.5mm and a single loose winding of nylon at a 5mm pitch, attached only at the ends of the graft to prevent unravelling. The reasoning for this was to try and imitate the response of elastin and collagen, the elastin taking up the initial stress and the collagen 'arresting' the graft distension at a certain pressure. The bead-cast grafts with this reinforcement had quite a low compliance (1.91%/100mm Hg static 80-120mm Hg range, and 1.46 %, dynamic 80-120mm Hg range), while the salt grafts had a higher compliance (4.38%, 2.68% for the same two tests respectively). Wrapping the nylon loosely around the salt graft was deemed unsuccessful, as the windings did not remain at a constant pitch and tended to shift along the length of the graft.

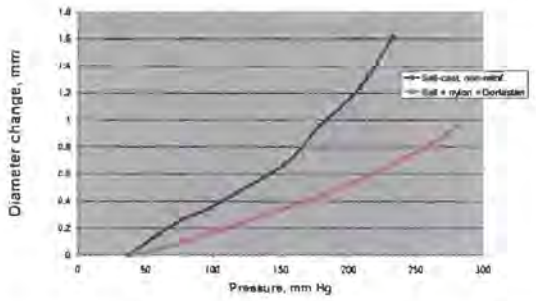

Static compliance plots of non-reinforced salt-cast graft compared to the graft reinforced with double Dorlastan winding at 1mm pitch and loose nylon fibre at 5mm pitch

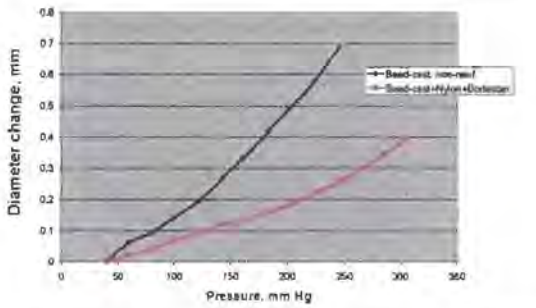

Static compliance plots of non-reinforced bead-cast graft compared to the graft reinforced with a single Dorlastan winding at 2.5mm pitch and single nylon fibre at 2.5mm pitch

Figure 5.22: Comparison of the static compliance plots of non-reinforced and reinforced salt and bead-cast grafts.

By comparing the static compliance plots in figure 5.22 above, it is easy to see the effect of reinforcement on the compliance: the non-reinforced grafts increase more in diameter per pressure increase, and are over-compliant. The reinforced grafts are about 50% less compliant, as indicated by the lower gradient of the curve. There is no sharp transition point on the curve where the nylon fibre comes into play however. This is most likely due to a to a longitudinal stress change, and being under a pre-tension, the increase in circumferential stress will result in a relaxing of the longitudinal stress. Hence some of the circumferential stress will be absorbed and the effect of the reinforcing will be less noticeable.

5.2.15 Reproducibility of the Compliance Results.

Results for static and dynamic compliance tests were found to be quite reproducible, although the correct setting up of the apparatus is very important (especially dynamic testing, where it is important to test at the same pressure ranges each time). A variation in the shape of the static pressure-diameter curve between samples is most likely the result of a variation in the properties of the porous graft. Only the best porous grafts were chosen for testing, but despite this, there are still some variation between the quality of one graft and the next. Often this is due to irregularities in the cast structure, (which mostly occur in the case of the bead-cast grafts). The curing and washing of the grafts is also important, as the amount of curing time will affect the strength of the polyurethane. Proper washing of the bead-cast grafts is important to ensure that all the pore-forming material (gelatin or salt) is extracted from the porous matrix. Residual gelatin will also

result in a variation in properties also. In this project, all bead and salt-cast grafts were cured and washed for equal periods, long enough to ensure the proper extraction of the pore-forming agent and curing of the polyurethane. In general most results were quite reproducible.

5.2.16 Sources of Error During Compliance Testing

While the effect of the latex inserts on the compliance measurements has been mentioned, there are other influences that could affect the readings obtained.

5.2.16.1 Linearity of the Linear Variable Displacement Transducers (LVDT) and the Measuring Pendulums.

The manufacturers specify a degree of linearity of the devices up to a certain range of movement. Since the range of movement of the graft walls was relatively small, this effect is negligible. However, there might also be a small amount of error associated with the radial movement of the measuring pendulums as the graft wall distends outwards (see figure 5.1 below). This means that the point of contact of the pendulums on the graft wall changes as the graft dilates, and this will result in some error in the actual diameter measurement

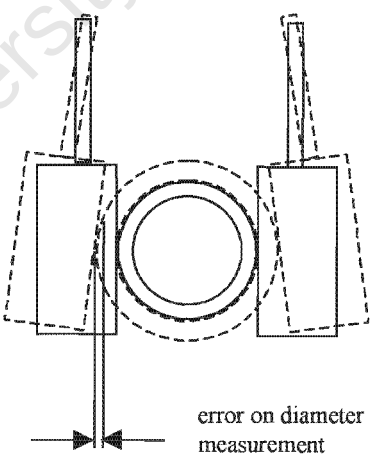

Figure 5.23 Source of error during diameter measurement of a distending graft.

One can calculate the percentage of error this would represent:

Assume a graft has a 6%/100mm Hg compliance in the 80-120mm Hg pressure range. Using a graft with an initial diameter of 8mm, this would translate to an increase in diameter of 0.192mm. Assuming the pendulums are deflected equally, this means 0.192÷2=0.096mm on each side. Now the amount of error can be defined as follows:

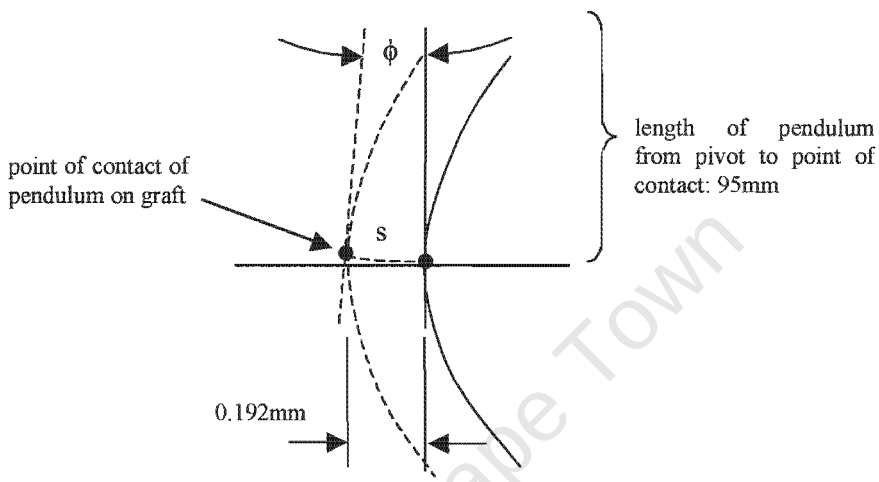

Figure 5.24: Calculating the percentage of error on the diameter measurement.

If ϕ is the angle subtended by the movement of the pendulum and s is the associated arc length, then the error will be:

actual diameter change (0.192mm) – arc length, s

Now, the arc length, s can be calculated from: $s = r \,.\, \phi$

where ϕ is in radians and r is the pendulum length (95mm).

And ϕ can be calculated using simple trigonometry from:

$$\tan \phi = \frac{0.192}{95} \Rightarrow \phi = 0.00202 rad$$

Therefore, s, the arc length is: $0.00202 \times 95 mm = 0.19199 mm$

Hence the error will be:

0.192mm – 0.19199mm = 0.00001mm (=0.0052% error)

As one can see, the error is very small indeed, but for larger deflections, would play more of a role.

5.2.16.2 Compression and Kinking of the Graft Wall During Testing

Since the diameter measurements were taken on the outside of the graft, compliance values were based on this measurement, and values were calculated based on the original internal diameter of the graft. There might be some resistance to the graft wall movement, due to the weight of the pendulums, and this might cause an indentation or kinking of the wall which would affect the diameter measurement (figure 5.25). Thinning of the wall will also occur during pressurisation, and therefore the measured outside diameter will not reflect the true increase in internal diameter (figure 5.25). Yeoman [56] in his thesis on modelling a fabric-reinforced graft, predicted a wall compression of 8.5% for a fabric-reinforced salt-cast graft at 100mm Hg. But it should be noted that this was a finite element model and one would have to correlate this value with biaxial test data to determine the actual amount of lateral compression when the material is tensioned (Poisson effect). However, the effect is real and will have some effect on the diameter measurements. A value of 0.3 for the Poisson's ratio was used in calculating the predicted compliance. This value was also obtained from Yeoman [56] who modelled the response of the same porous grafts using computational methods.

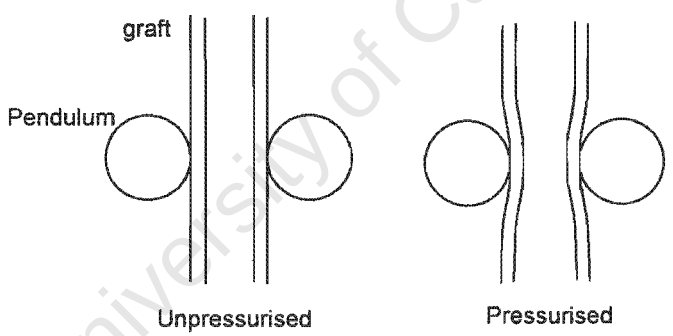

Figure 5.25: Kinking of the graft wall during testing

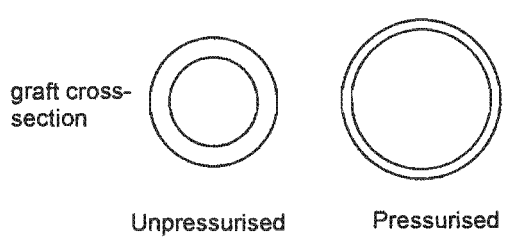

Figure 5.26: Compression of the graft wall when pressurised internally

5.3. BURST TESTING

5.3.1 Samples and Method

Burst testing was performed on selected grafts to ascertain the maximum internal pressure that they could stand until rupture (see table 5.9 below). Samples were inflated with water using the same apparatus as for compliance testing. Three samples of each graft type were tested and an average burst pressure calculated. In all cases latex liners were used to prevent leakage of the grafts. The graft was deemed to have failed once the wall had ruptured due to expansion of the latex liner. Grafts with strong reinforcement (nylon) and small winding pitch (1mm) or the combination reinforcements (nylon, Dorlastan®) were not tested due to the fact that very high pressures would have been needed to burst them. This would have exceeded the integrity of the fluid circuit (pressures above about 700mm Hg caused some leaking of the fittings in the circuit).

5.3.2 Results

Table 5.9: Bursting pressures of the grafts tested.

Graft type	Average bursting pressure, mm Hg
Salt-cast, non-reinforced	389.28 ± 33.15
Salt-cast + PU monofilament at 2.5mm pitch	525.32 ± 13.56
Bead-cast graft, non-reinforced	433.89 ± 3.59
Bead-cast + PU monofilament at 2.5mm pitch	652.22 ± 27.96
Bead graft + 33 dtex Dorlastan® at 1mm pitch	458.49 ± 37.81

The bead grafts reinforced with PU monofilament showed the highest failure strength of those tested, bursting at an average of 652mm Hg internal pressure (85.8 kPa). The strongly-reinforced grafts could well have burst strengths of in excess of 800mm Hg. Salt grafts reinforced with PU and at the same pitch showed a lower burst strength and this can be attributed to the weaker porous salt-cast structure. Non-reinforced bead-cast grafts were also stronger than the non-reinforced salt-cast grafts, with bursting pressures of 433.88 and 389.28mm Hg respectively. The

increase in strength offered by a Dorlastan reinforcement at 1mm wind pitch was only 25mm Hg, as evident from the testing of the bead-cast grafts reinforced this way. The non-reinforced grafts all failed in the circumferential direction, forming a tear line parallel to the longitudinal direction (see figure 5.27 below). This is expected, as the stress in the circumferential direction for thin-walled cylinders is always twice that in the longitudinal direction, as can be seen from the equations for thin-walled cylinders used before:

Circumferential or hoop stress:

$$\sigma_{\text{circ.}} = \frac{pd}{2t}$$

Longitudinal stress:

$$\sigma_{\text{long.}} = \frac{pd}{4t}$$

where p = internal pressure, d = tube diameter, t = wall thickness.

Therefore, σ_{circ} is always 2 x σ_{long} for any given pressure in the same graft.

In comparison, all the reinforced grafts failed perpendicular to the longitudinal axis, generally splitting between the windings. This is to be expected as the pressure will exceed the longitudinal strength of the graft before it is high enough to break the reinforcement.

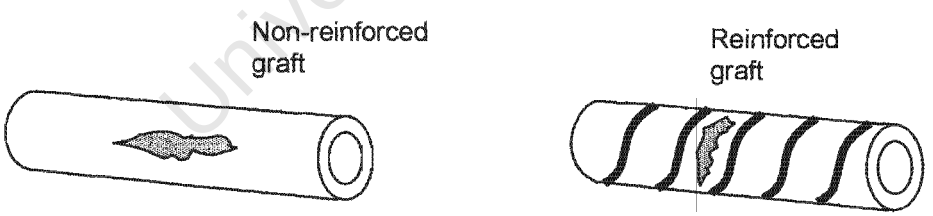

Figure 5.27: Modes of failure of the non-reinforced and reinforced grafts.

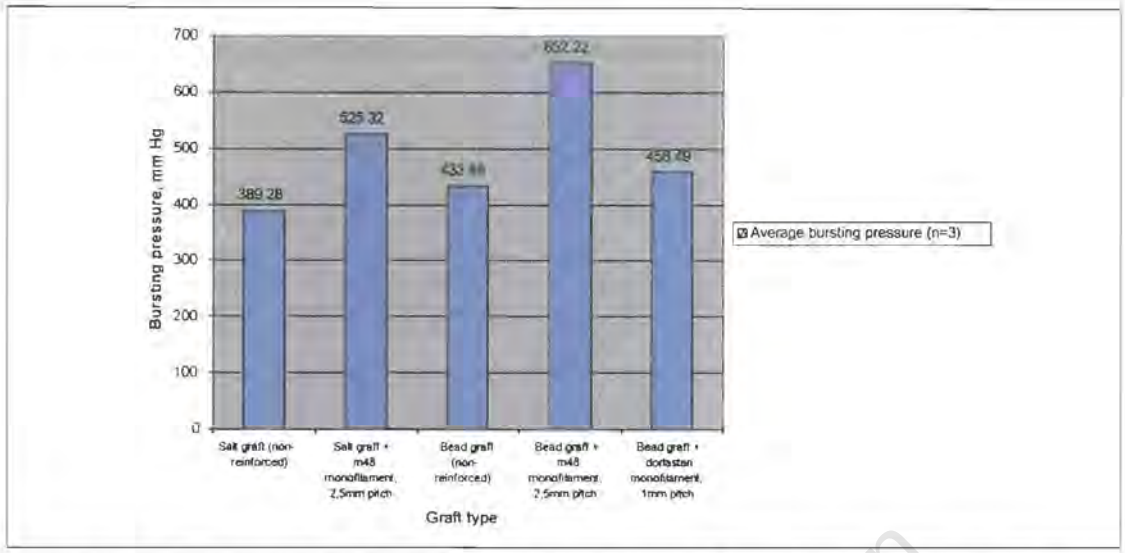

Figure 5.28: Burst pressure values of some of the non-reinforced and reinforced grafts.

5.4 CREEP TESTING (EXTENDED DYNAMIC TESTING) AND THE EFFECT OF TEMPERATURE ON COMPLIANCE

An extended dynamic test was performed on four graft types: a non-reinforced salt-cast graft, a salt-cast graft reinforced with a double winding of Dorlastan® filament, a bead-cast graft reinforced with a combination of Dorlastan® at 2.5mm pitch and nylon at 2.5mm pitch, and a bead-cast graft reinforced with polyurethane monofilament at 2.5mm pitch. This was to ascertain the effect of continued dynamic testing on the compliance of a non-reinforced graft at 37 deg. C and compare it to three reinforced grafts. Data sampling was taken at 0, 10, 20, 30, 60, 120 minutes, 4 hours and 20 hours. Testing was performed at the 80-120mm Hg pressure range. The change in original relaxed diameter was also measured. This was found to be an increase of 2.8% on the original diameter of 8.3mm on the non-reinforced graft and 2.86%, 3.15%, and 6.31% for the reinforced grafts respectively. As can be seen from the figures below, there is an increase in compliance of all the grafts tested. The compliance of the non-reinforced grafts showed an increase of 51.5%, the compliance at the start of testing being 4.95%, after 20 hours being 7.5%/100mm Hg. This proves the need for an adventitial reinforcement, especially in the case of the porous PU grafts, as they would most likely fail after only a short implant period. The reinforced grafts also showed an increase in compliance over the 20-hour period, and even the combination-reinforced bead-cast graft and polyurethane-reinforced graft seem to show an ever-increasing compliance. In the case of the combination-reinforced graft, this could be due to deterioration of the properties of the nylon fibre (nylon exhibits a degradation of mechanical

strength when immersed in water). The Dorlastan®-reinforced salt-cast graft seems to show a levelling-out of compliance after about 2 hours and is more stabilised, the values at 2 hours, 4 hours and 20 hours being 8.33%, 8.95% and 8.51%/100mm Hg respectively. So, although the compliance has increased significantly, it seems as though the reinforcement has prevented any further distension of the original diameter. Also, the polyurethane-reinforced graft seems to show a stabilised compliance of about 4.5%/100mm Hg after 2 hours of testing, after starting with a low compliance of 1.84%/100mm Hg. One would have expected after continued testing that the reinforced grafts would show 'bulging' between reinforcements as the porous material weakened, but this phenomenon was not really significant.

5.4.1 Non-reinforced Salt-cast Graft

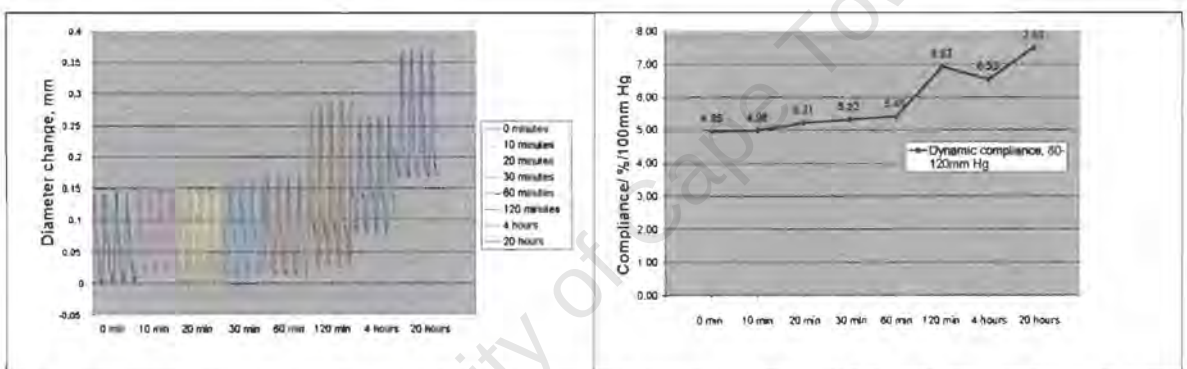

Increase in compliance with time of a non-reinforced salt-cast graft

Increase in compliance with time of a non-reinforced salt-cast graft – compliance values

Figure 5.29: Increase of dynamic compliance with time of non-reinforced salt-cast grafts.

5.4.2 Salt-cast Graft Reinforced With a Double Winding of Dorlastan® elastane monofilament

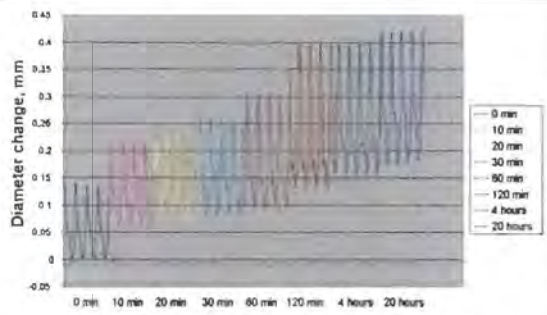

Increase in compliance with time of a Dorlastan® reinforced salt-cast graft

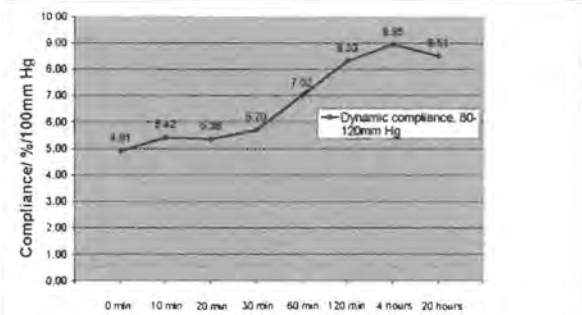

Increase in compliance with time of a Dorlastan® reinforced salt-cast graft – compliance values

Figure 5.30: Increase of dynamic compliance with time of Dorlastan®-reinforced salt-cast grafts.

5.4.3 Bead-cast Graft Reinforced with Single Winding of Dorlastan® Elastane Monofilament at 2.5mm Pitch Plus Single nylon Reinforcement at 2.5mm.

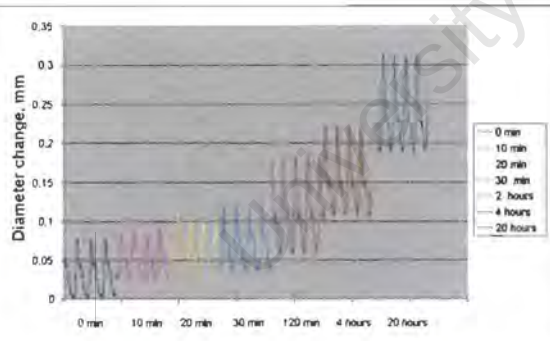

Increase in compliance of a bead-cast graft reinforced with a combination of Dorlastan® and nylon

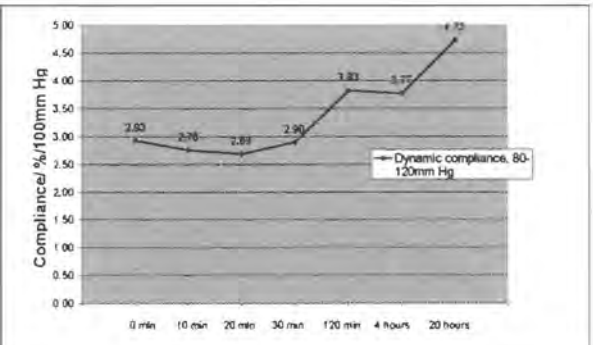

Increase in compliance of a bead-cast graft reinforced with a combination of Dorlastan® and nylon – compliance values

Figure 5.31: Increase of dynamic compliance with time of combination-reinforced bead-cast grafts.

5.4.4 Bead-cast Graft Reinforced with Single Winding of 290μm Polyurethane Monofilament at 2.5mm pitch.

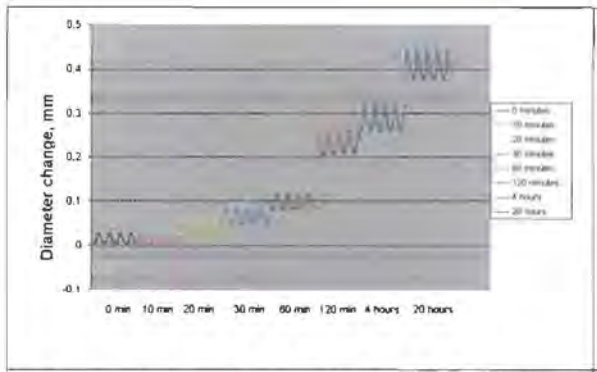

Increase in compliance with time of a bead-cast graft with a single PU reinforcement at 2.5mm pitch

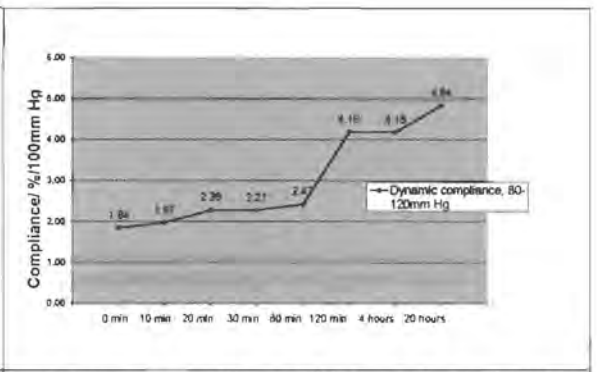

Increase in compliance with time of a bead-cast graft with a single PU reinforcement at 2.5mm pitch – compliance values

Figure 5.32: Increase of dynamic compliance with time of PU-reinforced bead-cast grafts.

5.4.5 The Effect of Temperature on Compliance.

The effect of temperature was also examined, by testing a non-reinforced salt graft. Testing compliance at 22 deg. C and 37 deg. C yielded a 67.3% increase in compliance, from 3.09% to 5.18%/100mm Hg respectively. Interestingly, this is almost in proportion to the 68.2% temperature increase but this could be coincidental. Also, this affirms the importance of testing at realistic temperatures when measuring compliance of the grafts.

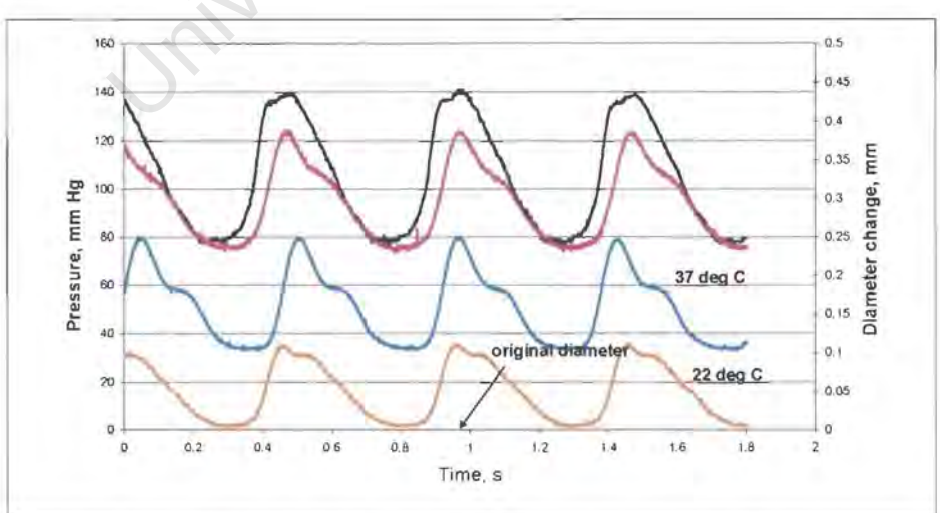

Figure 5.33: Increase in compliance with temperature.

5.5 SUTURE RETENTION TESTING

These tests were performed merely as a way of determining the suturability of the grafts, and what force would be needed to tear the graft with a suture passing through the graft wall. In the case of the reinforced grafts, the suture passes through at least two windings near the cut edge of the graft. Tests were conducted on the Instron tensile testing apparatus at a strain rate of 150mm/min. The non-reinforced salt grafts proved to be the weakest, with an average pull-out strength of 1.59N, while the non-reinforced bead graft gave a value of 3.28 (n=3). Again this is proof of the bead-cast structure being stronger than the salt-cast one. The strongest grafts tested were the bead-cast grafts reinforced with the PU fibre at 2.5mm pitch, with a suture pull-out load of 4.89N. One could also modify this test to see how well the reinforcing is 'glued' to the graft surface, by using the apparatus to pull the winding off the graft surface.

Table 5.10: Average failure strengths of the suture pull-out tests for some of the grafts tested.

Graft type	Average tearing strength, N
Salt-cast, non-reinforced	1.59 ± 0.19
Salt-cast + PU monofilament at 2.5mm pitch	3.52 ± 0.37
Bead-cast graft, non-reinforced	3.78 ± 1.33
Bead-cast + PU monofilament at 2.5mm pitch	4.89 ± 0.59
Bead graft + 33 dtex Dorlastan® at 1mm pitch	3.28 ± 0.58

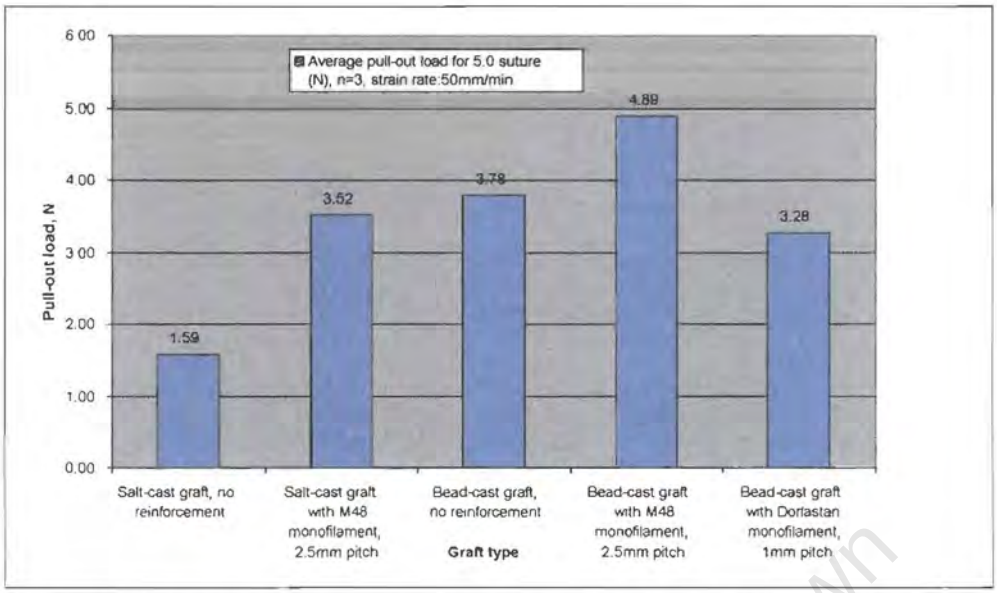

Figure 5.34: Suture retention strengths of some of the reinforced grafts tested.

6. Conclusions and Recommendations

This project provided some good insight as to the effect of reinforcement on porous polyurethane grafts. The effect of winding structure (winding pitch, number of traverses) and winding material is reflected by the compliance results obtained.

6.1 ANALYSIS OF THE COMPLIANCE RESULTS.

From the results obtained in this project, the intuitive correlation between graft reinforcement and compliance is confirmed. It was shown both mathematically and experimentally that there is a relation between compliance and winding angle of the reinforcement, as well as the type of reinforcement used.

6.1.1 Successful Modelling of a Synthetic Adventitia.

Although the focus of this project was on producing a synthetic adventitia, it was found that the compliance depends largely on the properties of the underlying porous graft. It was therefore difficult to appraise the properties of the synthetic reinforcement separately. Having shown the variation of compliance with winding angle and reinforcing material, and having shown that one can also to some degree predict the resulting compliance, one could manufacture grafts with specific compliance. That is to say, if a graft with a certain compliance is required, one could manufacture such a graft by adjustment of the reinforcing material and structure (winding angle). Although the mathematically predicted compliance was much lower that the actual measured compliance, one can see that the measured and predicted values follow each other quite well, and one could hence determine the ratio between the two. Thus one might be able to predetermine the compliance of a graft before it is manufactured, if one knows the reinforcing material and winding angle. Although the derivation of the formula for predicted compliance excludes any pre-tension during winding of the reinforcement, this effect could be added into the equation.

6.1.2 Variability of the Compliance Results

One can see from the results that there is some degree of variation, and there are some high standard deviations from the mean. In the case of the static tests, this depends largely on the shape

of the pressure-diameter curve generated. Some errors might occur due to friction in the diameter-measuring system (ie. friction in the pivot bearing) and this would undoubtedly affect the reading obtained. Since this is a random occurrence, it could explain for the high deviation of some of the values. Despite this, most of the static compliance pressure-diameter curves were quite reproducible. Another source of variation in the compliance values could be the quality of the underlying porous grafts. The homogeneity of the salt- and bead-cast polyurethane structures is very difficult to control, although the pore-forming agents were sieved to give a narrow size distribution (to produce a uniform porosity). The variations in graft microstructure would more likely come from the manufacturing process. During manufacture of the salt-cast grafts, 'weld-lines' are produced due to the rolling process (see 3.2: 'Manufacturing techniques'). These would result in variations of the graft wall-thickness and could influence the diameter measurement. Since the polyurethane cures by a phase inversion process, in which the curing agent displaces the polyurethane solvent, the curing time will also affect the strength of the porous structure. It should be pointed out however, that both the salt- and bead-cast grafts were cured for sufficient periods of time to allow proper development of strength. The grafts were all cured for equal periods of time. The properties of the bead-cast grafts might also be affected by the presence of residual gelatin in the porous matrix after the extraction process. However, all bead-cast grafts were washed thoroughly to ensure proper extraction. Variations in the properties of these grafts would more likely originate during the casting process, as the polyurethane solution travels through the gelatin-bead packed column (see 3.2.1.2: 'Bead-cast grafts'). The solution does not always travel evenly and proper dispersion of the polyurethane among the beads is not always ensured. This would result in some non-homogeneity. During the application of the synthetic adventitia, there are other variables that could influence the compliance of the graft. A significant cause could be the fibre tension during winding. Should the fibre be tensioned too much during application, this would result in a graft with an initial compressive stress in the wall and this would result in the graft being less compliant. To overcome this effect, the friction on the fibre was reduced to a minimum by using small spools that were free to rotate and caused minimal resistance. The only friction results from the fibre passing through the polyurethane solution before it is applied to the exterior of the graft. However this would have been a constant variable as all sets of grafts were reinforced together and friction on the fibre remained more or less constant.

6.2 COMPARISON OF THE COMPLIANCE RESULTS OBTAINED TO REALISTIC COMPLIANCE VALUES.

It is difficult to compare the results obtained in this project to those measured by others, as in most cases, they have employed different methods of compliance testing, and have used synthetic grafts manufactured by different methods. Although the definition of compliance is the same, given in terms of volume or diameter change per increase in internal pressure, the different methods of diameter measurement will give different results. Some researchers have opted for non-contact methods of measuring diameter such as video imaging systems, ultrasound and laser micrometers, but there are still possibilities of errors with these techniques. The contact-type systems are also not ideal as any mechanical part that makes contact with the graft will cause frictional effects and affect the distension of the vessel wall under pressure. The compliance of a human femoral artery is in the region of 6%/100mm Hg [19,28], and this has been used as the target compliance for the grafts in this work. The focus of this project was thus to see the effect of applying different types of external reinforcement to an existing porous polyurethane graft, and see how it would affect the compliance. As can be seen from the results, applying a very stiff fibre to the exterior of the graft causes a decrease in the compliance of the graft. Compliance is further decreased when the winding is applied at a small winding pitch ie. the reinforcements are close together, while the graft can be made less stiff in the circumferential direction by increasing the winding pitch. The non-reinforced salt- and bead-cast grafts would undoubtedly over-distend with time, as proven by the creep tests. The non-reinforced bead-cast graft has a better static compliance than the non-reinforced salt-cast graft (5.21% vs 9.21% over the 80-120mm Hg range), and applying reinforcement would perhaps make the graft too stiff. If a bead-cast graft could be manufactured with a thinner wall, then reinforcement could be applied until the correct compliance is attained. The salt- and bead-cast grafts, reinforced with the 33 dtex Dorlastan® fibre showed close static compliances to 6%/100mm Hg (7.77% and 7.47% respectively), and given the fact that this fibre has a non-linear stress profile, it could provide the correct behaviour of an adventitia. That is to say, with increased distension, the graft becomes less compliant (stiffer), which in the case of a natural vessel is due to the influence of the collagen in the adventitia. With the correct amount of tensioning of the fibre during winding, one could accurately adjust the compliance of the graft. From this research one can also conclude that it is possible to vary the compliance of a graft by use of different reinforcing materials and using different winding configurations. Natural vessels could be tested first on the compliance apparatus and grafts may then be manufactured and reinforced on the winding apparatus

according to the compliance required. It has been shown in this project that the porous polyurethane grafts definitely require a form of reinforcement because with extended exposure to physiological conditions over-distension of the graft occurs, as well as an increase in compliance. It was shown that by applying a combination reinforcement of nylon and Dorlastan® on a salt-cast graft, the compliance was quite close to a natural vessel (6.06%/100mm Hg, dynamic compliance 180-220mmHg range). However, the loose-wound nylon at 5mm pitch is not ideal as the windings tend to be easily displaced and would result in a variation of compliance along the length of the graft. The idea of this was that the Dorlastan would allow initial distension of the grafts wall until a certain pressure was reached. The loose nylon fibre, being secured only at the ends of the graft would not hinder this initial distension, but only come into play at higher pressures, thus creating a stiffening effect. Future reinforcement would have to be in the form of a mesh sleeve that arrests the distension of the graft wall at a certain pressure.

The burst tests proved that the reinforced grafts could withstand pressures of greater than 3 times normal physiological pressure, so there is no doubt of their reliability in this regard. However, future testing of the grafts could include a kink-resistance test that determines the amount of bending a graft can endure before the wall buckles inward. This characteristic of blood vessels is of vital importance, especially at positions in the body where there is high movement and bending (at joints etc.).

The suture-pull out tests showed the bead-cast grafts to be stronger than the salt-cast grafts again. Of those tested, the bead-cast graft reinforced with the polyurethane monofilament proved to be the strongest with a tearing strength of 4.89N. In terms of tearing strength, these grafts are much weaker than other commercial grafts due to the porous structure and weaker material properties of the polyurethane.

6.3 RECOMMENDATIONS FOR FUTURE COMPLIANCE TESTING METHODS AND APPARATUS

Although the apparatus developed and used in this project gave good results and relatively speaking the results obtained were concurrent with the predicted change in compliance, there are some modifications that could be made to improve on future compliance measurements.

6.3.1 Diameter-measuring System

The use of a contact-measuring system such as the one employed, does introduce some inaccuracies in the diameter measurement. The pendulums that make contact with the graft wall are heavy, because it was necessary to balance the weight of the linkage arm connected to the transducer probe. This results in a system which, although balanced in terms of weight, has a high moment of inertia, and testing at a higher pulse rate and pressures would result in the pendulums not following the graft wall very well (as indicated by the dynamic porcine aorta tests). In future, a light, spring-loaded mechanism could be employed, as shown in figure 6.1 below, the spring ensuring that the measurement piece remains in contact with the graft wall at all times. Of course, one would have to use a very light spring so as not to cause excessive compression of the graft wall.

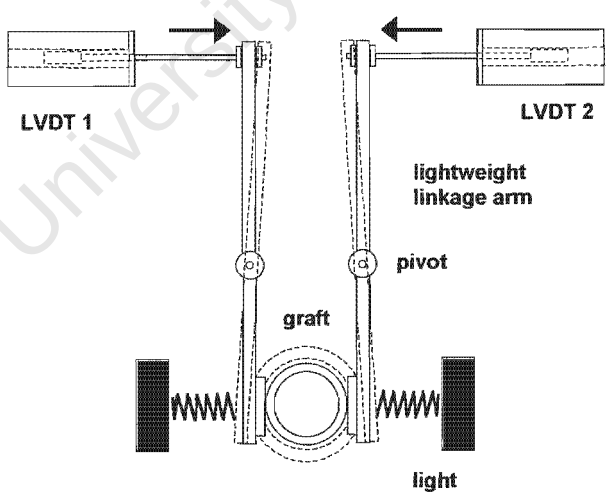

Figure 6.1: Suggested modification to the diameter-measuring system

Alternatively, one could opt for a more costly non-contact measurement system, such as a laser micrometer, which would be optimal in the sense that there is no interference of the measuring

system with the graft wall movement. With an optical system such as this however, there are other errors that have to be accounted for (diffraction of the laser beam when passing through the fluid-filled testing chamber, etc.).

6.3.2 Axial Tensioning of the Graft

It was hoped that by the use of an air bearing isotonic compliance testing would have been possible (constant axial tension). This would have allowed for longitudinal elongation of the graft during testing, which would give more accurate diameter measurements. Under isometric conditions (fixed length), an increase in internal pressure causes the graft to bulge to the side or downwards. This results in a volume change due to increase in length as opposed to an increase in diameter, and would not reflect a true compliance measurement. To overcome this effect, an initial axial tension was applied to the grafts before fixing the length. In principle, the air-bearing would have provided the axial float necessary, but because the level of the bearing is below the level of the fluid in the testing chamber, an o-ring seal was needed to prevent leakage. This seal caused too much friction on the sliding tube, and any axial elongation due to pressurisation of the graft was prevented. Thus it was decided to pre-tension and test under fixed length conditions. Some researchers have used an air bearing in compliance testing (Charara, Ruel et al, 116), but this was placed outside the fluid-filled testing chamber and hence no seals were needed (see figure 6.2 below). However, due to the design of the system, a counterweight was needed to balance the axial tension applied to the graft. The apparatus could be modified to incorporate such a linear air bearing in future.

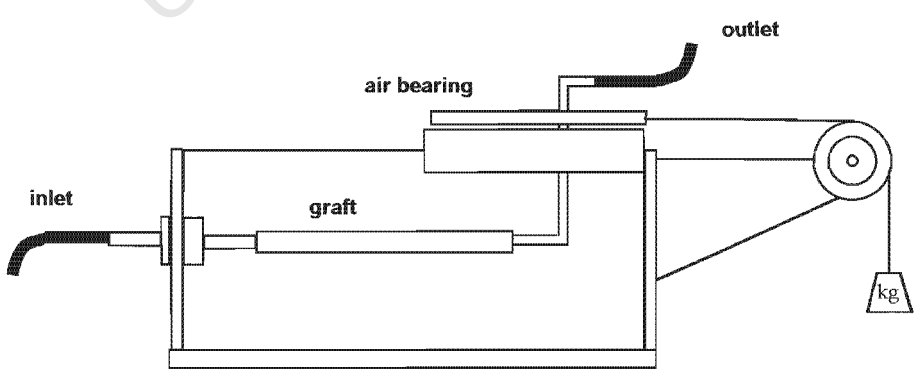

Figure 6.2: Use of a linear air-bearing for axial tensioning

6.3.3 Modifications to the Fluid Circuit

Some modifications could be made to the pulsatile loop to facilitate easier testing and a quicker setup time (especially with regard to the dynamic compliance testing). The re-adjustment of the pressure regulator and pinch valves requires much time before the desired systolic and diastolic pressure levels are attained. Also, this adjustment has to be completed before the pressure reservoir empties. The pinch valve could be modified such that the amount of pinch on the tube can be accurately controlled. Adjustment of the valve and regulator might even be done electronically, and fine control of the pressure waveforms could be achieved by an electronic feedback system. The pressure pulse could be 'read' digitally and compared to the desired pressure pulse, the pinch valves may then be adjusted until the correct waveform is achieved.

6.3.4 The Latex Inserts

Unfortunately, since the grafts were porous it was necessary to use latex inserts to prevent leakage and loss of pressure through the graft. Obviously, they would have an effect on the compliance values obtained. A graphical method of subtracting the effect of the latex was used (see 3.2.6: Compensation for the effect of the latex liners). However, this method was difficult to apply in the case of the weaker grafts, as the latex has more of an effect on the compliance (ie. the grafts appear stiffer due to the latex). The latex inserts acquired from Roynhardt Jhb. were perhaps too strong and thick-walled, having a wall thickness of around 200μm. However, according to the AAMI standards, the inserts still meet the specifications for inserts (the diameter of the insert at 120mm Hg should be at least 1.05 x the relaxed internal diameter). The Roynhardt inserts have a diameter at 120mm Hg of 1.09 x the relaxed diameter. In future though, it would be better to use thinner-walled latex that has a smaller effect on the compliance of the grafts.

6.3.5 Data Acquisition Software

While the data acquisition software used in this project proved to be satisfactory, it is run in a Dos environment which makes file management somewhat cumbersome. Also, the program only displays the voltage output of each of the channels being sampled. There is no way of adding conversion factors to the plots ie. to convert the volts display into the desired units (pressure, diameter, flow etc.). Currently there are programs available that are more advanced and have more capability (Maclab, Daisy, Winview etc.).

References

1. D.E. Hokanson, D.E. Strandness, *Stress-strain characteristics of various arterial grafts*, **Surgery, Gynecology & Obstetrics** July 1968 pp57-60.

2. N. L'Heureux, S. Paquet, R. Labbé et al, *A completely biological tissue-engineered human blood vessel,* **FASEB Journal**, vol 12 1998, pp 47-56.

3. J.A.M. Ramshaw, D.E. Peters, J.A. Werkmeister, *Collagen organisation in mandrel-grown vascular grafts,* **Journal of Biomedical Materials Research** vol 23 1989, pp 649-660.

4. W.E. Burkel, *The challenge of small diameter vascular grafts,* **Medical Progress Through Technology** 14 1988, pp 165-175.

5. A.N. Nicolaides, *Haemodynamic aspects of vascular grafting*, **Acta Chir. Scand.** Suppl. 529:7-16, 1985 pp 7-16.

6. J. Leidner, E.W.C. Wong, D.C. McGregor, G. J. Wilson, *A novel process for the manufacturing of porous grafts: Process description and product evaluation,* **Journal of Biomedical Materials Research** vol 17 1983 pp 229-247.

7. G.J. Wilson, D.C. McGregor et al, *Anisotropic polyurethane nonwoven conduits: a new approach to the design of a vascular prosthesis,* **Transactions of the American society of Artificial Internal Organs** vol 29 1983 pp 260-268.

8. G. Hellener, D. Cohn, G. Marom, *Elastic response of filament wound arterial prostheses under internal pressure*, **Biomaterials** 1994, vol 15:14 pp1115-1121.

9. B. Gershon, D. Cohn G. Marom, *Utilisation of composite laminate theory in the design of synthetic soft tissues for biomedical prostheses*, **Biomaterials**, 1990, vol 11 October pp 548-552.

10. B.S. Gupta, V.A. Kasyanov, *Biomechanics of human common carotid artery and design of novel hybrid textile compliant vascular grafts,* **Journal of Biomedical Materials Research** vol 34 1997 pp 341-349.

11. K. Hayashi, K. Takamizawa, T. Saito, K. Kira et al, *Elastic properties and strength of a novel small-diameter, compliant polyurethane vascular graft,* **Journal of Biomedical Materials Research: applied biomaterials** vol 23 no. A2 1989 pp 229-244.

12. Schugens, Maquet, Grandfils,, Jerome, Teyssie, *Polylactide microporous biodegradable implants for cell transplantation. II. Preparation of polylactide foams by liquid-liquid phase separation,* **Journal of Biomedical Materials Research**, vol 30 1996 pp449-461.

13. A. Edwards, R.J. Carson, S. Bowald, W. C. Quist, *Development of a microporous compliant small bore vascular graft,* **Journal of Biomaterials Application** vol 10 Oct 1995 pp171-187.

14. R.R. Kowligi, W.W. von Maltzahn, R.C. Eberhart, *Fabrication and characterisation of small-diameter vascular prostheses,* **Journal of Biomedical Materials Research: applied biomaterials**, vol 22 no. A3 1988 pp245-256.

15. K.B. Chandran, Y-H Kim, *Mechanical aspects of vascular graft-host artery anastomoses*, **IEEE Engineering in Medicine and Biology** Aug/sept 1994.

16. I. G. Kidson, *The effect of wall mechanical properties on patency of arterial grafts.* **Annals of the Royal college of Surgeons of England** 1983, vol. 65, pp24-29.

17. I.G. Kidson, W.M. Abbott, *Low compliance and arterial graft occlusion*, **Circulation**, vol 58 no. 3 Sept. 1978 supl. no. 1 I1-I4.

18. R. Walden, G.J. L'italien et al, *Matched elastic properties and successful arterial grafting*, **Arch. Surgery**, vol 115 Oct. 1980 pp 1166-1169.

19. G. Stansby, C. Berwanger, N. Shukla, T. Schmitz-Rixen, G. Hamilton, *Endothelial seeding of compliant polyurethane vascular graft material,* **British Journal of Surgery**, 1994 no. 81 pp 1286-1289.

20. A. Giudiceandrea, A.M. Seifalian, B. Krijgsman, G. Hamilton, *Effect of prolonged pulsatile shear stress in vitro on endothelial cell seeded PTFE and compliant Polyurethane vascular grafts,* **European Journal of Endovascular Surgery** 1998 15, pp147-154.

21. R.A. White, S. R. Klein, E. Shors, *Maintenance of compliance in a small diameter arterial prsothesis*, **Trans. Am. Soc. Artif. Organs** 1996 vol 32, pp601-604.

22. H.P. Griesler, K.A. Joyce, *Spatial and temporal changes in compliance following implantation of bioresorbable vascular grafts*, **Journal of Biomedical Materials Research**, Vol 26, 1992, 1449-1461.

23. M.W. Weston, K. Rhee, J.M. Tarbell, *Compliance and diameter mismatch affect the wall shear rate distribution near an end-to–end anastomosis*, **Journal of Biomechanics**, vol29 no. 2 1996 pp 187-198.

24. Robert E. Shadwick, *Elasticity in arteries*, **American Scientist**, vol 86 Nov – Dec 1998 pp 535 – 541.

25. M.F. O'Rourke, H.R. Brunner, *Introduction to arterial compliance and function,* **Journal of Hypertension** 1992 vol 10 (suppl. 6) S3-S5.

26. G. Belz, *Elastic properties and Windkessel function of the Human aorta,* **Cardiovascular Drugs and Therapy**, 1995, vol. 9 pp73-83.

27. C.E. Kinley, A.E. Marble, *Compliance: a continuing problem with vascular grafts*, **Journal of Cardiovascular Surgery**, vol 21 1980 pp 163-170.

28. P.D. Ballyk, C. Walsh, J. Butany, M. Ojha, *Compliance mismatch may promote graft-artery intimal hyperplasia by altering suture-line stresses*, **Journal of Biomechanics** vol 31 1998 pp 229-237.

29. B. Gershon, D. Cohn, G. Marom, *Compliance and ultimate strength of composite arterial prostheses*, **Biomaterials** 1992 vol 13 no. 1 pp 38-43.

30. L.H. Peterson, R.E. Jensen, J. Parnell, *Mechanical properties of arteries in vivo*, **Circulation Research**, vol 8, May 1960 pp622-639.

31. B.A. MacWilliams, A.H. Hoffman, B.J. Savilonis, *Variation of arterial compliance within the cardiac pressure pulse*, **Journal of Biomechanics**, 31 1998 pp 867-871.

32. M.H. Sherebrin, S.H. Song, M. R. Roach, *Mechanical anisotropy of purified elastin from the thoracic aorta of dog and sheep*, **Canadian Journal of Physiology and Pharmacology**, vol 61 1983, pp 539-545.

33. Y.C. Fung, **Biomechanics: Mechanical Properties of Living Tissues**, 2nd edition, 1993, Springer-Verlag, New York, pp 243-263.

34. Q. Yu, J. Zhou, Y.C. Fung, *Neutral axis location in bending and Young's modulus of different layers of arterial wall,* **American Journal of Physiology** 265 (heart circ. physiology, 34) H52-H60, 1993.

35. A.A. Mangoni, L.Mircoli et al, *Heart rate-dependence of arterial distensibility in vivo*, **Journal of Hypertension**, vol 14 1996 pp 897-901.

36. R.F. Labadie, J.F. Antaki, J.L. Williams et al, *Pulsatile perfusion system for ex vivo investigation of biochemical pathways in intact vascular tissue*, **American Journal of Physiology** vol 270 (heart circ. physiol.) 1996 H760-768.

37. A.M. Brant, V.G.J. Rodgers, H.S. Borovetz, *Measurement in vitro of pulsatile arterial diameter using a helium-neon laser*, **Journal of Applied Physiology** 62(2) 1987 pp 679-683.

38. Y.F. Law, R.S.C. Cobbold, K.W. Johnston, P.A.J. Bascom , *Computer-controlled pulsatile pump system for physiological flow simulation*, **Medical & Biological Engineering & Computing** 1987 vol 25 pp590-595.

39. D.W. Holdsworth, D.W. Rickey, M. Drangova, D.J.M. Miller, A. Fenster, *Computer-controlled positive positive displacement pump for physiological flow simulation*, **Medical & Biological Engineering & Computing** 1991, vol 29 pp 565-570.

40. H. Schima, S. Tsangers, P. Zilla et al , *Mechanical simulation of shear stress on the walls of peripheral arteries*, **Journal of Biomechanics**, vol 23 no. 8 1990 pp845-851.

41. R.N. Baird, I. G. Kidson, G.J. L'italien, W.M. Abbott, *Dynamic compliance of arterial grafts*, **American Journal of Physiology** 233(5) (heart circ. physiology), 1977 H568-H572.

42. J.P. Murgo, R.G. Cox, L.H. Peterson, *Cantilever transducer for continuous measurement of arterial diameter in vivo*, **Journal of Applied Physiology**, Vol 31 no. 6 Dec. 1971 pp 948-953.

43. R.W. Stadler, W.C. Karl, R.S. Lees, *New methods for arterial diameter measurement from B-mode images*, **Ultrasound in Medicine & Biology** vol 22 no. 1 1996 pp 25-34.

44. J-J. Meister, Y. Tardy, N. Stergiopulos, *Non-invasive method for the assessment of non-linear elastic properties and stress of forearm arteries in vivo, compliance* **Journal of Hypertension**, 1992 vol 10 (suppl. 6) S23-S26.

45. M.J. Roman, R. Pini, et al, *Non-invasive measurements of arterial compliance in hypertensive compared with normotensive adults,* **Journal of Hypertension**, 1992 vol 10 (suppl. 6) S115-S118.

46. N. Uchida, H. Kambic et al, *Compliance effects on small diameter polyurethane graft patency*, **Journal of Biomedical Materials Research**, vol 27 1993 pp 1269-1279.

47. C. Giannattasio, M. Failla, A.A. Mangoni et al , *Evaluation of arterial compliance in humans*, Clinical and experimental hypertension Vol 18(3&4) 1996 pp 347-362.

48. J.M. Gosline, C.J. French, *Dynamic mechanical properties of elastin,* **Biopolymers**, Vol 18, 1979, pp 2091-2103.

49. L. Debelle, A.M. Tamburro, *Elastin: molecular description and function,* **International Journal of Biochemistry and Cell Biology**, vol 31, 1999, pp 261-272.

50. N. Sasaki, S. Odajima, *Stress-strain curve and Young's modulus of a collagen molecule as determined by the x-ray diffraction technique*, **Journal of Biomechanics**, 29:5 1996, pp 655-8.

51. Harley et al, *Phonons and the elastic modulus of collagen and muscle,* **Nature**, vol. 267 May, 1977, pp285-287.

52. P. Fratzl, K. Misof, I. Zizak, *Fibrillar structure and mechanical properties of collagen,* **Journal of Structural Biology**, 122, 1997 pp 119-122.

53. A.J. Bank, H. Wang, J.E. Holte, *Contribution of collagen, elastin and smooth muscle to in vivo human brachial artery wall stress and elastic modulus*, **Circulation**, 1996 vol 94 pp 3263-3270.

54. F.L. Wuyts, V.J. Vanhuyse, G.J. Langewouters et al, *Elastic properties of human aortas in relation to age and artherosclerosis: a structural model*, **Physics in Medicine and Biology**, 40:10 Oct 1995, pp 1577-97.

55. R.W. Carton, J. Dainauskas, J.W. Clark, *Elastic properties of single elastic fibres*, **Journal of Applied Physiology**, 17(3), 1962, 547-551.

56. M. Yeoman, *The design and optimisation of a fabric reinforced porous prosthetic graft using finite element methods and a genetic algorithm,* Masters thesis, Department of Cardiovascular Research, University of Cape Town, 2001.

57. E. Rosset, C. Brunet, R. Rieu, *Visco-elastic properties of human arteries. Methodology and preliminary results*, **Surgical and Radiologic Anatomy** 1996 18, pp 89-96.

58. A. Giudiceandrea, A.M. Seifalian, B. Krijgsman, G. Hamilton, *Effect of prolonged pulsatile shear stress in vitro on endothelial cell seeded PTFE and compliant Polyurethane vascular grafts,* **European Journal of Endovascular Surgery** 1998 15, pp147-154.

59. J-H Chen, R-F Laiw, S-F Jiang, Y-D Lee, *Microporous segmented polyurethane vascular graft: dependency of graft morphology and mechanical properties on compositions and fabrication conditions*, **Journal of Biomedical Materials Research** (applied biomaterials) 1999 vol 48 pp235-245.

60. H. Martz, G. Beaudoin, R. Paynter, M. King, D. Marceau, R. Guidoin, *Physiochemical characterisation of a hydrophilic microporous vascular graft*, **Journal of Biomedical Materials Research**, vol 21 1987 pp399-412.

61. B.M. Learoyd, M.G. Taylor, *Alterations with age in the visco-elastic properties of Human arterial walls,* **Circulation Research**, vol. 18 1966, pp 278-292.

62. Y.C. Fung, S.Q. Liu, *Determination of the mechanical properties of the different layers of blood vessels in vivo,* **Proc. National Academy of Science** USA, vol 92 March 1995, pp2169-73

63. J. Michael Lee, G.J. Wilson, *Ansiotropic tensile visco-elastic properties of vascular graft materials tested at low strain rates*, **Biomaterials** 1986, vol 7 November pp423-431.

64. V.L. Streeter, W.Ford Keitzer, D.F. Bohr, *Pulsatile pressure and flow through distensible vessels*, **Circulation Research** vol 13, July 1963 pp3-18.

65. K.S. Haas S.J Phillips, A.J. Comerota, J.V. White, *The architecture of adventitial elastin in the canine infrarenal aorta*, **The Anatomical Record** 1991 vol 230 pp 86-96.

66. B.I. Levy, *The mechanical properties of the arterial wall in hypertension*, **Prostaglandins, Leukotrienes and Essential Fatty Acids** 1996 vol 54 pp 39-43.

67. M. Hasegawa, T. Azuma, *Mechanical properties of synthetic arterial grafts*, **Journal of Biomechanics** vol 12 1979, pp509-517.

68. G.J. L'italien, N.R. Chandrasekar, G.M. Lamuraglia et al, *Biaxial elastic properties of rat arteries in vivo: influence of vascular wall cells on anisotropy*, **American Journal of Physiology** 267 (heart circ. physiol. 36) 1994 H574-H579.

69. K.Takamizawa, K. Hayashi, T. Matsuda, *Isometric biaxial tension of smooth muscle in isolated cylindrical segments of rabbit arteries*, **American Journal of Physiology** 263 (heart circ. physiol. 32) 1992 H30-H34.

70. J.T. Apter, *Correlation of visco-elastic properties with microscopic structure of large arteries, IV. Thermal responses of collagen, elastin, smooth muscle, and intact arteries*, **Circulation Research** , vol 21 Dec 1967 pp 901-918.

71. D.J. Patel, J.S. Janicki, *Static elastic properties of the left coronary circumflex artery and the common carotid artery in dogs*, **Circulation Research**, vol 27 Aug 1970 pp 149-158.

72. R.H. Cox, *Three-dimensional mechanics of arterial segments in vitro: methods*, **Journal of Applied Physiology** vol 36 no 3 March 1974 pp 381-384.

73. T.V. How, R.M. Clarke, *The elastic properties of a polyurethane arterial prosthesis*, **Journal of Biomechanics**, vol 17 no.8 pp597-608.

74. N. Uchida, H. Emoto, H. Kambic, et al, *Compliance effect on patency of small diameter vascular grafts*, **Trans Am. Soc. of Artificial Internal Organs**, vol 35 1989 pp 556-558.

75. V.G.J. Rodgers, M.F. Teodori, H.S. Borovetz, *Experimental determination of mechanical shear stress about an anastomotic junction*, **Journal of Biomechanics**, vol 20 no. 8 1987 pp 795-803.

76. A.J. Bank, R.F. Wilson, S.H. Kubo et al, *Direct effects of smooth muscle relaxation and contraction on In vivo human brachial artery elastic properties*, **Circulation Resesarch** vol 77 no. 5 Nov. 1995 pp 1008-1016.

77. C.J. Chuong, Y.C. Fung, *Three-dimensional stress distribution in arteries*, **Journal of Biomechanical Engineering** vol 105 Aug 1983, transaction of the ASME pp 268-274.

78. W.-W. von Maltzahn, D. Besdo, W. Wiemer, *Elastic properties of arteries: a nonlinear two-layer cylindrical model*, **Journal of Biomechanics**, vol 14 no.6 1981 pp 389-397.

79. R.H. Cox, *Anisotropic properties of the canine carotid artery in vivo*, **Journal of Biomechanics**, vol 8 1975 pp 293-300.

80. R.P. Vito, J. Hickey, *The mechanical properties of soft tissues-II: The elastic response of arterial segments*, **Journal of Biomechanics** vol 13 1980 pp 951-957.

81. A.J. Bank, D.R. Kaiser, *Smooth muscle relaxation: effects on arterial compliance, distensibility, elastic modulus and pulse wave velocity*, **Hypertension** vol 32 1998 pp 356-359.

82. J. Melbin, P.C. Ho, *Stress reduction by geometric compliance matching at vascular graft anastomoses*, **Annals of Biomedical Engineering** vol 25 1997 pp 874-881.

83. R.L. Binns, D.N. Ku, M.T. Stewart et al, *Optimal graft diameter: effect of wall shear stress on vascular healing* , **Journal of Vascular Surgery**, 1989 vol 10 pp 326-37.

84. P. B. Dobrin, R. Mrkvicka, *Estimating the elastic modulus of non-atherosclerotic arteries,* **Journal of Hypertension**, 1992 vol 10 (suppl.6), S7-S10.

85. X. J. Girerd, C. Acar, J-J. Mourad et al, *Incompressibility of the human arterial wall: an in vitro ultrasound study,* **Journal of Hypertension** 1992 vol 10 (suppl. 6) S11-S114).

86. C. Giannattasio, B. M. Cattaneo, A. Mangoni et al, *Changes in arterial compliance induced by physical training in hammer-throwers,* **Journal of Hypertension**, 1992 vol 10 (suppl. 6), S53-S55.

87. C.M. Quick, D.S. Berger, A. Noordergraaf, *Apparent arterial comliance,* **American Journal of Physiology** (Heart, circ. Physiol.) vol 43 1998, H1393-1403.

88. N.R.M Tai, A. Guidiceandrea et al, *In vivo femoropopliteal arterial wall compliance in subjects with and without lower limb disease,* **Journal of Vascular Surgery** 1999, vol 30 pp 936-945.

89. C.M. Brophy, *The dynamic regulation of blood vessel caliber,* **Journal of Vascular Surgery**, vol 31, Feb 2000 pp 391-5.

90. T. Tanabe, Y. Kubo, M. Hashimoto, *Wall reinforcement with highly porous Dacron® mesh in aortic surgery,* **Annals of Surgery**, April 1980 pp 452-455.

91. T.M. Sullivan, M.M. Dunn, *Effect of external reinforcement on the patency of infrainguinal polytetrafluoroethylene arterial grafts,* **Journal of the American College of Surgeons**, March 1996 Vol 182 pp 211-214.

92. N. Nazem, Zakhariev, Tschirkov, *Spiral plastic stent for external reinforcemnt of prosthetic vascular grafts in pressure and bending areas in the course of aorto-femoral/bifemoral by-pass,* **Journal of Cardiovascular Surgery** 1994; 35 pp277-8.

93. H.D. Berkowitz, L.J. Perloff, B. Roberts, *Pseudointimal development on microporous polyurethane lattices,* **Transactions of the American Society of Artificial Internal Organs** vol 28 1972 pp 25-29

94. G. Roberts, H. McCormack, V. Ketharanathan, D.G. Macleish et al, *The role of physical and chemical characteristics in assessing the performance of a new biological vascular graft,* **Journal of Biomedical Materials Research**, vol 23 1989, pp 443-450.

95. W. J. Drasler, M.L. Jenson, S. A. George et al, *A unique casular graft concept for coronary and peripheral applications,* **Transactions of the American Society of Artificial Internal Organs** vol 34 1988 pp 769-772.

96. E. Wintermantel, J. Mayer, J. Blum K.-L. Eckert, P. Lüscher, M. Mathey, *Tissue engineering scaffolds using superstructures,* **Biomaterials**, vol 17 no. 2 1996 pp 83-91.

97. S. Masuda, K. Doi, S. Satoh et al, *Vascular endothelial growth factor enhances vascularisation in microporous small caliber polyurethane grafts,* **ASAIO Journal**, 1997, vol 43, M530-534.

98. Y. Marois, R. Guidoin, X. Deng et al, *The Dialine II graft: A new collagen-impregnated warp-knitted vascular prosthesis,* **Annals of Vascular Surgery**, 1997 vol 11 pp 133-140.

99. J.G.F. Bots, L. van der Does, A. Bantjes, *Small diameter blood vessel prostheses from polyethers,* **Polymers in Medicine II** New York Plenum press 1986 pp 223-234.

100. R. Tu, E. Wang et al, *A compliant vascular prosthesis,* **International Journal of Artificial Organs**, vol 16 no. 3 1993, pp 141-145.

101. A. Eberhart, Z.Zhang R. Guidoin et al, *A new generation of polyurethane vascular prostheses: rara avis or ignis fatuus?,* **Journal of Biomedical Materials Research** (appl. biomaterials), vol 48 1999, pp 546-558.

102. W.L.J. Hinrichs, H-P Zweep et al, *Supporting, microporous, elastomeric degradable prostheses to improve the arterialisation of autologous vein grafts,* **Biomaterials**, 1994, vol 15, no. 2 pp 83-91.

103. Z. Zhang, M.W. King, R. Guidoin et al, *Morphological, physical and chemical evaluation of the Vacsugraft® arterial prosthesis: comparison of a novel polyurethane device with other micoporous structures,* **Biomaterials**, 1994 vol 15 no. 7 pp 483-501.

104. H. Jerius, D.R. Karolyi et al, *Endothelial-dependent vasodilation is associated with increases in the phosphorylation of a small heat shock protein*, **Journal of Vascular Surgery**, vol 29 1999 pp678-84.

105. K. Hayashi, T. Nakamura, *Material test system for the evaluation of mechanical properties of biomaterials*, **Journal of Biomedical Materials Research** vol 19 1985 pp133-144.

106. R. Bozzi, J.C. Conti, D. Rhode et al, *Relating the frequency dependent radial compliance to the tensile modulus of polyurethane vascular grafts*, **Fifth World Biomaterials Congress** May 29 – June 2 1996, Toronto, Canada.

107. R.C. Peterson, R. Tu et al, *Dynamic internal compliance measurements of fresh and fixed artery*, **ASAIO Transactions** 1990 vol 36: M766-M769.

108. D.J. Lyman, F.J. Fazzio et al, *Compliance as a factor effecting the patency of a copolyurethane vascular graft*, **Journal of Biomedical Materials Research**, vol 12, 1978 pp 337-345.

109. N Stergiopulos, J-J, Meister, N. Westerhof, *Evaluation of methods for estimation of total arterial compliance*, **American Journal of Physiology** 268 (heart circ. physiology), 1995 H1540-H1548.

110. G.S. Schajer, S.I. Green, A.P. Davis, Y.N.-H. Hsiang, *Influence of elastic nonlinearity on arterial compliance*, **Journal of Biomechanical Engineering**, Nov. 1996 vol 118 pp 445-451.

111. R.N. Baird, I. G. Kidson, G.J. L'italien, W.M. Abbott, *Dynamic compliance of arterial grafts*, **American Journal of Physiology** 233(5) (heart circ. physiology), 1977 H568-H572.

112. D.M. Stump, V.G. Hart, S.L. Tuttle, *Circumferentially flexible vascular grafts*, **Journal of Biomechanics**, 31 1998 pp705-71.

113. K.B. Chandran, D. Gao, G. Han et al, *Finite-element analysis of arterial anastomoses with vein, Dacron® and PTFE grafts*, **Medical & Biological Engineering & Computing**, July 1992 vol 30 pp 413-418.

114. J.C. Conti, E.R. Strope et al, *Frequency dependent radial compliance of latex tubing*, **Biomedical Science Instrumentation**, 33 1997 pp524-529.

115. **Proceedings of the Annual Meeting of ASME**, Mechanical division, Nov 30 1966, New York: Biomechanics.

116. J. Charara, J. Ruel, C.J. Doillon, *Development of a flow simulator to study haemodynamic behaviour of a natural and artificial blood vessels under physiologic flow conditions.* **Journal of Medical Engineering & Technology** vol 23, no. 3 , May, June 1999 pp 83-95.

117. D.V. Carmines, J.H. McElhaney, R. Stack, *A piece-wise non-linear elastic stress expression of human and pig coronary arteries tested in vitro,* **Journal of Biomechanics** Vol 24 no 10 1991 pp899 – 906.

118. M.M. Werneck, N.B. Jones, J. Morgon, *Flexible hydraulic simulator for cardiovascular studies*, **Medical & Biological Engineering & Computing** Jan 1984 vol 22 pp86-89.

119. T. Kiyose, A. Kusaba, M. Kamori, K. Inokuchi, Y. Takamatsu, H. Takahara, *Development of Pump system for experimental model simulation of blod flow in peripheral artery,* **Fukuoka Acta Medica** vol 68(2) 1977 pp86-91.

120. F.C.P. Yin, C-T. Ting, *Compliance changes in physiological and pathological states,* **Journal of Hypertension** 1992 vol 10 (suppl. 6) S31-S33.

121. S. Trazzi, S. Omboni, C. Santucciu, *Variability in arterial diameter and compliance* **Journal of Hypertension**, 1992 vol 10 (suppl. 6) S41-S43.

122. D.J. Patel, B.R. Coleman, R. Carpentier, *Clinical relevance of distal arterial compliance,* **Journal of Hypertension**, 1992 vol 10 (suppl. 6) S15-S17.

123. S.N. Finkelstein, J.N. Cohn, *First- and third-order models for determining arterial compliance,* **Journal of Hypertension**, 1992 vol 10 (suppl. 6) S11-S14.

124. Y. Qiu, J.M. Tarbell, *Computational simulation of flow in the end-to-end anastomosis of a rigid graft and a compliant artery,* **ASAIO Journal**, 1996, vol 42 M702-M709.

125. N.R.M Tai, A. Giudiceandrea et al, *In vivo femoropopliteal arterial wall compliance in subject with and without lower limb vascular disease,* **Journal of Vascular Surg**. , 1999, vol 30, pp936-45.

126. M. Cengiz, L.R. Sauvage et al, *Effects of compliance alteration on healing of a porous Dacron® prosthesis in the thoracic aorta of the dog.,* **Surgery, gynecology & obstetrics**, Feb 1984, vol 158 pp 145-151.

127. A.M. Brant, J.F. Chmielewski et al, *Simulation in vitro of pulsatile vascular haemodynamics using a CAD/CAM designed disc and roller-follower.,* **Artif. Organs**, vol. 10 no. 5 1986, pp419 – 421.

128. R. Burattini, S. Natalucci, *Complex and frequency-dependent compliance of visco-elastic windkessel resolves contradictions in elastic windkessels.,* **Medical Eng. & Physics** 20 1998 pp 502-514.

129. M. Stevanov, J. Baruthio, B. Eclancher, *Fabrication of elastomer arterial models with specified compliance,* **Journal of Applied Physiology**, 2000 vol 88 pp 1291-1294.

130. C.P. Winlove, K.H. Parker, *Influence of solvent composition on the mechanical properties of arterial elastin*, **Biopolymers**, vol 29, 1990, pp729-735.

131. S. Cusack, A. Miller, *Determination of the elastic constants of collagen by Brillouin light scattering,* **Journal of Molecular Biology**, 1979 vol 135 pp 39-51.

132. H. Liao, S. Belkoff, *A failure model for ligaments,* **Journal of Biomechanics**, vol 32 1999, pp 183-188.

133. J.F Chapuis, P. Agache, *A new technique to study the mechanical properties of collagen lattices,* **Journal of Biomechanics**, vol 25 no. 1 1992, pp 115-120.

134. F. Bonne, P. Baldet, F. Blotman, *Biomécbanique du tissu conjonctif,* **Annales du Biologie Clinique**, 1986 vol 44, pp 156-161.

135. J.I. Thompson, J.T. Czernuszka, *The effect of two types of cross-linking on some mechanical properties of collagen,* **Biomedical Materials and Engineering**, vol 5 no. 1 1995 pp 37-48.

136. **AAMI** (Association for the advancement of medical instrumentation) American national standard: Cardiovascular Implants – vascular prostheses. 1994 ISBN: 1-57020-025-4.

137. Rhodin, **Handbook of physiology**, sec. 2: The Cardiovascular system.

ADDENDUM I –Operation of the adjustable pressure reservoir & flow waveforms

A1: Operation of the Adjustable Pressurised Reservoir

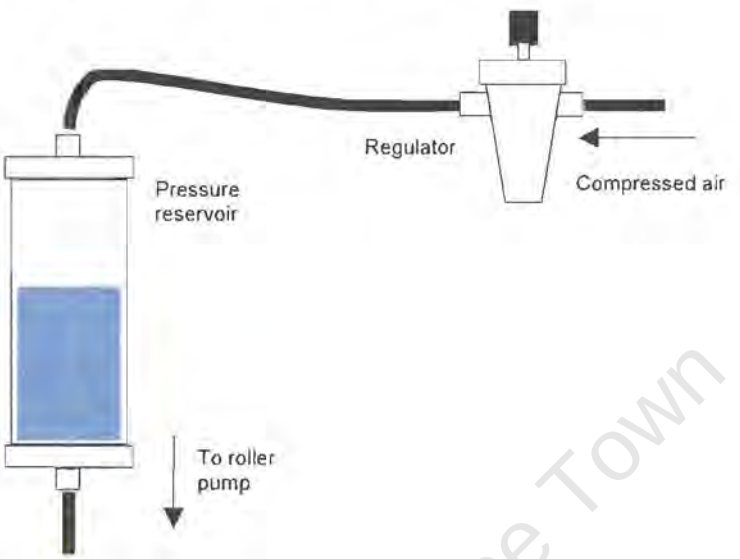

Adjustment of the air pressure in the airspace at the top of the reservoir is achieved by adjustment of the regulator

A2: Examples of the different waveforms achieved by varying certain parameters in the fluid circuit.

Waveform	Description / circuit conditions
a	74 beats per min, Windkessel 1 full, Windkessel 2 90%, control valve 80% closed.
b	120 bpm, same as above
c	120 bpm, same windkessel levels, control valve open
d	120 bpm, same windkessel levels, control valve 90% closed
e	120 bpm, windkessel 1 2/3 full, windkessel 2 90% full, valve 90% closed.
f	120 bpm, windkessel 1 80%, windkessel 2 90%, valve 90% closed
g	120 bpm, windkessel 1 full, windkessel 2 90%, valve 90% closed.
h	200 bpm, windkessel 1 full, windkessel 2 90%, valve 90% closed.

Proximal pressure
Distal pressure
Flow

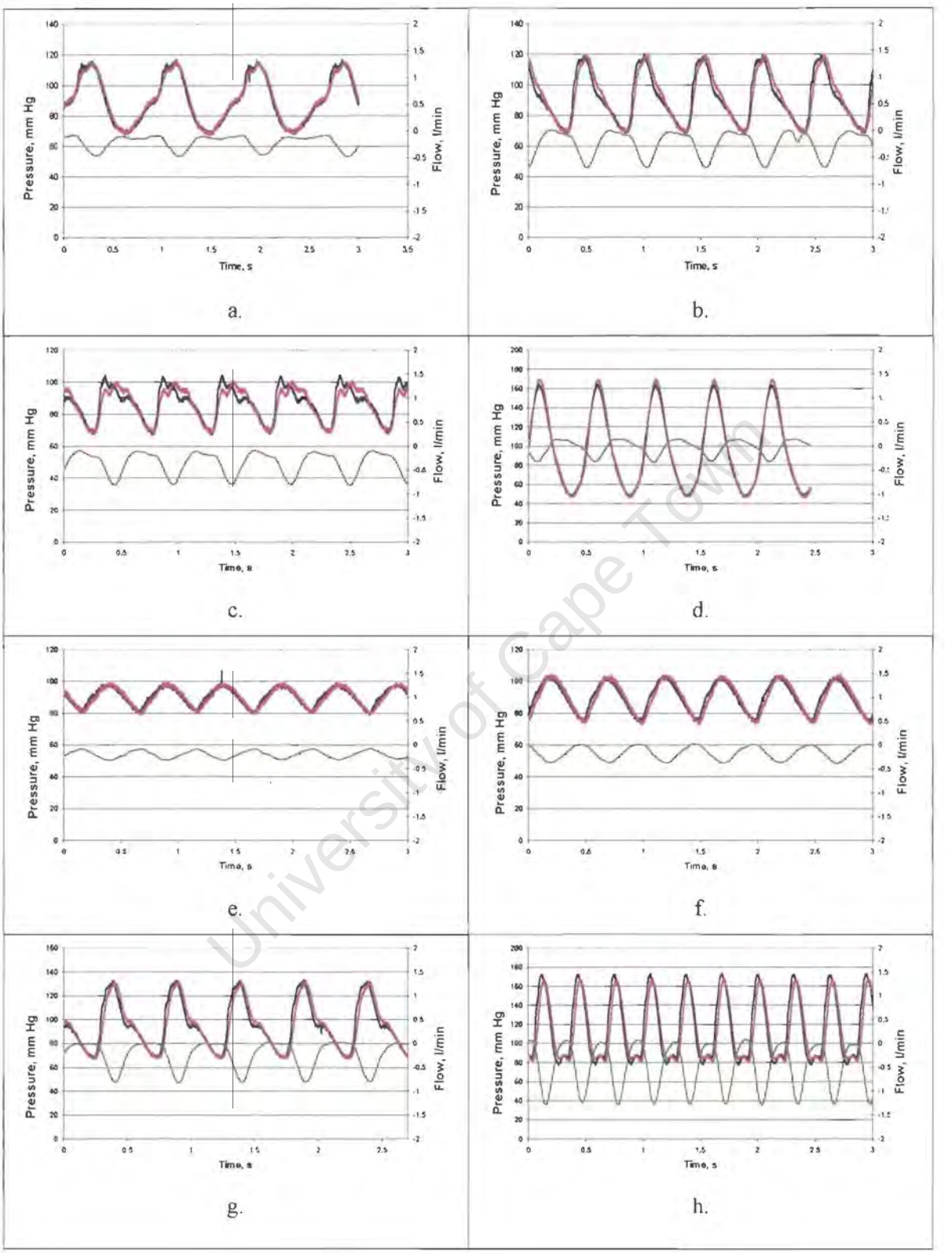

ADDENDUM II – Compliance results

NOTE: For the dynamic compliance tests graphs, the following legend applies in all tests:

Proximal pressure
Distal pressure
Diameter change

A1: Porcine aorta

Static testing

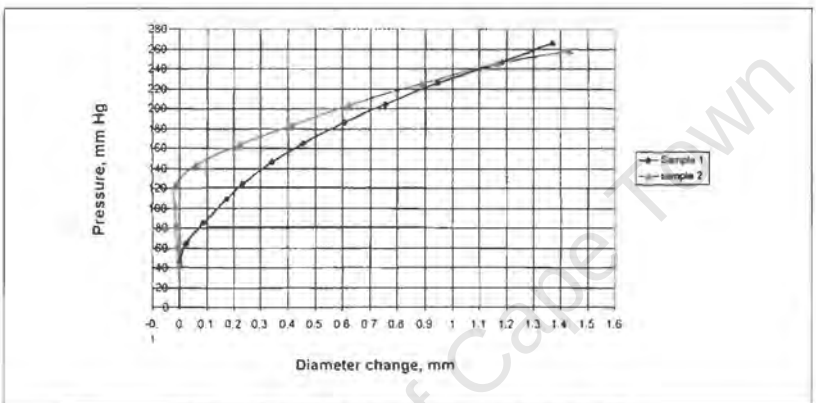

2 Samples of Porcine aorta tested statically

Dynamic testing

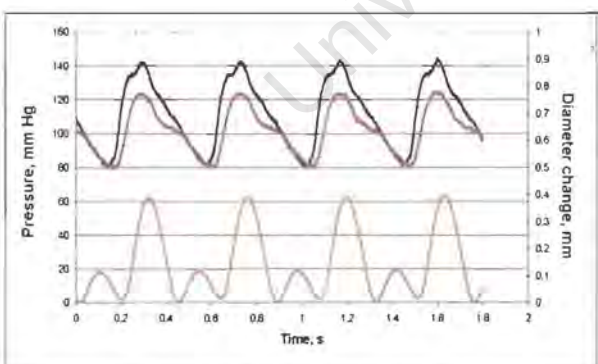

Sample 1: 80-120mm Hg

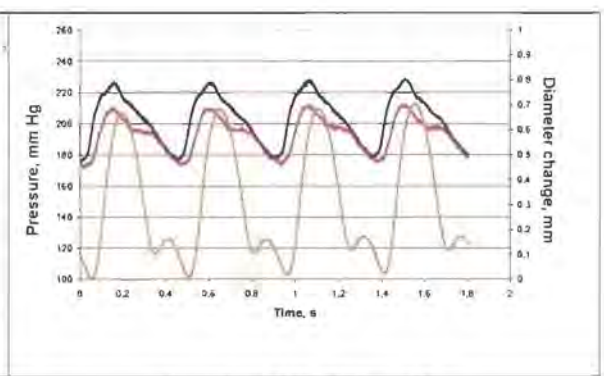

Sample 1: 180-220mm Hg

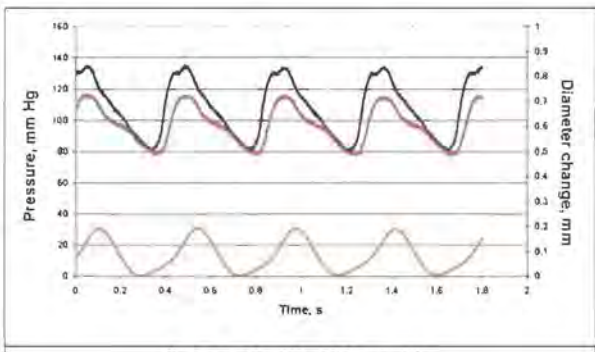

Sample 2: 80-120mm Hg

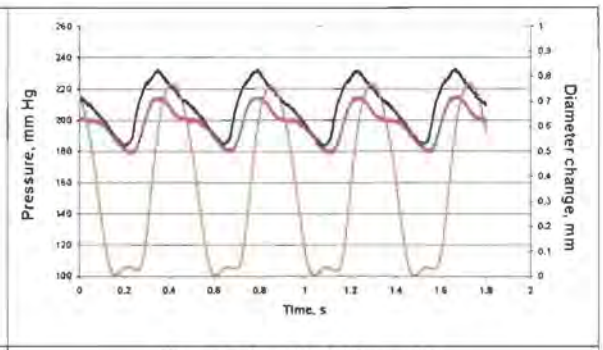

Sample 2: 180-220mm Hg

A2: Latex graft liners (static testing only)

Six samples of latex tubes tested statically. Wall thickness: 200µm. (2 samples cut from 3 lengths of tube 200mm long)

A3: Salt-cast grafts

a) Non-reinforced salt-cast grafts

Static testing

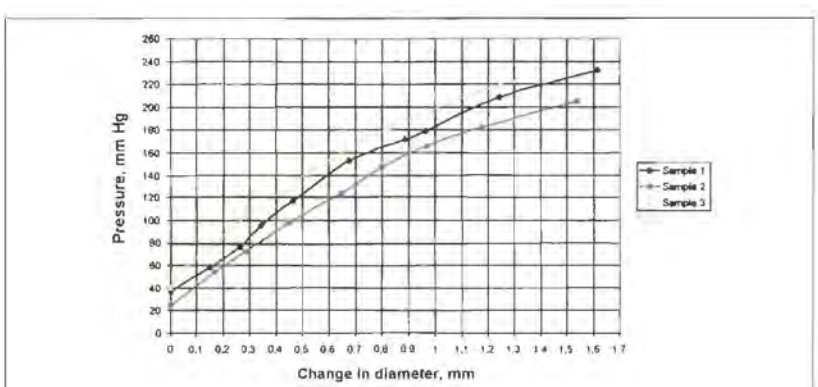

3 Samples of salt-cast grafts tested statically

Dynamic testing

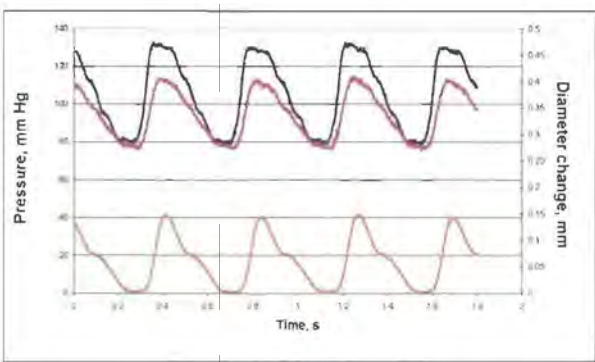

Sample 1: 80-120mm Hg

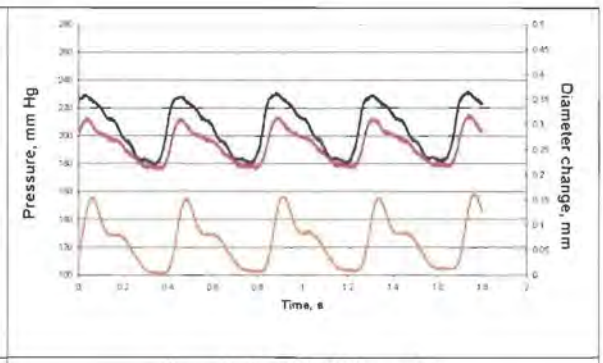

Sample 1: 180-220mm Hg

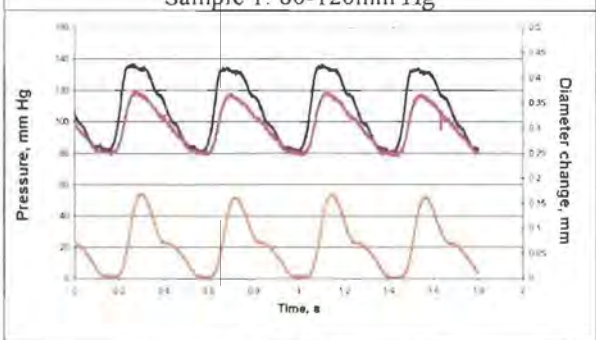

Sample 2: 80-120mm Hg

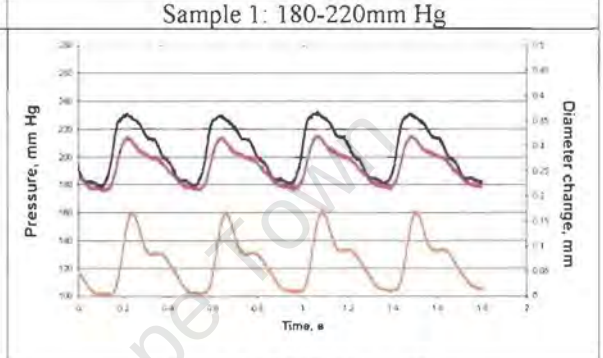

Sample 2: 180-220mm Hg

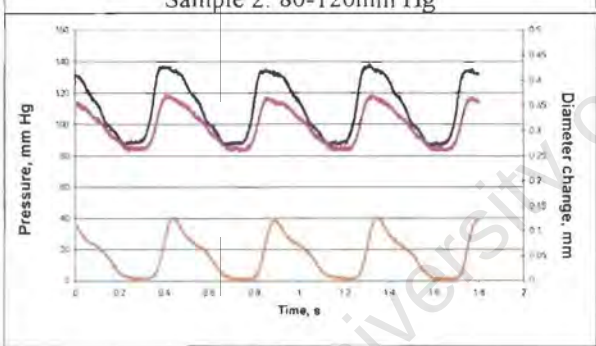

Sample 3: 80-120mm Hg

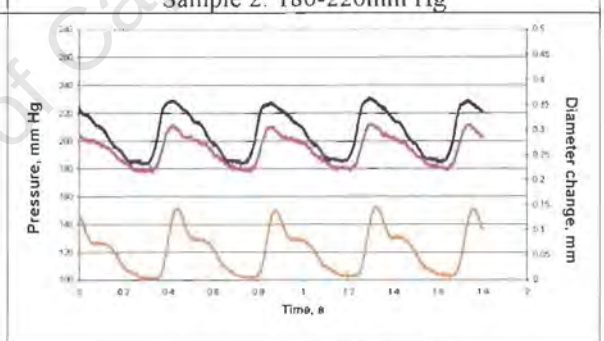

Sample 3: 180-220mm Hg

b) Salt graft reinforced with single wrapping of polyurethane monofilament at 2.5mm pitch.

Static testing

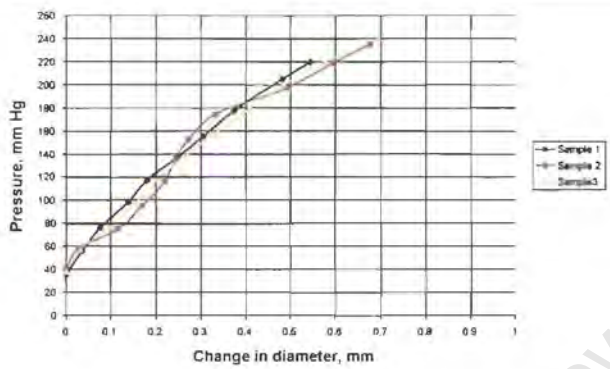

3 Samples of salt-cast grafts with a single wrapping of polyurethane monofilament.

Dynamic testing

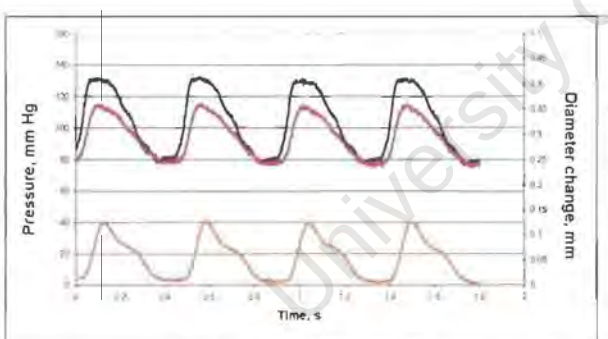

Sample 1: 80-120mm Hg

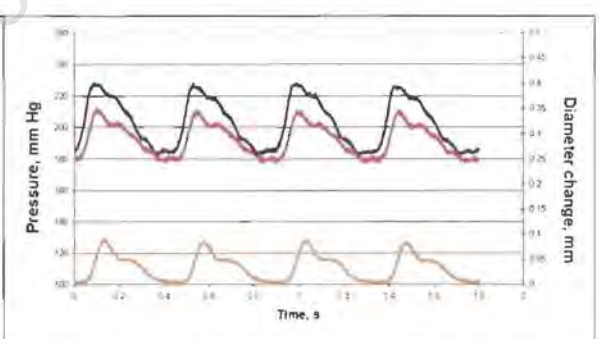

Sample 1: 180-220mm Hg

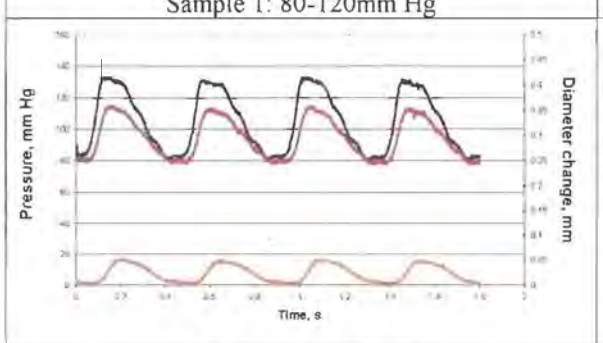

Sample 2: 80-120mm Hg

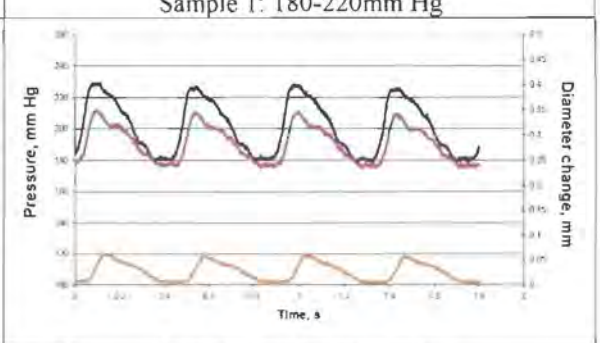

Sample 2: 180-220mm Hg

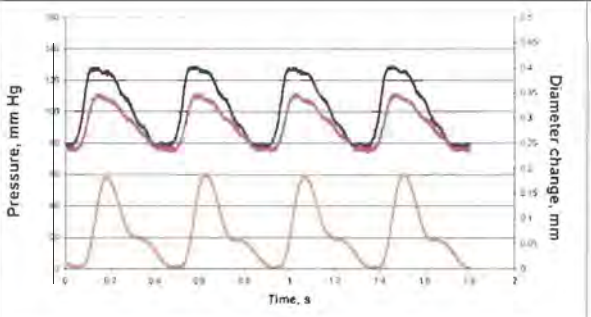

Sample 3: 80-120mm Hg

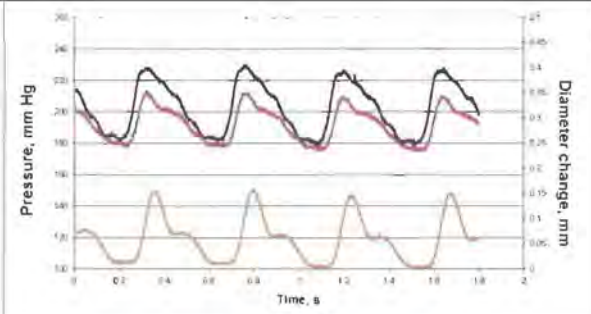

Sample 3: 180-220mm Hg

c) Salt-cast graft reinforced with single wrapping of 33 dtex Dorlastan® monofilament at 2.5mm pitch

Static testing

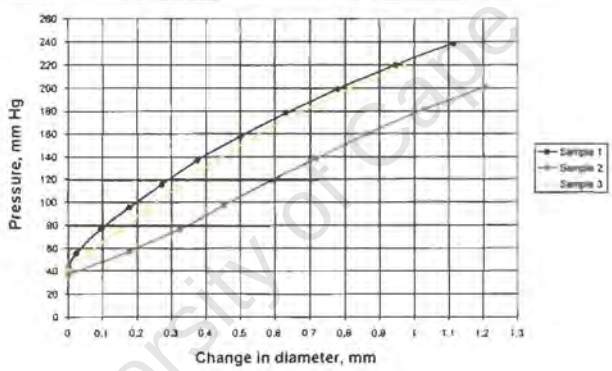

Static compliance of 3 samples of salt cast grafts reinforced with a single wrapping of 33 dtex Dorlastan monofilament at 2.5mm pitch

Dynamic testing

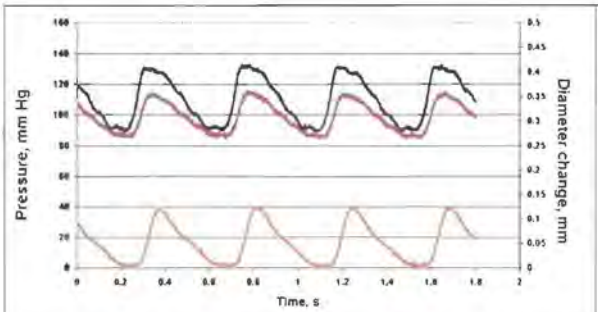

Sample 1: 80-120mm Hg

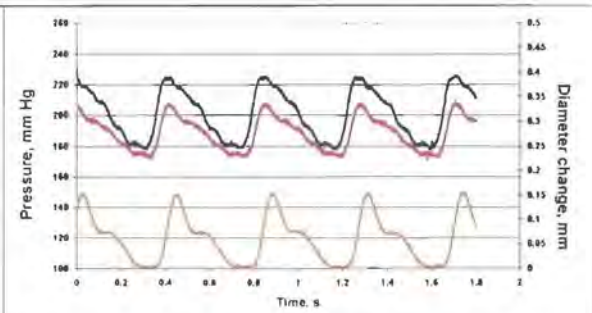

Sample 1: 180-220mm Hg

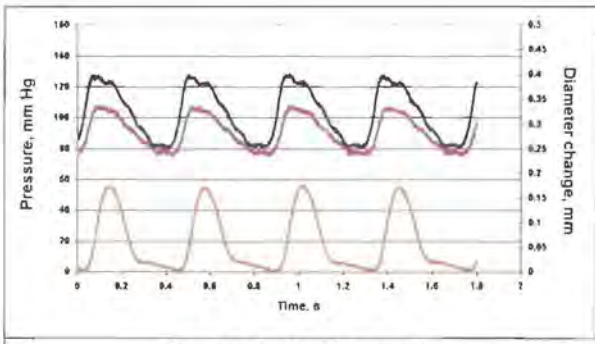

Sample 2: 80-120mm Hg

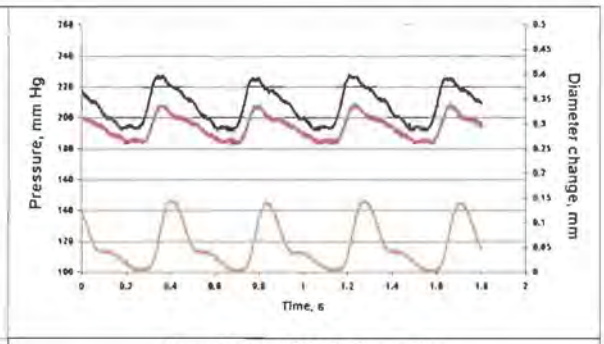

Sample 2: 180-220mm Hg

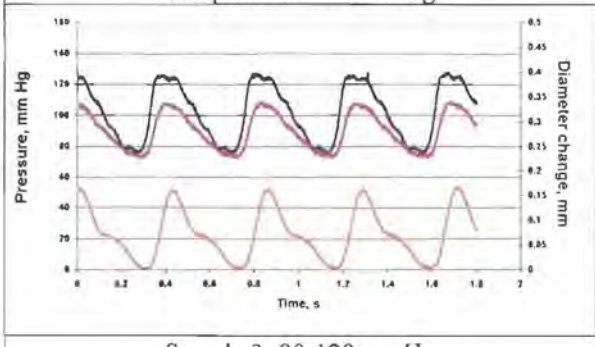

Sample 3: 80-120mm Hg

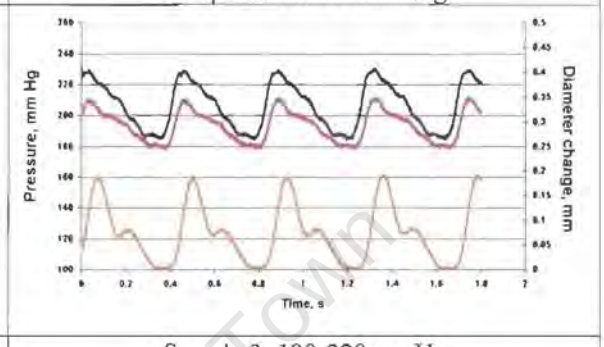

Sample 3: 180-220mm Hg

d) Salt-cast grafts reinforced with 33dtex Dorlastan® monofilament at 2.5mm pitch, double winding.

Static testing

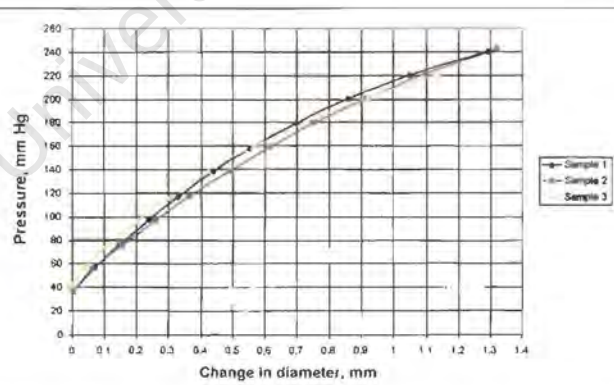

Static compliance of 3 samples of salt cast grafts reinforced with a double wrapping of 33 dtex Dorlastan® monofilament at 2.5mm pitch

Dynamic testing

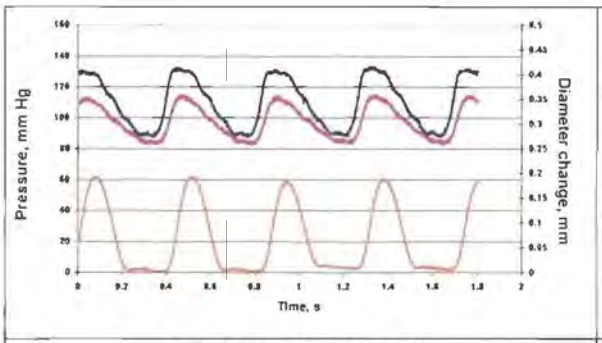

Sample 1: 80-120mm Hg

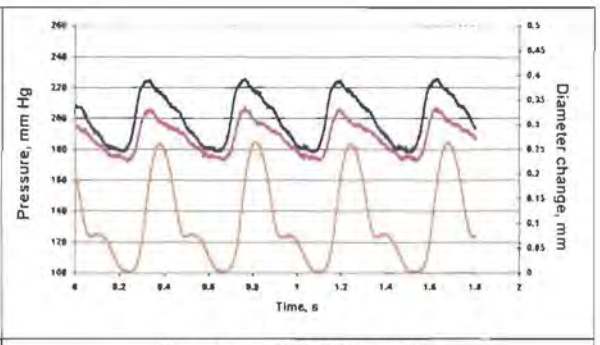

Sample 1: 180-220mm Hg

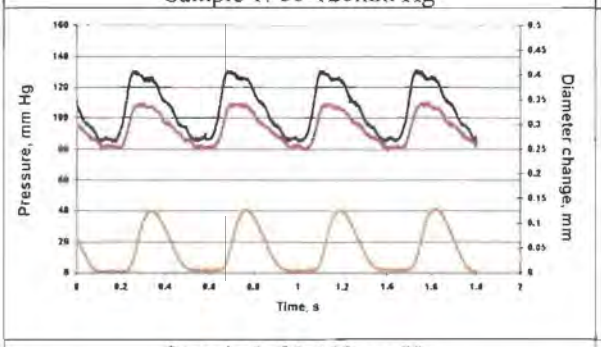

Sample 2: 80-120mm Hg

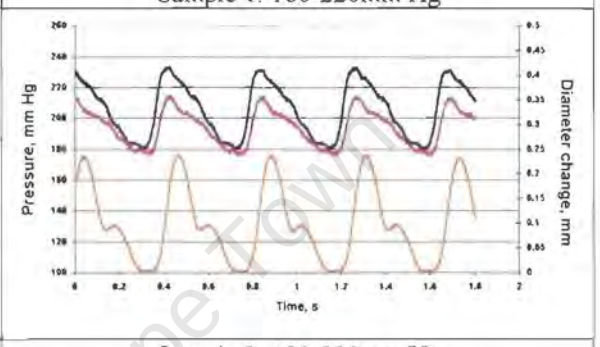

Sample 2: 180-220mm Hg

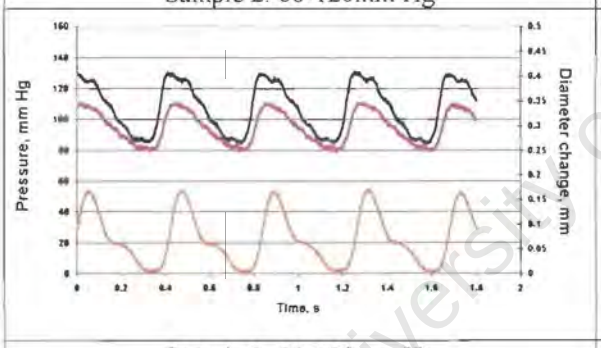

Sample 3: 80-120mm Hg

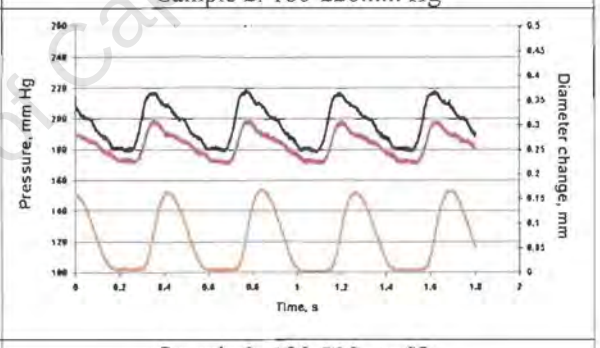

Sample 3: 180-220mm Hg

e) Salt-cast grafts reinforced with nylon monofilament at 1mm pitch (single wrapping)

Static testing

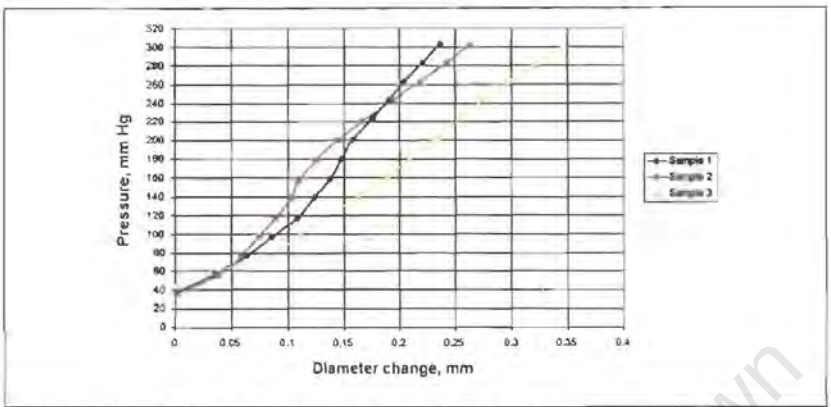

3 Samples of salt-cast grafts reinforced with nylon monofilament at 1mm pitch.

Dynamic testing

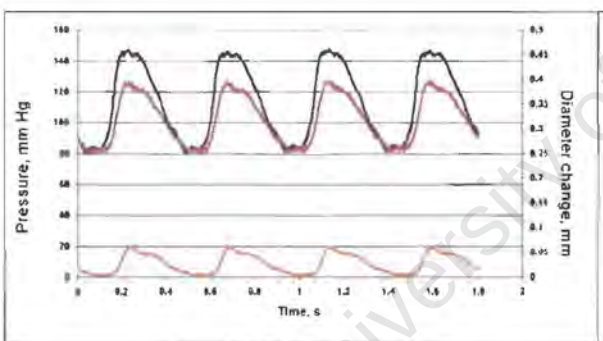

Sample 1: 80-120mm Hg

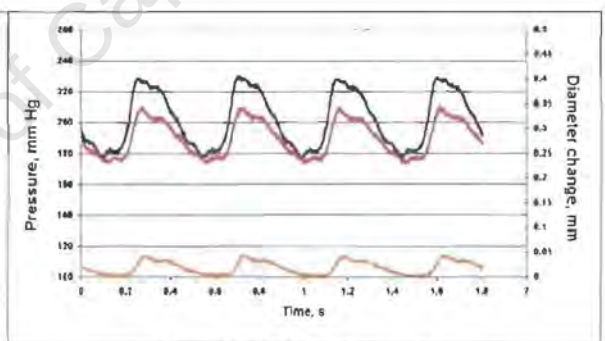

Sample 1: 180-220mm Hg

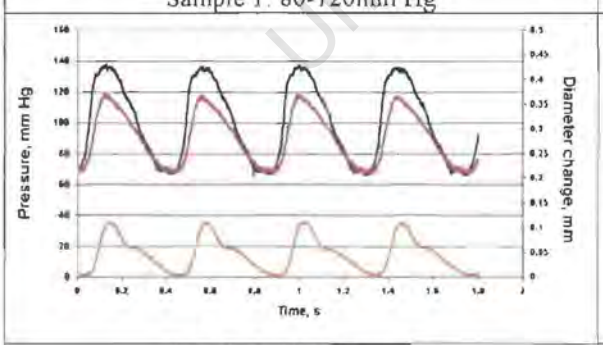

Sample 2: 80-120mm Hg

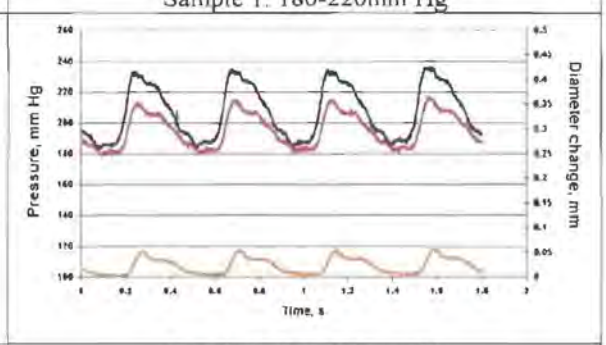

Sample 2: 180-220mm Hg

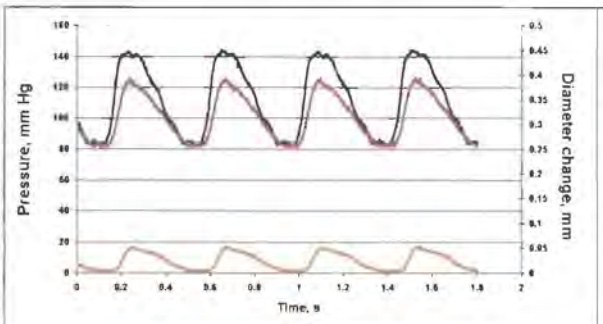

Sample 3: 80-120mm Hg

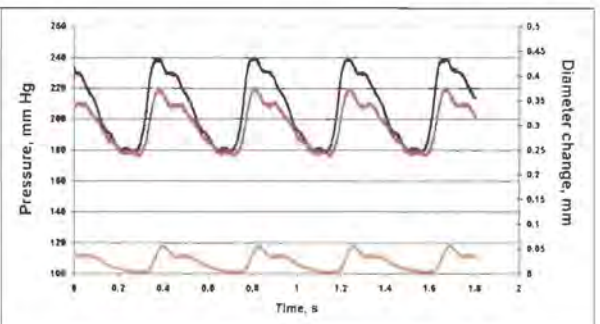

Sample 3: 180-220mm Hg

f) Salt-cast grafts reinforced with nylon monofilament at 2.5mm pitch (single wrapping)

Static testing

3 sample of salt-cast grafts reinforced with nylon monofilament at 2.5mm pitch.

Dynamic testing

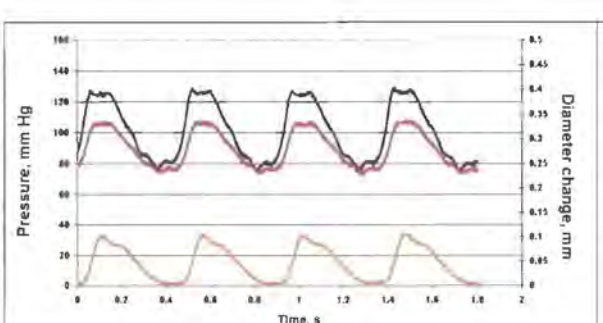

Sample 1: 80-120mm Hg

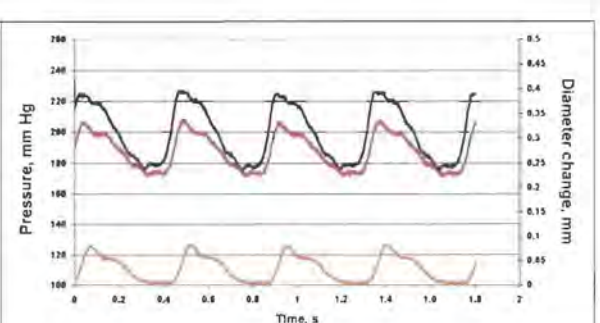

Sample 1: 180-220mm Hg

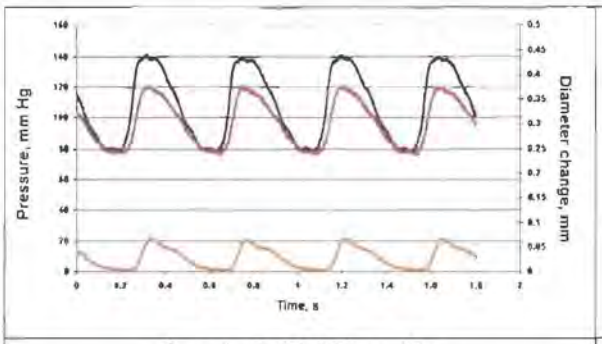

Sample 2: 80-120mm Hg

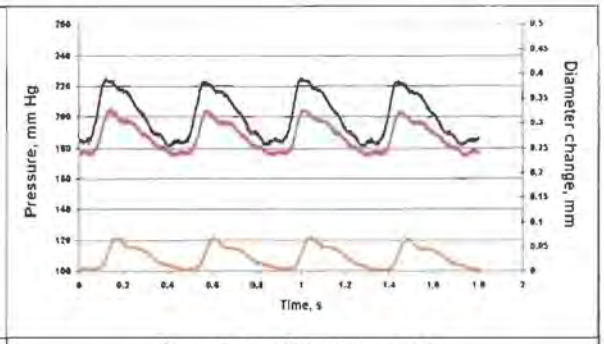

Sample 2: 180-220mm Hg

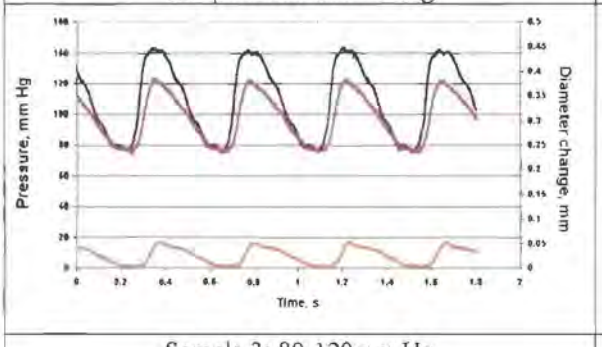

Sample 3: 80-120mm Hg

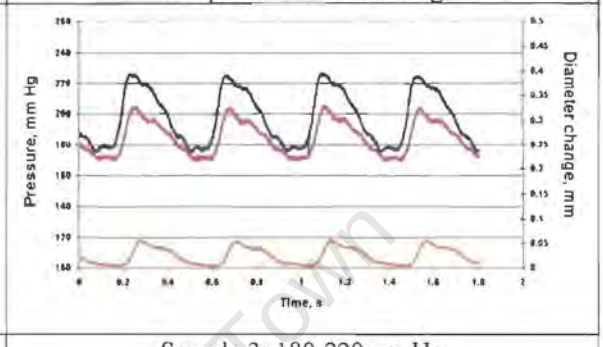

Sample 3: 180-220mm Hg

g) Salt-cast grafts reinforced with nylon monofilament at 5mm pitch (single wrapping)

Static testing

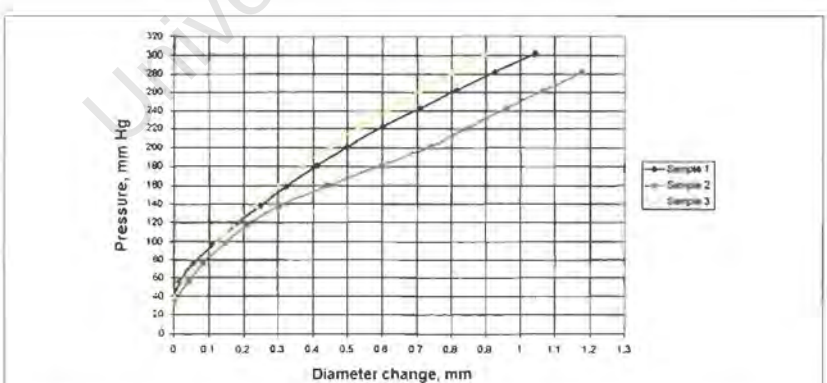

3 Samples of salt-cast grafts reinforced with single wrapping of nylon monofilament at 5mm pitch

Dynamic testing

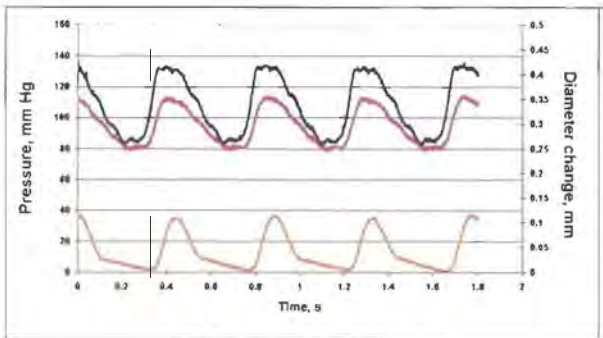

Sample 1: 80-120mm Hg

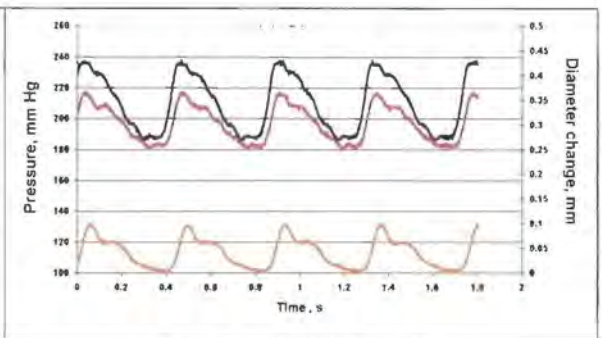

Sample 1: 180-220mm Hg

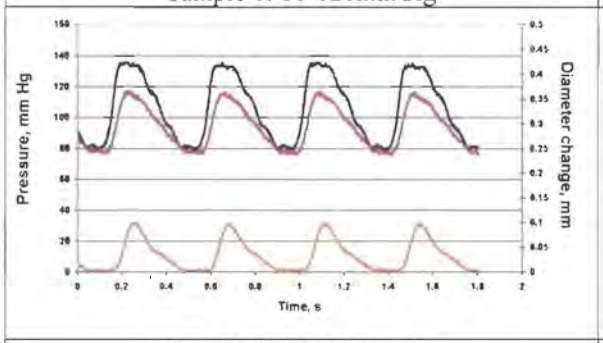

Sample 2: 80-120mm Hg

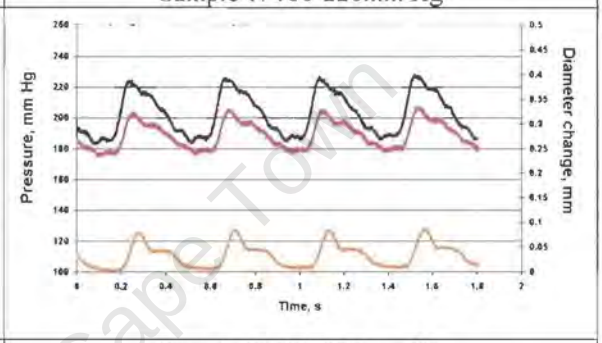

Sample 2: 180-220mm Hg

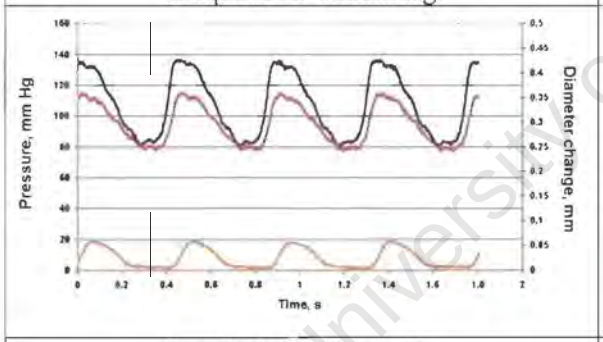

Sample 3: 80-120mm Hg

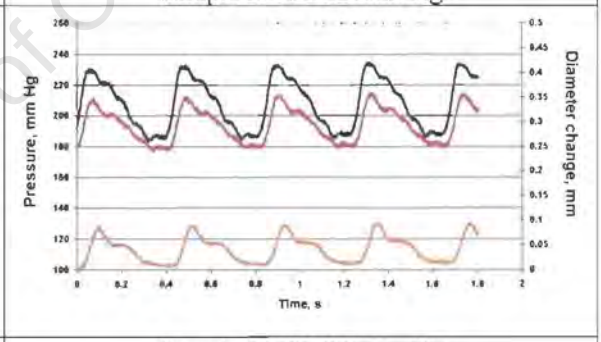

Sample 3: 180-220mm Hg

b) Salt-cast grafts reinforced with combination reinforcement: double wrapping of Dorlastan® 33 dtex at2.5mm pitch plus loose winding of nylon monofilament at 5mm pitch (attached only at ends of grafts).

Static testing

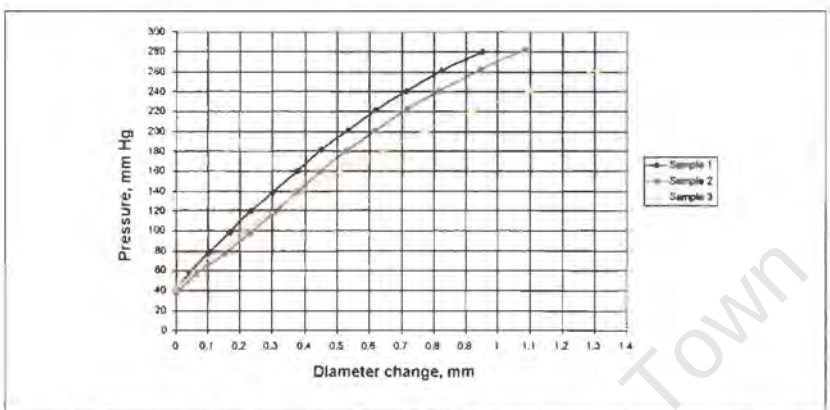

3 Samples of salt-cast grafts with combination reinforcement of Dorlastan® and nylon

Dynamic testing

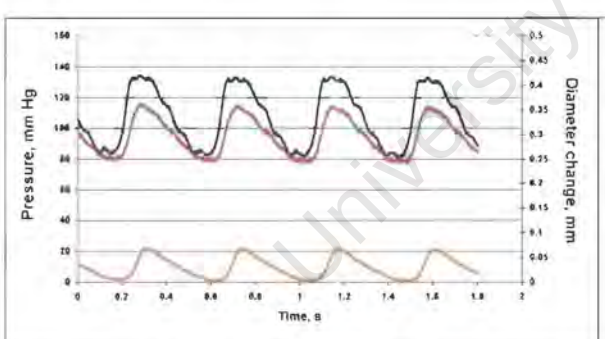

Sample 1: 80-120mm Hg

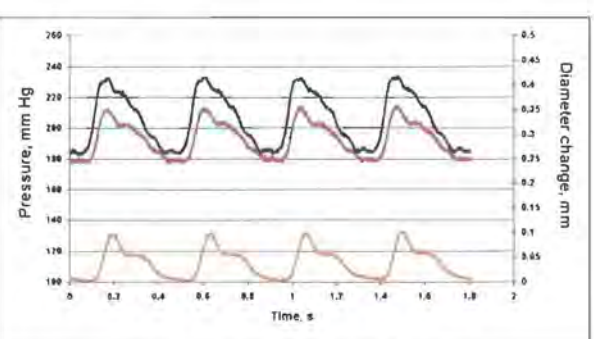

Sample 1: 180-220mm Hg

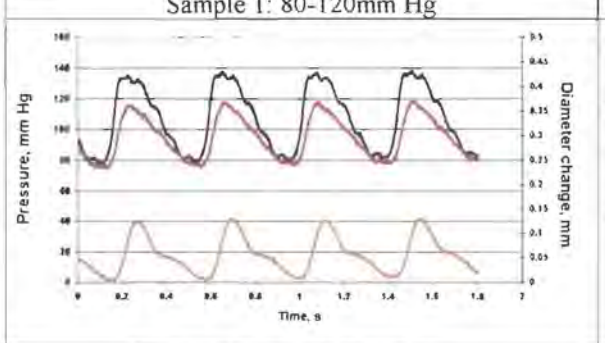

Sample 2: 80-120mm Hg

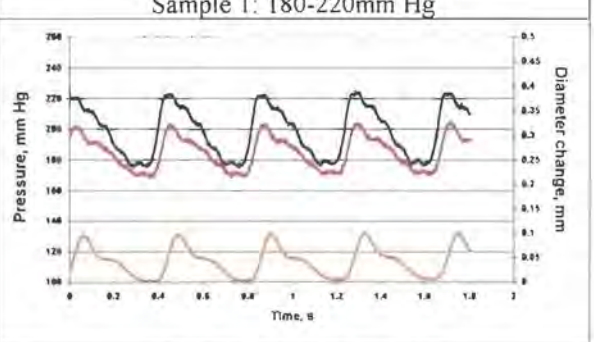

Sample 2: 180-220mm Hg

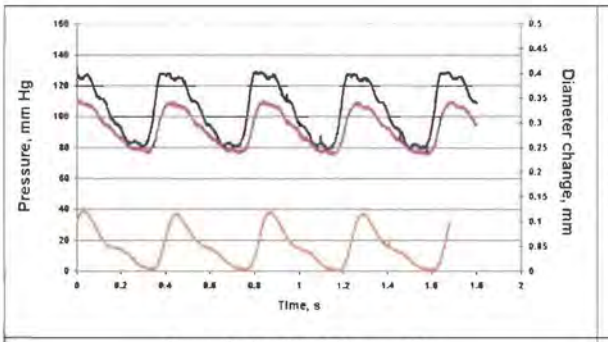

Sample 3: 80-120mm Hg

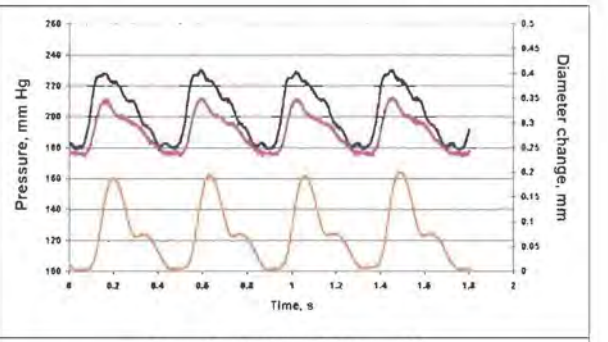

Sample 3: 180-220mm Hg

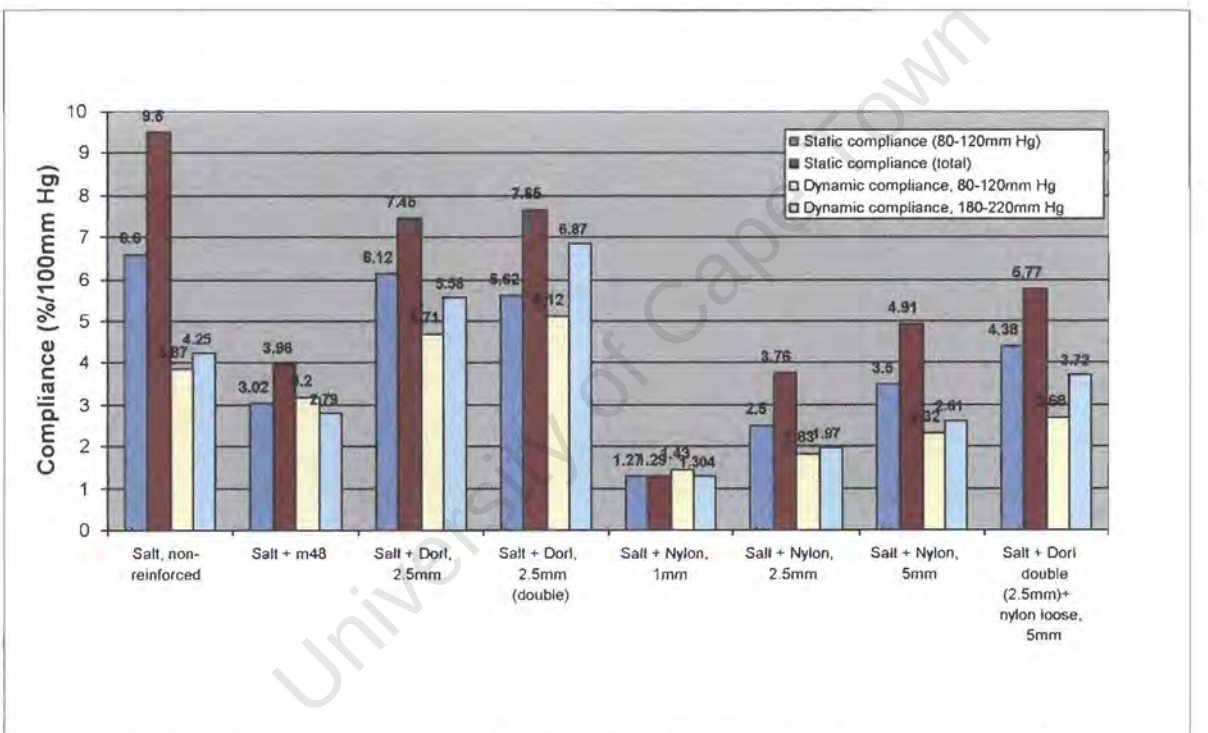

Static and dynamic compliance values of the various types of reinforced salt-cast grafts

A4: Bead-cast grafts

a) Non-reinforced bead-cast grafts

Static testing:

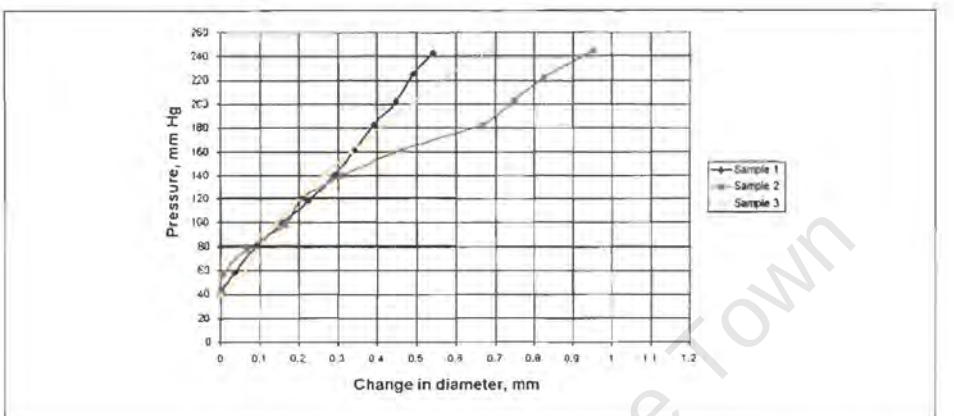

3 Samples of bead-cast grafts with no reinforcement

Dynamic testing:

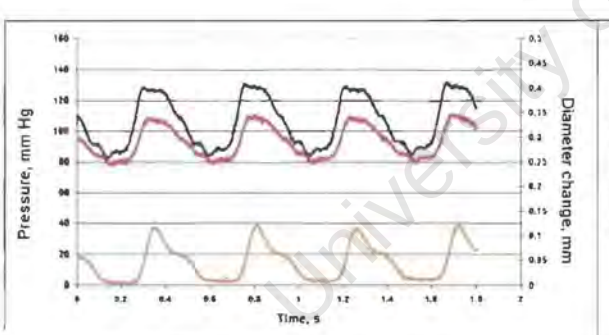

Sample 1: 80-120mm Hg

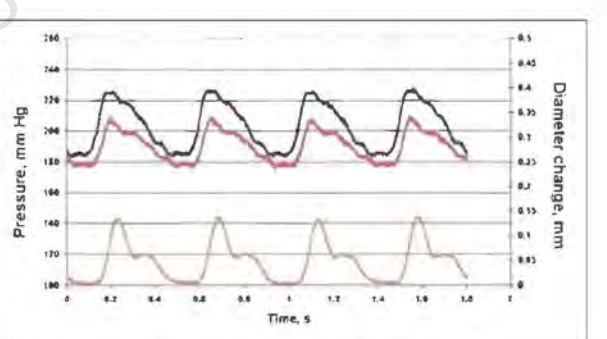

Sample 1: 180-220mm Hg

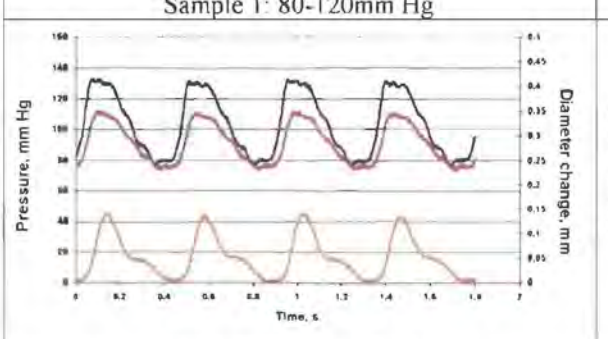

Sample 2: 80-120mm Hg

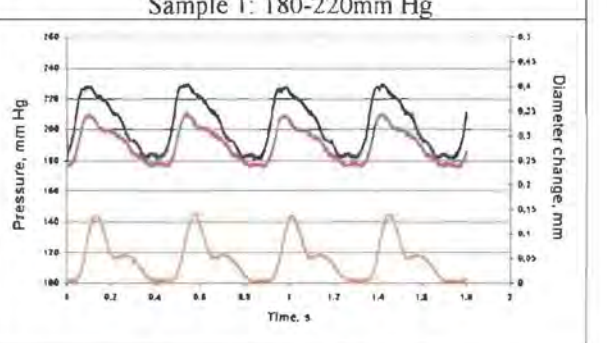

Sample 2: 180-220mm Hg

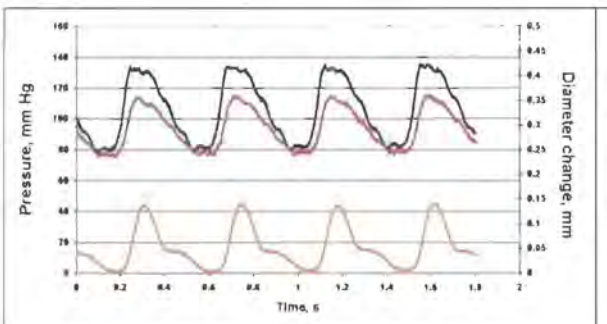

Sample 3: 80-120mm Hg

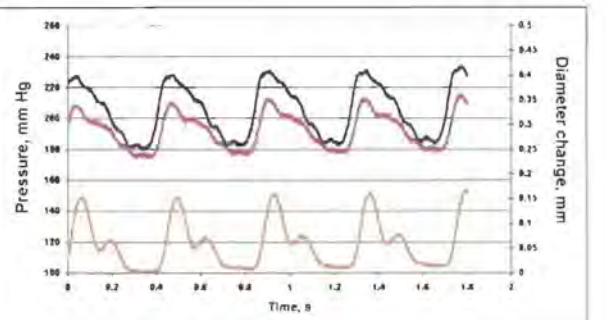

Sample 3: 180-220mm Hg

4 Bead-cast grafts with a single wrapping of polyurethane monofilament

Static testing:

3 Samples of bead-cast grafts with a single wrapping of polyurethane monofilament.

Dynamic testing:

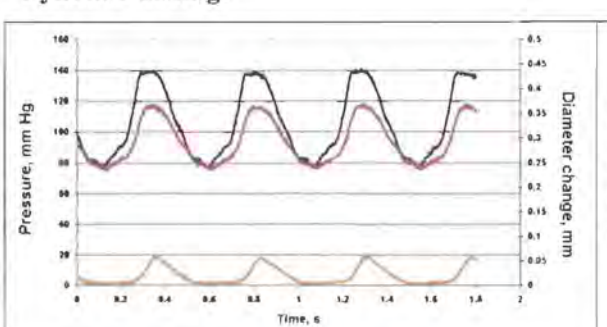

Sample 1: 80-120mm Hg

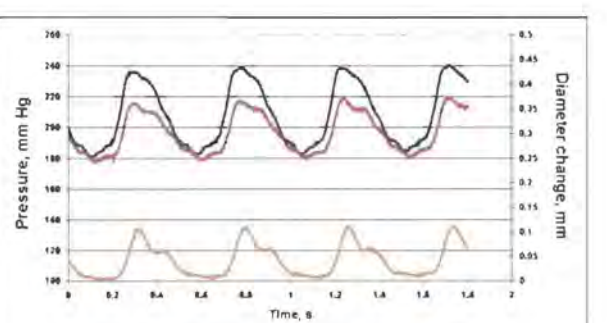

Sample 1: 180-220mm Hg

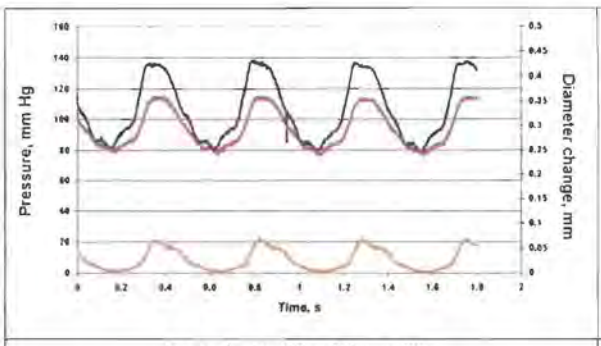

Sample 2: 80-120mm Hg

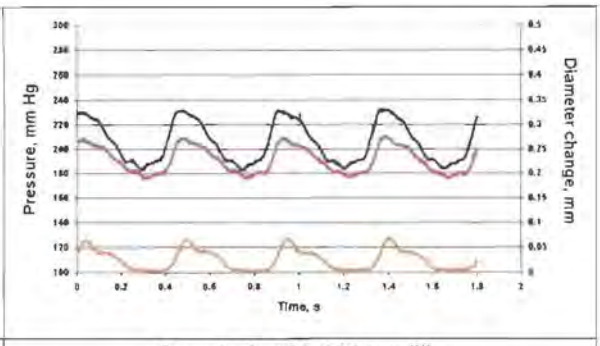

Sample 2: 180-220mm Hg

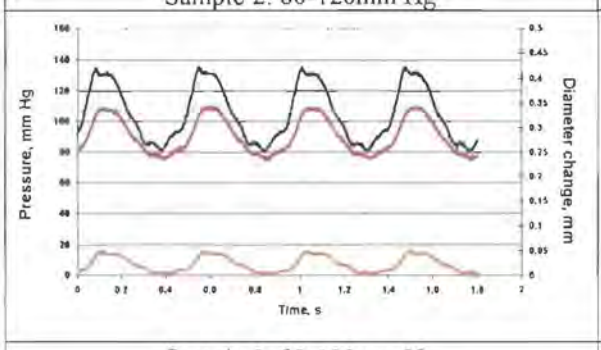

Sample 3: 80-120mm Hg

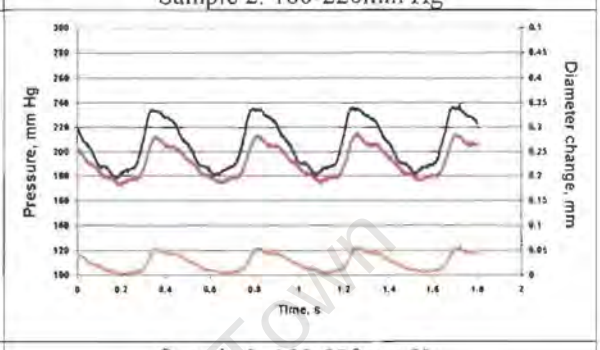

Sample 3: 180-220mm Hg

5 Bead-cast grafts with a single wrapping of Dorlastan® monofilament at 1mm pitch

Static testing

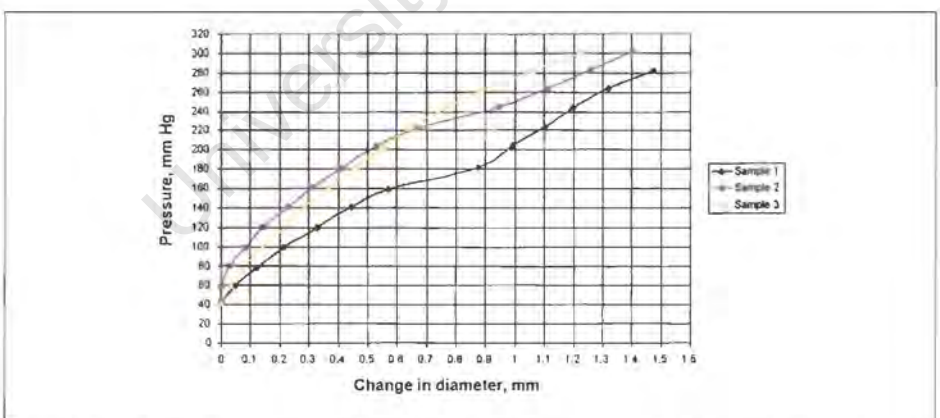

3 Samples of bead-cast grafts with a single wrapping of 33 dtex Dorlastan® monofilament at 1mm pitch

Dynamic testing:

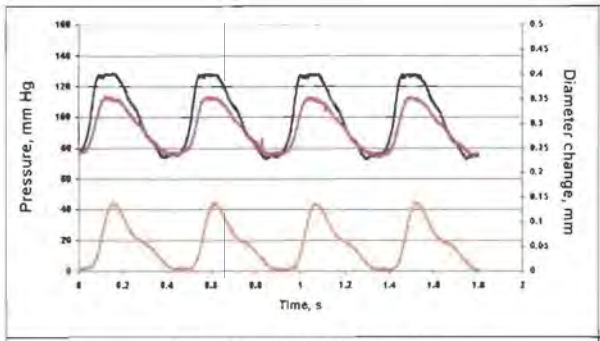

Sample 1: 80-120mm Hg

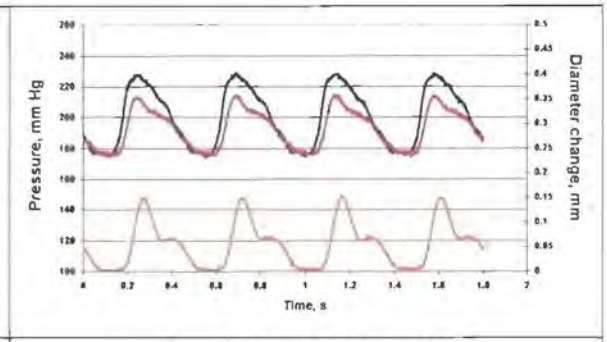

Sample 1: 180-220mm Hg

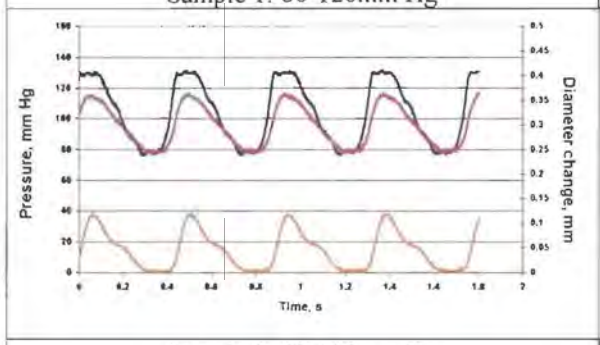

Sample 2: 80-120mm Hg

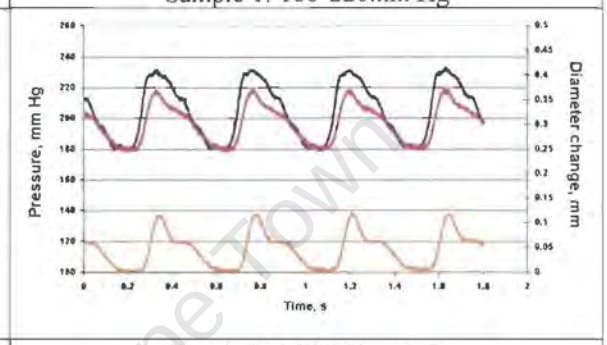

Sample 2: 180-220mm Hg

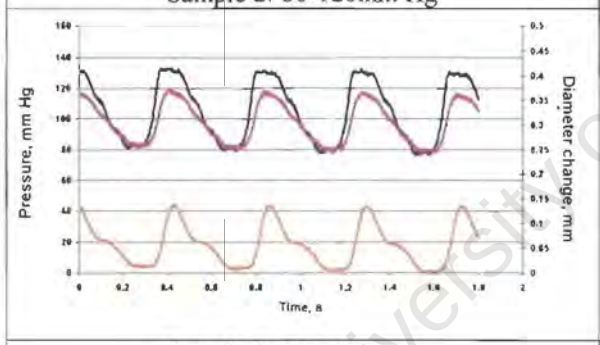

Sample 3: 80-120mm Hg

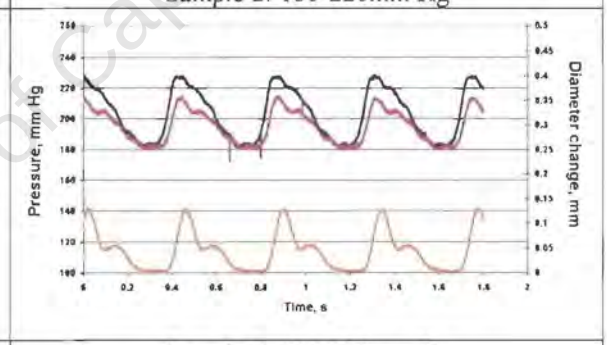

Sample 3: 180-220mm Hg

d) Bead-cast graft with a combination-reinforcement: Single wrapping of 33 dtex Dorlastan® at 2.5mm pitch and single wrapping of nylon monofilament at 2.5mm pitch.

Static testing:

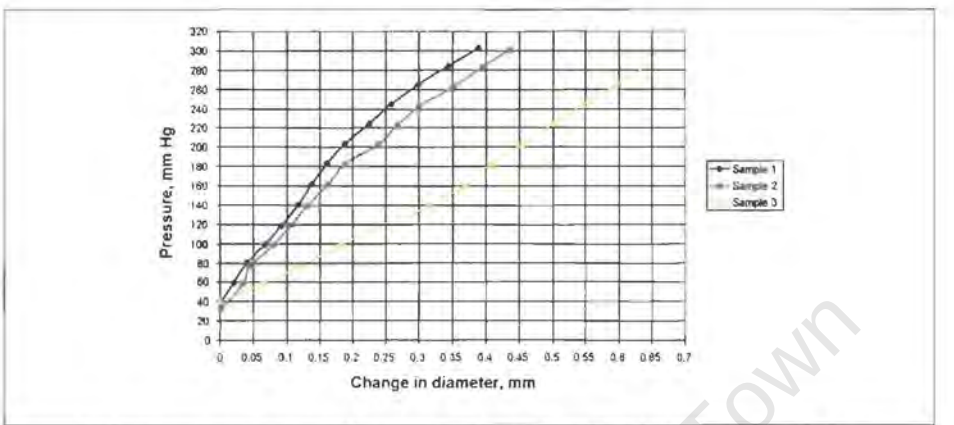

Static compliance tests of 3 samples of bead grafts reinforced with 33 dtex Dorlastan® monofilament and 130µm nylon monofilament

Dynamic testing:

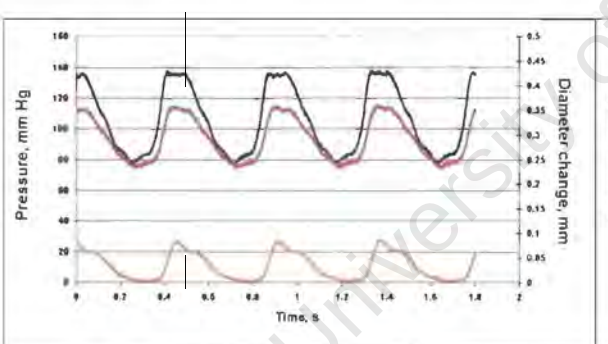

Sample 1: 80-120mm Hg

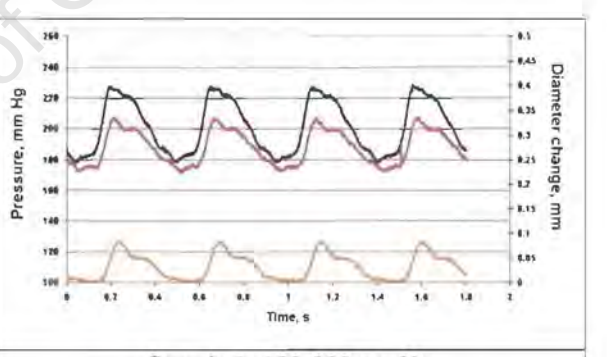

Sample 1: 180-220mm Hg

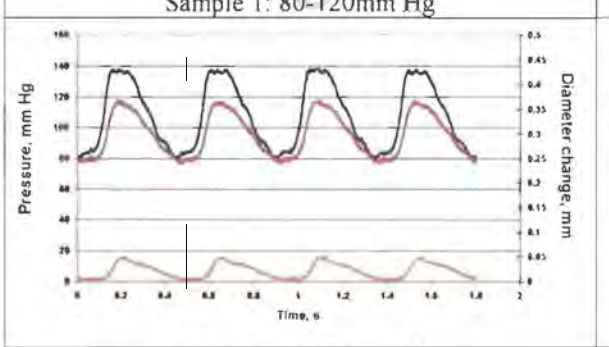

Sample 2: 80-120mm Hg

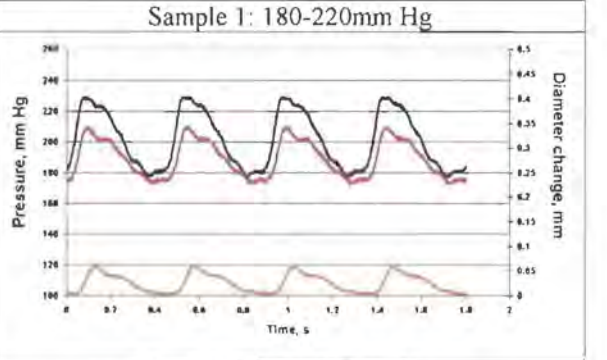

Sample 2: 180-220mm Hg

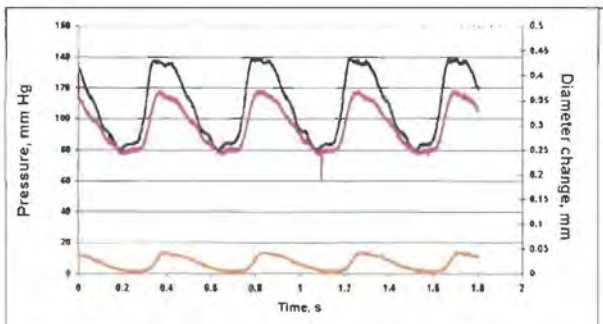

Sample 3: 80-120mm Hg

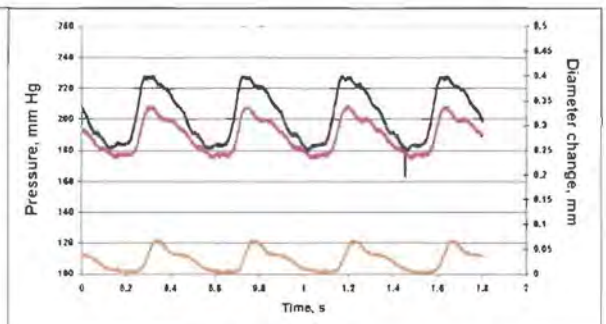

Sample 3: 180-220mm Hg

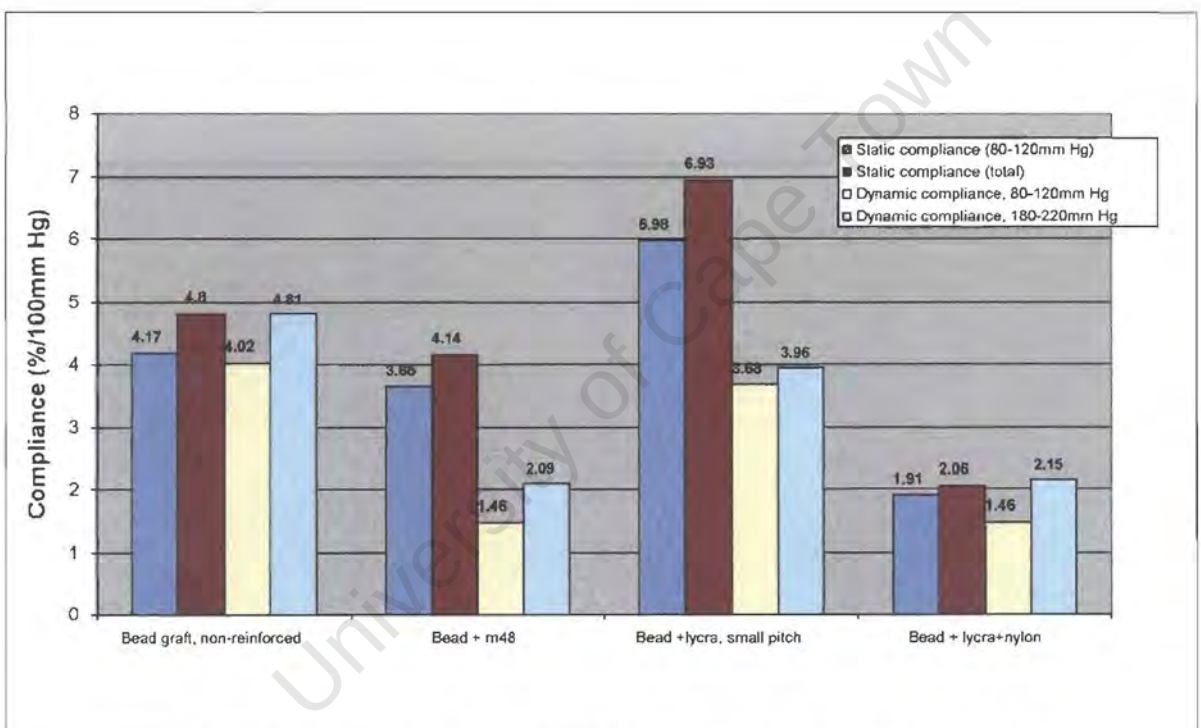

Static and dynamic compliance values of the various reinforced bead-cast grafts

A5: Commercial PTFE (Teflon®) 4mm id. grafts

Static testing

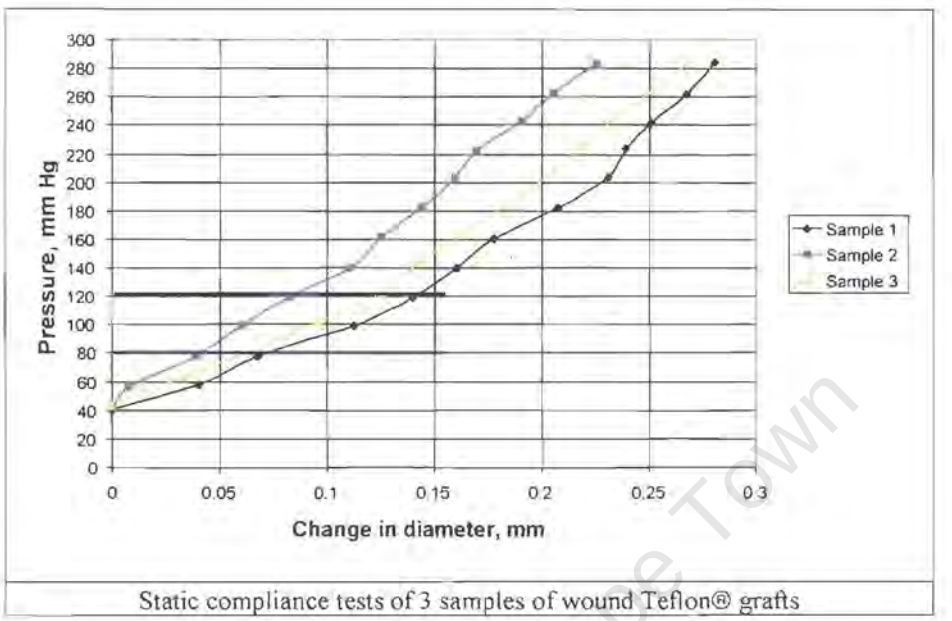

Static compliance tests of 3 samples of wound Teflon® grafts

Note: only static testing was carried out on the Teflon® grafts – dynamic testing resulted in negligible graft wall movement since these were very stiff grafts.

ADDENDUM III – Latex compensation

The following are graphs of the static compliance curves plotted for each graft type tested with the latex inserts compared to the static curve of the latex tested separately. The equations used used as best-fit plots to calculate the compensated pressure range are shown on each graph.

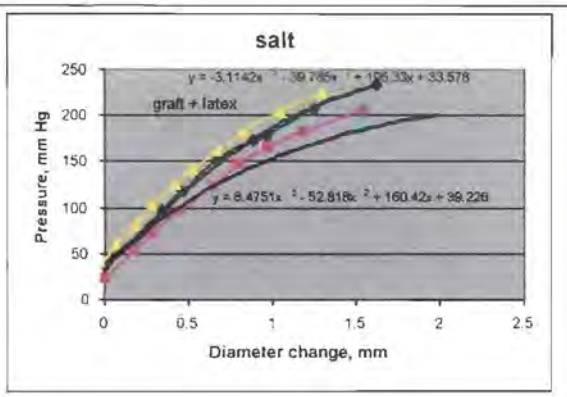

Non-reinforced salt-cast graft

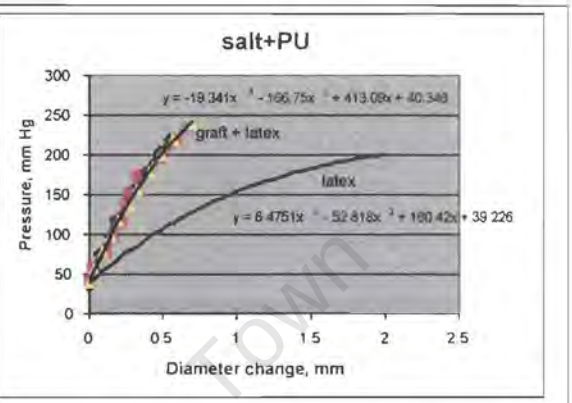

PU-reinforced salt-cast graft

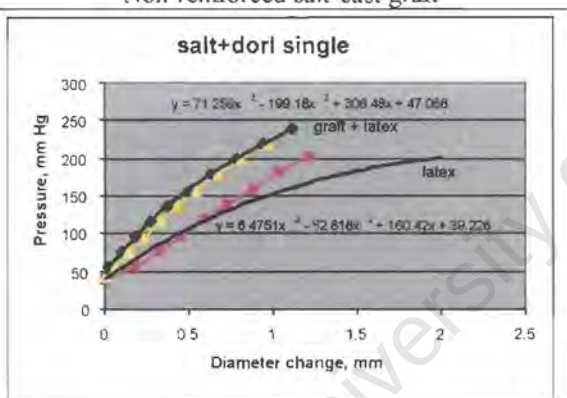

Salt-cast graft with single wrapping of Dorlastan®.

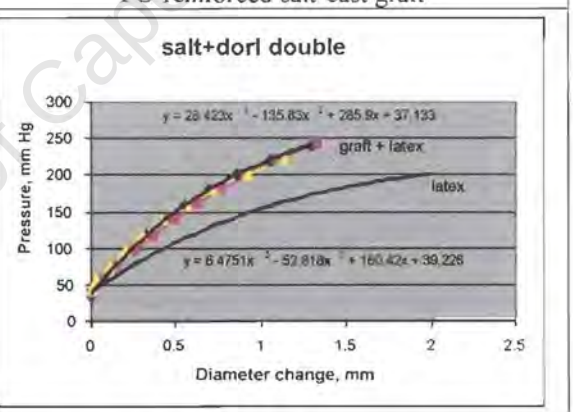

Salt-cast graft with double wrapping of Dorlastan®.

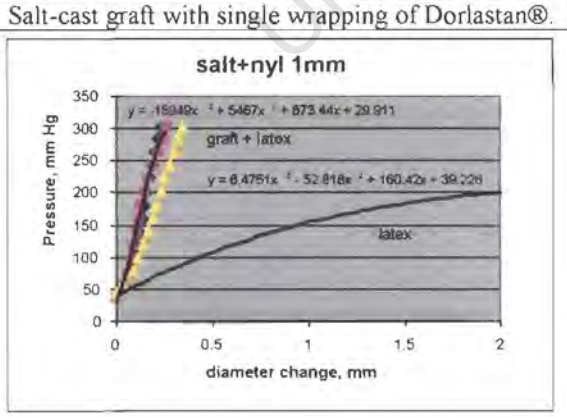

Salt-cast graft with single wrapping of nylon at 1mm pitch

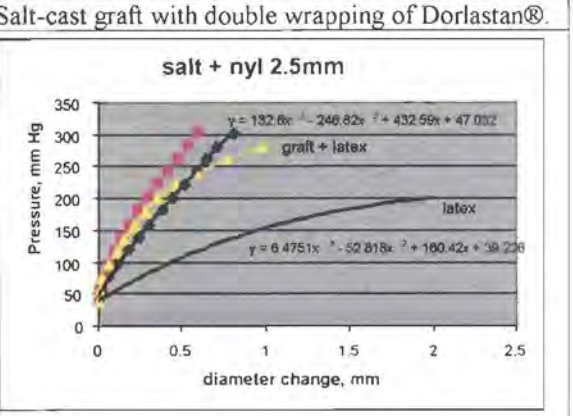

Salt-cast graft with single wrapping of nylon at 2.5mm pitch

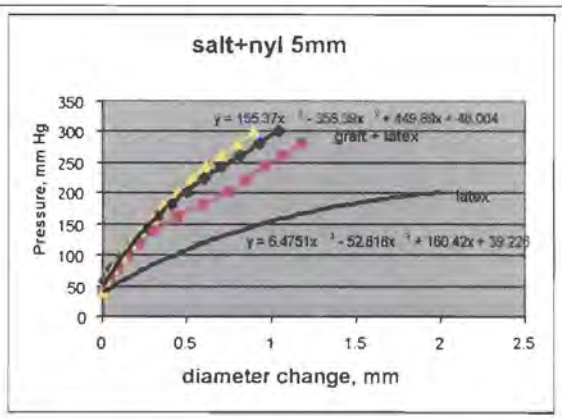

Salt-cast graft with single wrapping of nylon at 5mm pitch

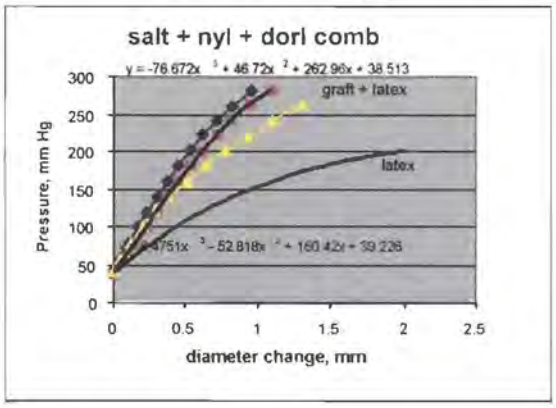

Salt-cast graft with combination reinforcement of Dorlastan® and nylon.

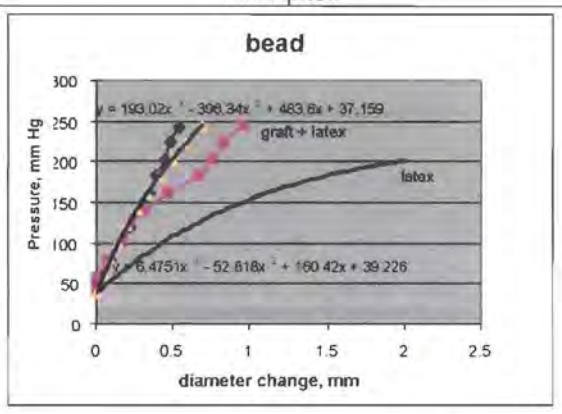

Non-reinforced bead-cast graft

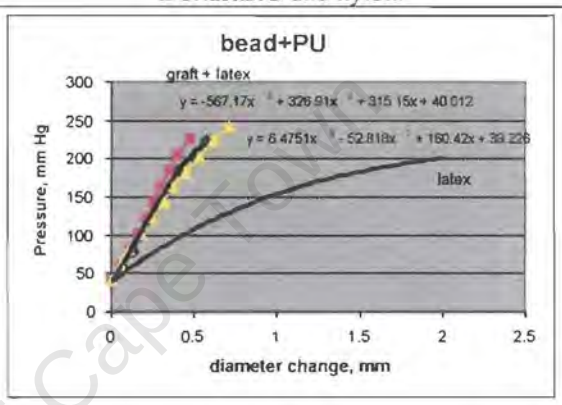

Bead-cast graft reinforced with PU monofilament

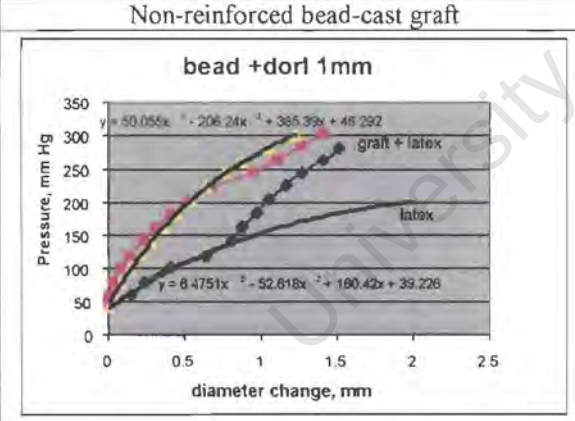

Bead-cast graft reinforced with Dorlastan® at 1mm pitch

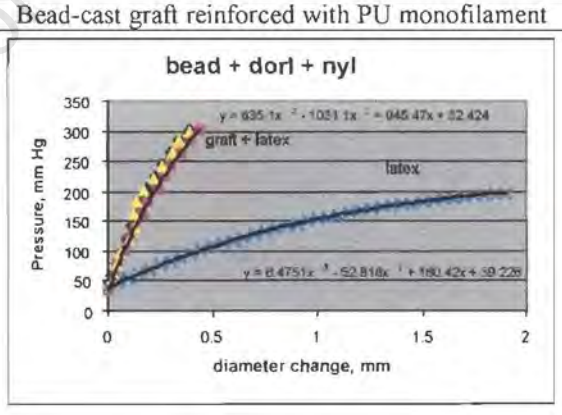

Bead-cast graft reinforced with combination of Dorlastan® and nylon

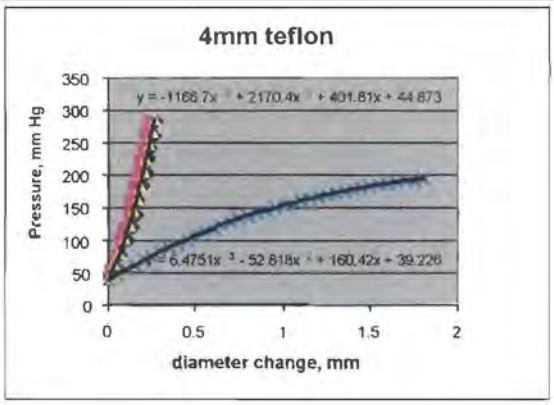

4mm commercial Teflon® graft

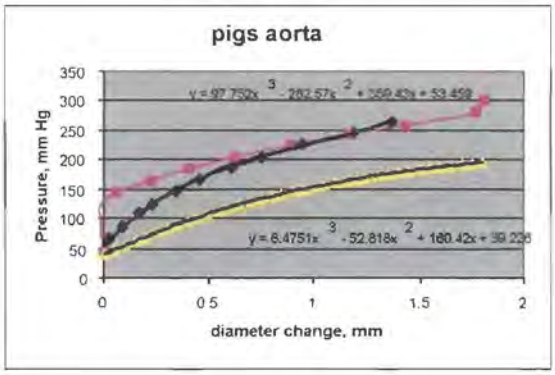

Porcine aorta (6-9mm internal diameter).